RESTRAINED ROCKING RESPONSE

OF EQUIPMENT

ON RIGID FLOORS

by

AHMED M. EL-HOSSIENY, B.Sc., M.Sc.

A Thesis

Submitted to the School of Graduate Studies

in Partial Fulfillment of the Requirements

for the Degree

Doctor of Philosophy

September 1985

RESTRAINED ROCKING RESPONSE

OF EQUIPMENT

ON RIGID FLOORS

DOCTOR OF PHILOSOPHY (1985)
(Civil Engineering and
Engineering Mechanics)

McMASTER UNIVERSITY
Hamilton, Ontario

TITLE: Restrained Rocking Response of Equipment on Rigid Floors

AUTHOR: Ahmed Maged Mohammed Abdel Monem El-hossieny,

             B.Sc.   (Ain Shams University)

             M.Sc.   (Ain Shams University)

SUPERVISOR: Dr. W. K. Tso

NUMBER OF PAGES: xix, 214

ABSTRACT

Equipment can be mounted on rigid floors by placing the equipment freely on the floor without fastening, fixing it tightly to the floor, or partially fixing it to the floor. This study investigates the rocking response of equipment resting freely on rigid floors and also the effect of restrained rocking on the response of partially fixed equipment under seismic excitations.

Equipment which rests freely on rigid floors is simulated as a rigid rectangular block. The overturning of rigid blocks is studied under the effect of three types of base motion, namely, pulsive, critical, and harmonic excitations.

When the effect of pulse shapes on the overturning potential of rigid blocks under pulsive excitations is examined, it is found that the rectangular pulse will require the least peak acceleration for a specified duration. Under critical excitations, it is found that the extent of response amplification depends on the coefficient of restitution and the initial angle of rotation in addition to the peak acceleration of the pulses. To amplify the motion by a specified ratio, pulses with lower peak accelerations are required for cases of large initial angles and for cases with large values of the coefficient of restitution. Under harmonic excitation, the conditions for steady-state periodic motion are derived. It is also found that as the coefficient of restitution decreases, the system becomes more stable against overturning and can withstand higher accelerations.

iii

Also in this research, the response of partially fixed equipment resting on rigid floors under the effect of harmonic and earthquake excitations is investigated. For systems restrained by non-yielding bolts, it is found that the existence of gaps has the effect of decreasing the deformation of the mounted equipment relative to the base compared to the case of complete fixation. The existence of gaps also decreases the natural frequency of the system. In systems with yielding bolts, the presence of the gaps affects the deformation of the equipment more than in systems with non-yielding bolts. In the latter, the total rocking angle after all stretching takes place is not sensitive to the initial gap size, and depends only on the level of excitation.

Based on this study, it is recommended that equipment systems be allowed to rock on their bases by providing gaps in their anchorage systems. This kind of mounting has the advantage of allowing the equipment to rock without the risk of overturning. Also, larger gaps are recommended for higher floor acceleration levels.

ACKNOWLEDGEMENTS

TABLE OF CONTENTS

viii

LIST OF FIGURES

LIST OF TABLES

LIST OF SYMBOLS

A	Equipment shear cross-sectional area
A_n	Arbitrary constant for the response of the nth half-cycle of the steady-state periodic motion
A_o	Arbitrary constant for the response of the periodic motion
A^*	Constant base acceleration that will cause one bolt to yield.
a	Peak base acceleration
a_o, a_1, a_2	Coefficients of second order algebraic equation (4.30)
B_n	Arbitrary constant for the response of the nth half-cycle of the steady-state periodic motion
B_o	Arbitrary constant for the response of the periodic motion
B_1, B_2	Constants in equation (2.27)
b	Half width of base plate
C	Input parameter in the steady-state response expression (4.4)
$C-J$	Address of case referred to, in row C and column J, in table (3.1)
C_o	Parameter in equations (3.41) and (3.42)
c	Damping coefficient for the equipment system
c_1, c_2	Coefficients of second order algebraic equation (2.16)
c^*	Generalized damping coefficient for the equipment system
D	Damping parameter for the steady-state periodic motion
D_o	Parameter in equations (3.41) and (3.42)
D_y	Elastic deformation of bolts just before yielding

E_{max} Maximum energy a bolt can absorb before failure

F Frequency (Hz) of the base harmonic excitation

F_y Bolt yielding force

F_1, F_2 Tension forces in the left and right bolts respectively

F^* Parameter in equation (5.5)

f Parameter in equation (3.5)

f_o Natural frequency of equipment on a fixed base (Hz)

G Shear modulus for the shear beam model

G_o Parameter in equations (3.41) and (3.42)

g Acceleration due to gravity

g_o Initial gap size

g_r Gap ratio which is equal to $g_o/1$.

g_t Total gap size including bolt stretching

H Parameter for the steady-state periodic motion depending on the frequency of the base motion and the restitution coefficient

h height of the mass center above the rigid floor

I Label of the curve representing the upper limit of existence of the in-phase periodic motion

I_o Mass moment of inertia of the equipment about the centre of rotation.

I_1, I_2, I_3 Integration parameters in equation (2.27)

J Parameter which depends on the normalized duration for the half-sine pulse

K Normalized amplitude of base acceleration = $a/(g\alpha)$

K_o Critical normalized acceleration for steady-state motion

K^* Generalized stiffness of the equipment system

1 Distance between the centre of rotation o and point p

M	Equipment Mass
M^*	Generalized mass of equipment
m	Equipment mass per unit length
N	Label for curve representing the minimum acceleration required to start tilting
N^*	Parameter for the generalized forces in equation (5.3)
p	$=[WR/I_o]^{1/2}$
Q_1, Q_2	Parameters in the stability condition (4.29) of the steady-state periodic motion
q	Frequency parameter for the steady-state periodic motion
R	Distance between the center of mass and the center of rotation
r	Amplification factor for the response due to critical excitation
S	Label for the curve representing the upper limit for stability of steady-state periodic motion
s	Distance between the differential mass element and the centre of rotation
T	Period of response
t	Time variable
t_b	Time of impact of base plate with bolt head
t_i	Time of start of tilting for rigid block subjected to triangular pulse of type 2
t_j	Length of time interval between the impact of rigid block with floor and the end of rectangular pulse
t_m	Length of time interval between the start of triangular pulse and the impact of rigid block with floor
t_n	Length of time interval between the start of rectangular pulse and the impact of rigid block with floor
t_s	Half length of time duration of critical triangular pulse

u	Displacement due to deformation of the equipment of point at height y relative to the base plate
U	Displacement, due to deformation, of the equipment top point in the direction parallel to the base plate
V_o	Static base shear which is equal to (Ma)
v	Normalized angle of rotation, θ/α
v_n	Normalized angle of rotation for the nth half-cycle of the steady-state periodic motion, θ_n/α
W	Equipment weight
X	Parameter for the steady-state periodic motion depending on the input parameters of the base motion and the restitution coefficient
x	Total floor displacement in the horizontal direction
$\bar{x}_g$	Ground acceleration in the horizontal direction
x^r	Floor displacement relative to the foundation system in the horizontal direction
y	Height of differential mass element above the base plate in the rest position
Z	Label of curve representing the minimum conditions for steady-state periodic motion
α	The angle between the diagonal of the rectangular block and its vertical edges
β	Ratio defined as $\beta = p/\Omega$
$\Delta A_n, \Delta B_n, \Delta \tau_n$	Disturbances for the response parameters A_n, B_n, τ_n respectively in the nth half-cycle to examine the stability of steady-state periodic motion
$\Delta_a, \Delta_b, \Delta_t$	Disturbances applied to the response parameters A_n, B_n, τ_n respectively at the zero half-cycle to examine the stability of the steady-state periodic motion
Δ_p	Displacement of point p' on the base plate in the axial direction of the bolt
δ	Restitution coefficient
δ^*	Impulsive force due to impact between the base plate and

xviii

the bolt

n Factor defined in equation (2.21)

θ Angle of rotation of equipment base relative to the floor

θ_n Angle of rotation of equipment relative to rest position during the nth half-cycle of the steady-state response

θ_0 Angle of rotation of equipment when the base plate has just touched the bolt head

λ Parameter defined in equation (4.28) to describe the disturbance to the steady-state periodic motion in the nth half-cycle

ξ Damping ratio for the equipment system

ξ_s Damping ratio for the structure to which the equipment is mounted

σ Factor defined in equation (2.26)

τ Normalized time equal to Ωt

τ_n Normalized time of the nth impact with the floor

τ_0 Phase angle for the steady-state periodic motion

ϕ Shape function for the deformation of the equipment

ϕ Phase angle

Ω Angular frequency of the harmonic excitation

Ω_r Ratio between the excitation frequency and the natural frequency of the equipment on a fixed base

ω Natural frequency of the equipment on a fixed base

ω_s Natural frequency of the structure to which the equipment is mounted

$\cdot$ First derivative with respect to time

$\cdot\cdot$ Second derivative with respect to time

CHAPTER 1

INTRODUCTION

1.1 General

Equipment can be mounted on rigid floors by placing the equipment freely on the floor without fastening, fixing it tightly to the floor, or partially fixing it. If equipment is fastened rigidly to the floor, it can be idealized as a structure which is fixed to its foundation. At the other extreme, equipment can be placed on the floor without fastening. In this case, the equipment may slide on the floor under the effect of seismic excitation if friction between the equipment base and the floor is relatively low. This behaviour is most probable for squat bodies. If the equipment is slender, the sliding response is less probable and the equipment may start to rock on its edges when the base acceleration exceeds a certain level. The amplitude of the rocking angle depends on the excitation level, the equipment geometry, and the conditions of contact between the equipment base and the floor. If the rocking angle amplitude exceeds a certain level, the equipment may overturn. During the rocking of unattached equipment, the characteristic response parameter is the angle of tilt, with the major concern being overturning. In general, the part of the lateral displacement caused by the rigid body motion is larger than that caused by the equipment's elastic deformation. Thus, to study the problem of overturning, the equipment model is often approximated as a rigid block.

1

During the rocking response, some of the system's kinetic energy is dissipated through the impact with the floor. This portion of energy lost is small for slender systems and large for squat ones.

If equipment is fastened to the floor loosely, it is able to rock without overturning. In this case, the amplitude of the rocking angle depends on how loose the system is. Also, the displacement components corresponding to the rigid body motion may be of the same order as those produced by the elastic deformation of the equipment. Hence, it becomes necessary to take into account the deformation of the system when modelling the partially fixed equipment.

The phenomena of rocking attracted the attention of researchers in the latter part of the 19th century. They attempted to define criteria for overturning of equipment and furniture inside buildings during earthquakes. Tombstones and monumental columns overturned by earthquakes had been used to estimate the peak ground acceleration of the earthquakes. Formulas were derived to calculate the ground acceleration sufficient to overturn rigid bodies. The formulas were applied in the seismological observatories to determine the peak ground acceleration during earthquakes.

Despite the availability of modern strong-motion accelerographs in many places, there are wide gaps in present-day seismic contour maps because strong earthquakes are rare and may occur in uninstrumented areas. Thus it is still desirable to make use of the information provided by the overturning of slender monument columns to estimate the ground motion intensity for the old and recent earthquakes where no instrument recordings are available.

Another reason for the study of rocking behaviour in earthquake engineering arises from observations that apparently unstable structures had survived major earthquakes after the entire structures had rocked on their base foundations. Tall petroleum towers survived major earthquakes by rocking on their foundations and stretching their anchor bolts. Several golf-ball-on-a-tee types of elevated reinforced concrete water tanks incurred minimal damage during the Chilean earthquakes of 1960 by rocking on their foundations and stretching their anchor bolts. On the other hand, more statically-stable ground-supported reinforced concrete tanks were severely damaged. These observations would suggest that making use of rocking to dissipate the kinetic energy of the systems during earthquakes may decrease the deformations of such systems, and therefore can be used to advantage in seismic design.

1.2 Literature Survey

The research work done to investigate the rocking behaviour of systems under dynamic excitation can be classified into the following four categories according to the rigidity of the rocking systems and the base condition:

a) rigid blocks rocking on rigid floors,

b) flexible systems rocking on rigid floors,

c) rigid systems rocking on flexible foundations, and

d) flexible systems rocking on flexible foundations.

In this section, the work done for each of these problems will be presented.

1.2.1 Rigid Blocks Rocking on Rigid Floors

A fundamental study of the problem was made by Housner (1963), who showed that the impact of a rocking body with a rigid floor plays a role in dissipating the kinetic energy of the system. He derived the expressions governing the free vibration of a block rocking on a rigid floor and showed that the period of free vibration depends on the rocking amplitude. Housner developed a theory to incorporate the energy lost by impact with the floor, assuming that the angular momentum of the system about the edge of impact was conserved during the impact with the floor. Assuming that the rigid block would not bounce after the impact, he defined a restitution coefficient for the angular velocity which could be expressed in terms of the geometric parameters of the rigid rectangular block. Finally, he considered the overturning of rigid blocks subjected to base excitations in the form of a rectangular pulse, a half-sine pulse and white noise excitation. An important conclusion from his study was that a scale effect exists in rocking which makes a large block more difficult to overturn by base motion than a small block, assuming that both blocks have the same aspect ratio.

Yim, Chopra and Penzien (1980) adopted a probabilistic approach and utilized the results obtained from the rocking of rigid blocks to estimate the intensity of ground shaking from its observed effects on tombstones, monumental columns and other similar objects. The study was made, using 20 different artificial earthquake records created from the same spectrum and with the same peak acceleration. They concluded that the response of a rigid block is very sensitive to small changes in its size and slenderness ratio and to the details of ground motion. No

consistent trend is apparent, i.e., the overturning potential of rigid blocks does not change monotonically with the parameters. The probability of overturning, however, shows some consistent trend.

Aslam (1980) did a theoretical and experimental analysis to study the sensitivity of the response of rigid blocks rocking on rigid floors, using harmonic and earthquake excitations. He concluded that the response is very sensitive to the contact conditions between the block and the floor. The experimental results on harmonic excitation agreed with the theoretical work for motions of low frequencies and large amplitudes. For earthquake excitation, there existed little correlation between the experimental and the calculated results, as the experimental response was not repeatable because of a limitation in the shaking table used. Parametric study showed the sensitivity of the response to the aspect ratio, the block size, and the restitution coefficient. Aslam concluded that the tendency for rigid blocks to overturn is smaller with a lower restitution coefficient, a smaller aspect ratio, and larger blocks. There were, however, exceptions for all cases.

Ogawa (1980) studied the periodic response of rigid blocks subjected to sinusoidal excitation. Using the linearized differential equations of motion, and assuming the impact with the floor to be impulsive, he derived approximate response expressions for the steady-state periodic motion. He derived the conditions of existence for the steady-state periodic motion and investigated the stability of such motion. Further, he carried out shaking table experimental work to

verify his theoretical findings.

Spanos and Koh (1984) used the linearized equations of rocking motion to derive the response equations for the steady-state periodic motion of rigid blocks under the effect of harmonic excitation. They calculated the corresponding frequency-response curves and investigated the stability of the obtained response. They also indicated that a periodic motion with non-zero mean is likely to occur. Using a trial method, they divided the frequency-acceleration domain into no-motion, safe and unsafe regions, the latter referring to the overturning of rigid blocks during the transient response stage for initially quiescent blocks.

Ishiyama (1982) suggested a criterion for the rocking and overturning of rigid blocks subjected to earthquake excitations. The criterion is based on the peak ground acceleration and velocity. He verified his theory by an analytical study, in which he used a "general motion" model for the rigid blocks that allowed sliding and jumping responses. He also defined a horizontal restitution coefficient and introduced the concept of a tangent impulse at the moment of impact. He examined cases with different restitution coefficients and concluded that the coefficient of friction between the rigid block and the ground must be greater than the breadth-height ratio so that the block can rock. Also, taking into account the peak values of both the velocity and acceleration of the ground improves the description of the ground motion which will cause overturning of the blocks.

1.2.2   Flexible Systems Rocking on Rigid Floors

Beck and Skinner (1974) examined the response of a simple model of a 200-foot high stepping pier, under earthquake excitation. They considered two states of vibration, i.e., no uplift axial oscillations and rocking vibrations. They found that if damping were not taken into account in the model, stepping with large amplitudes would occur. Introducing some structural damping would marginally reduce the stepping of the pier. When energy absorbing devices were introduced into the mathematical model, however, both the amplitude and the number of stepping cycles were decreased.

Meek (1975) developed a theory for a single degree of freedom (SDOF) system attached to a rigid foundation which is allowed to rock on the ground. He applied the theory to the analysis of the rocking of a slender building. He found that the lateral deflection of the system, relative to the base, and the base shear were considerably reduced, relative to the case of a fixed base where the base was not allowed to uplift. In the case of a squat structure, however, the decrease was not large. He concluded that the effect of rocking in reducing the structure response can be considered in structures whose heights are significantly greater than their widths.

Sexton (1976), in his discussion of Meek's paper, indicated that the reduction of frequency in the response of the rocking structure does not necessitate a decrease in the response amplitude or the state of stress.

Meek (1978) suggested a simplified model for the analysis of multi-storey buildings supported laterally by cores which are allowed to

rock on their foundations. He assumed the foundation to be rigid. The core was assumed to deform in a prescribed triangular mode. He assumed that, at the instant of impact, the vertical momentum was dissipated completely while the lateral momentum remained-unchanged. This assumption implies that the cores stop rotating after each impact. The response spectra of the cores subjected to earthquake excitation indicated that the cores with small natural frequencies did not uplift. At intermediate frequencies, the overall response was reduced by the uplift. For cores with high natural frequencies, however, the response of the cores for the uplift cases was higher than that of the cores on fixed bases. Also, slender structures showed larger reductions in the response than squat ones.

Huckelbridge (1977) performed shaking table tests on a nine-storey steel frame. The columns of the three-bay frame were allowed to uplift under the effect of strong motion in some tests and were fixed in other tests. The results showed an increase in the lateral relative displacement for the uplift cases relative to the cases of complete fixation and a redistribution of the axial forces between columns.

1.2.3 Rigid Systems Rocking on Flexible Foundations

Evison (1977) carried out experimental work to verify the natural decay of rocking motions analysed by Housner. Evison also investigated the rocking response caused by sinusoidal and earthquake excitations. He suggested an iterative method using the response spectrum of linear SDOF systems to estimate the structure's peak rocking displacement. The design approach was based on an analogy between the

viscous SDOF system and the rocking block in the rate of energy loss during the free vibration. Computer analysis indicated that a significant reduction in design accleration could be achieved when rocking was allowed on a flexible foundation but such a reduction could not be achieved with a rigid foundation.

Wolf (1976-77) used the finite element technique to study the effect of uplift on atomic reactors subjected to travelling shear waves. His results indicated that the uplift may lead to reductions in the total horizontal acceleration, the lateral displacement, and the overturning moment of the structure, compared to the results of standard soil-structure interaction in which uplift is not permitted. Accordingly, he concluded that there is no need to prevent uplift in structures.

Psycharis (1981), in his analytical work, investigated the effect of uplift on the dynamic response of both rigid and flexible superstructures. The foundation was considered to be elastic with viscous dashpots. Then, the Winkler foundation was approximated by an equivalent two-spring model. Constant soil coefficients were assumed. He set the problem in two states, the full-contact state (no-uplift) and the uplift state. In the second state, because the contact length of the base with the ground varies with time, an equivalent contact length was used in the analysis. The model was subjected to impulsive excitations. He also assumed no slipping between the base and the ground. He concluded that uplift reduces the apparent fundamental resonance frequency to a value below that of the no-uplift model and

that, of the superstructure. Uplift also decreases the critical damping of the apparent fundamental mode with the amount of uplift. However, no clear trend in the response values for the flexible system was found.

1.2.4 Flexible Systems Rocking on Flexible Foundations

Yim and Chopra (1983) studied the rocking of structures on flexible foundations. They modelled the superstructure as a SDOF system attached to a rigid mat. Two models for the foundation system were used. The first was a two-spring damper foundation. The second was the Winkler foundation. The whole system, which was prevented from sliding, had three degrees of freedom, namely, the deformation of the SDOF system, relative to the base mat, the base mat rotation, and the vertical displacement of the centre of the base mat. They eliminated the effect of the third mode (vertical displacement) on the response, however, as it was found to have a relatively high frequency. They concluded that for structures with a small natural frequency the base shear was less than the static value at incipient uplift and the foundation mat did not uplift. For structures with a high natural frequency, however, uplift took place and the base shear was reduced relative to the bonded case. As a result, they recommended that it would be desirable to permit uplift in structures.

1.3 Objectives and Scope of Research

The previously mentioned research work indicates that permitting the equipment to rock on the mounting surface may be desirable for the following reasons. Allowing the equipment to rock may be better than designing it to withstand larger overturning moments. The equipment

frames, instead of being designed as fully ductile, can be designed to remain elastic during earthquakes. This will reduce the post-earthquake repair cost relative to the case of ductile frames which may suffer large permanent deformations under some earthquakes. Thus, allowing the equipment to rock may increase the survival probability of equipment under seismic excitation.

As was indicated earlier, equipment can be mounted on the floor in one of three ways, namely, free resting, complete fixation, or partial fixation. In the case of free-resting equipment, the benefit of rocking can be achieved, but the risk of the system overturning exists. If the rocking is restrained, as in the case of partial fixation, the risk of overturning is eliminated while the benefit of rocking can still be gained. The aim of this research, is to study the overturning potential of equipment free to rock, and the effect of restrained rocking on its response. The overturning potential of unrestrained rocking of equipment will be studied under the effect of:

1. pulsive excitations (chapter 2)

2. series of pulsive excitations (critical excitations)(chapter 3)

3. harmonic excitation (chapter 4).

The response of partially fixed equipment under the effect of harmonic and earthquake excitations is studied in chapters 5 and 6. In chapter 5, the system is considered to rock with constant maximum rocking amplitudes. In chapter 6, the effects of possible yielding and failure of the restrainers are taken into account.

The main objectives of this research are to define criteria for

the overturning of equipment which is free to rock under the effects of pulsive, harmonic, and critical excitations and to investigate the effect of restrained rocking on the response of mounted equipment, when it is subjected to harmonic and earthquake excitations.

CHAPTER 2

OVERTURNING OF FREELY RESTING EQUIPMENT

BY

PULSIVE EXCITATIONS

2.1 Introduction

As was mentioned in the previous chapter, equipment can be mounted on rigid floors by placing the equipment freely on the floor without fastening, fixing—it—tightly to the floor, or partially fixing it. In Chapters 2, 3 and 4, the first case, where the equipment is free to rock on the floor, will be studied.

Equipment that is free to rock on the floor is not usually of great height because the main engineering problem in this case is the possibility of the equipment overturning under seismic excitation. When such equipment is subjected to static loads, the overturning problem can be solved by assuring that the sum of moments of the counter-acting weights about the edge of overturning is greater than the overturning moment of the applied loads. In the case of dynamic excitation, the system will overturn if its total energy (potential and kinetic) is sufficient to cause it to tilt, so that the effect of the system's weight will no longer provide a resisting moment. The problem is complicated because the build-up of energy in the system is dependent on the excitation time history and the system characteristics. If the system is rocking under the effect of periodic or earthquake excitations, the work done by the effective force is positive during

13

some time intervals and negative during others. In Chapters 2 and 3,
the problem associated with the rocking of equipment subjected to
particular types of excitation will be studied. The effective forces
considered will always exert positive work on the system. Two types of
dynamic excitation will be considered, namely pulsive excitations
(Chapter 2) and critical excitations (Chapter 3). In the case of
pulsive excitations, the base acceleration is unidirectional. Critical
excitations, however, are composed of successive pulses of alternate
direction with variable durations. These kinds of dynamic excitation
present some of the most favorable conditions for overturning. This
study will provide information on the lower bound of dynamic excitations
which will overturn equipment.

In this chapter, the minimum conditions for the overturning of
equipment free to rock on rigid floors and excited by different types of
pulsive excitation are studied. A comparison is made, whenever
applicable, with results in the existing literature.

2.2 Mathematical Modelling of Equipment Free to Rock on Rigid Floors

The following assumptions are made in this analysis. It is
assumed that the amplitudes of deformations of equipment rocking freely
on a rigid floor are much less than the amplitudes of displacements
resulting from the rigid body motion taking place. Therefore, the
equipment deformations can be ignored and the equipment can be assumed
to be a rigid body. Also, it is assumed that the system rocks without
sliding on a rigid floor. As a result, the system has only one degree
of freedom, which is denoted by θ, the angle of rotation of the system

relative to the rest position. Because the rocking of a rigid body is governed by the base width and the location of the center of gravity, the rigid block can be represented by a rigid rectangular block of width 2b and height 2h, where h is the height of the equipment mass center above the rigid floor, as shown in Fig. (2.1). The block base will be assumed to be slightly concave such that rocking takes place on only one edge of the base. Accordingly, at the instant of impact of the rocking system with the floor, the center of rotation is changed instantaneously from one edge to the other.

The differential equations of motion can be derived by using the principle of dynamic equilibrium. If the rectangular block is excited by a total floor acceleration $\ddot{x}$, as shown in Fig. (2.2), the sum of moments of all forces about the center of rotation "o" should vanish. Mathematically, this condition can be expressed as

$$M \ddot{x} R \cos(\alpha-\theta) - I_o \ddot{\theta} - W R \sin(\alpha-\theta) = 0 \qquad \theta > 0 \qquad (2.1.a)$$

where

    M is the equipment mass

    R is the distance between the center of mass and the center of rotation

    α is the angle between the diagonal of the rectangular block and its vertical edges.

    I_o is the mass moment of inertia about the center of rotation "o"

    W is the equipment weight

and the dots represent differentiation with respect to time t.
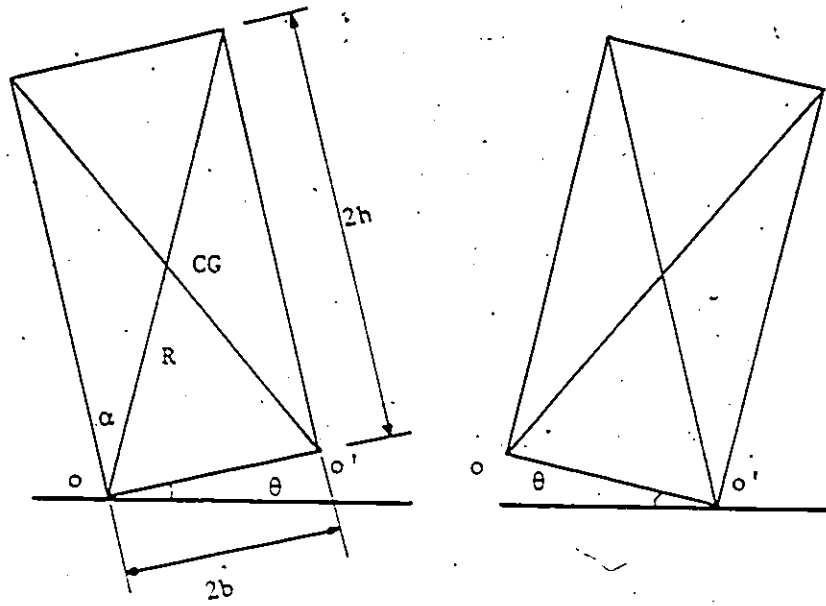
Fig. (2.1) . Block geometry
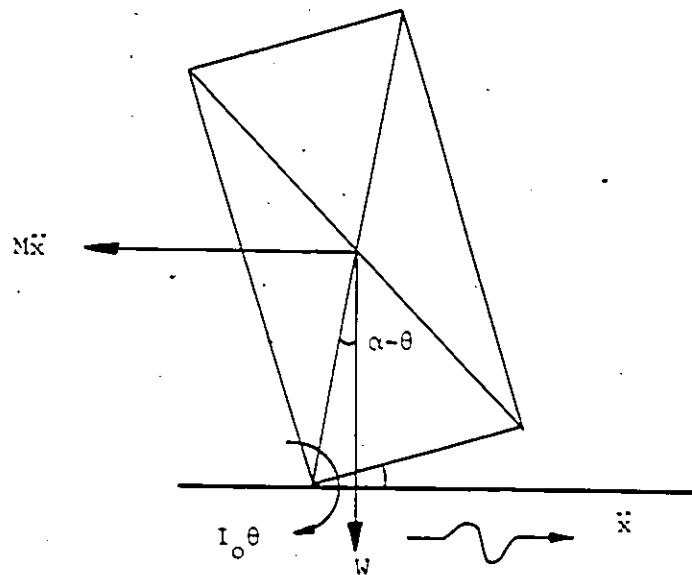
Fig. (2.2)   Forces acting on the rigid block

Equation (2.1.a) applies when the angle of rotation θ is positive, i.e. for anticlockwise rotations. If the angle of rotation is negative and the block is rocking about the edge o', the equation of motion becomes:

$$M \ddot{x} R \cos(\alpha+\theta) - I_o \ddot{\theta} + W R \sin(\alpha+\theta) = 0 \qquad \theta < 0 \qquad (2.1.b)$$

Equations (2.1.a) and (2.1.b) can be expressed and combined in the following form:

$$\ddot{\theta} = \frac{p^2}{g} \ddot{x} \cos(\theta \mp \alpha) + p^2 \sin(\theta \mp \alpha) \qquad \theta \gtrless 0 \qquad (2.1.c)$$

where
     g is the acceleration due to gravity
and
$$p^2 = W R/I_o \qquad (2.2)$$

For rectangular blocks, equation (2.2) has the following simpler form:

$$p^2 = \frac{3g}{4R} \qquad (2.3)$$

The coefficient p expressed by equation (2.3) is a measure of the block size irrespective of the aspect ratio defined by the angle α. Large values of p correspond to blocks with small sizes.

When the block is at rest and is then subjected to a base acceleration, it will not rock until the overturning moment about one of the base edges exceeds the weight resisting moment. This condition may be expressed as follows:

$$\left| M \ddot{x} h \right| > W b$$

which can be reduced to the form:

$$|\ddot{x}| > g \tan(\alpha) \qquad (2.4)$$

If the rigid block is slender, it is possible to approximate the trigonometric functions in the equations of motion as follows:

$$\sin(\theta \mp \alpha) = \theta \mp \alpha$$

$$\cos(\theta \mp \alpha) = 1 \qquad (2.5)$$

These approximations will linearize the differential equation (2.1.c), which takes the form:

$$\ddot{\theta} - p^2 \theta = \frac{p^2}{g} \ddot{x} \mp p^2 \alpha \qquad \theta \gtrless 0 \qquad (2.6)$$

Equation (2.6) was derived by Housner (1963). Although equation (2.6) is linear, the change of the differential equation governing the system after each impact with the floor is one of the main sources of nonlinearity.

In this study, it is assumed that the impact of the block with the floor is completely plastic and bouncing does not happen after the impact. At the instant of impact with the floor, some of the kinetic energy of the system is lost and the angular velocity of the system is reduced according to the relation:

$$\dot{\theta}_2 = \delta \dot{\theta}_1 \qquad (2.7)$$

where

$\dot{\theta}_1$ and $\dot{\theta}_2$ are the angular velocities of the system just before and just after the impact respectively

δ is a fraction which is less than unity, defined as the coefficient of restitution.

The coefficient of restitution can be determined either analytically (Housner,1963) or experimentally (Evison,1977). Housner (1963) derived an expression for δ, assuming that during the impact with the floor, the angular momentum of the rocking system about the edge of impact is conserved. Conservation of the angular momentum is expressed as

$$I_o \, \dot{\theta}_2 = I_o \, \dot{\theta}_1 - 2 \, MR^2 \, \dot{\theta}_1 \, \sin^2(\alpha) \qquad (2.8)$$

When equation (2.7) is substituted into equation (2.8), the coefficient of restitution can be expressed as follows:

$$\delta = 1 - \frac{2MR^2 \sin^2(\alpha)}{I_o} \qquad (2.9)$$

In the following sections, the overturning of the rigid block caused by pulsive excitation is considered. This represents the simplest type of dynamic excitation and there is no rocking of the block in this case.

2.3 Overturning of Rigid Blocks Subjected to Pulsive Excitations

2.3.1 Type 1-Triangular Pulse with Decreasing Intensity

Figure (2.3.a) illustrates a single decreasing triangular pulse with maximum intensity at the beginning of the pulse. The maximum intensity of the pulse is greater than the minimum value specified in equation (2.4) to cause the tilting of the block. The base acceleration at time t can be expressed as

$$\ddot{x} = a - at/t_1 \qquad (2.10)$$

where

t_1 is the pulse duration

and

     a   is the peak base acceleration

The linearized differential equation (2.6) is now expressed as:

$$\ddot{\theta} - p^2\theta = \frac{p^2}{g} a(1 - t/t_1) - p^2 \alpha \qquad (2.11)$$

Subjected to the initial conditions:

$$\text{At } t = 0, \qquad \theta(0) = 0 \quad \text{and} \quad \dot{\theta}(0) = 0 \qquad (2.12)$$

the response of the system is given by the following equation:

$$\theta(t) = (-\alpha + \frac{a}{g}) \cosh(pt) - \frac{a}{gpt_1} \sinh(pt) + \alpha - \frac{a}{g} (1 - \frac{t}{t_1})$$

$$(2.13)$$

The effective force $M\ddot{x}$ will exert work on the rocking system until the end of the pulse at time t_1. At the end of the pulse, the total work done is just sufficient to let the system overturn. In other words, the work done is equal to the potential energy of a system which is moved such that the center of mass is just above the center of rotation. Mathematically, this condition of overturning is expressed as

$$\int_0^{t_1} M \ddot{x} h \dot{\theta} \, dt = W R (1 - \cos\alpha) \qquad (2.14)$$

When equation (2.13) is differentiated, and is substituted, together with equation (2.10), into equation (2.14), and the integration is calculated, the following equation results:

$$\frac{Wha\alpha}{g} \left[p(k-1) \quad \frac{\sinh(pt_1)}{p^2 t_1} - \frac{1}{p} + \frac{K}{2} + \frac{K}{t_1} \quad \frac{-\cosh(pt_1)}{p^2 t_1} - \frac{1}{p^2 t_1} \right] = \frac{WR\alpha^2}{2}$$

$$(2.15)$$

where $\quad K = \dfrac{a}{g\alpha}$

Equation (2.15) can be rearranged to the following form:

$$c_2 K^2 - c_1 K - 1 = 0 \qquad (2.16)$$

where

$$c_1 = 2 \sinh(pt_1)/(pt_1) - 2 \quad .$$

and

$$c_2 = \frac{2 \sinh(pt_1)}{pt_1} + \frac{2 - 2 \cosh(pt_1)}{p^2 t_1^2} - 1 \quad .$$

Equation (2.16) is a second order algebraic equation which can be solved to give two values for K as follows:

$$K = \frac{c_1 \pm \left[c_1^2 + 4 c_2 \right]^{1/2}}{2 c_2} \qquad (2.17)$$

Numerical values indicate that one of the roots given by equation (2.17) is positive, while the other is negative. The positive root relates the peak base acceleration "a" to the pulse duration t_1.

2.3.2 Type 2-Triangular Pulse with Increasing Intensity

Figure (2.3.b) shows a single triangular pulse with zero intensity at the beginning and with intensity increasing linearly to a maximum base acceleration "a" at time t_1. The block will remain at rest until the base acceleration has the value $g.\tan(\alpha)$ at time t_1, where

$$t_i = g \tan(\alpha) \, t_1/a$$

For slender blocks, α is small and the above expression can be simplified to

$$t_i = g \, \alpha \, t_1/a$$

For simplicity, the time origin, for the purpose of analysis, will be shifted such that at $t=0$, $\ddot{x}(0)=g\alpha$. With the new time origin, the base acceleration can be expressed as

$$\ddot{x} = g\alpha + a \, t/t_1 \tag{2.18}$$

When equation (2.18) is substituted into the differential equation of motion (2.6), it takes the form:

$$\ddot{\theta} - p^2\theta = \frac{p^2 a}{g} \left[\frac{t}{t_1} + \frac{1}{K} \right] - p^2 \, \alpha \tag{2.19}$$

The general solution of equation (2.19), with initial conditions of zero rotation and zero angular velocity, is given by:

$$\theta(t) = \frac{a}{g} \left[\frac{\sinh(pt_1)}{pt_1} - \frac{t}{t_1} \right] \tag{2.20}$$

The overturning condition of the block, caused by the pulsive excitation, is the same condition described earlier in section (2.3.1). The total work done by the effective force at the pulse end should be equal to the potential energy of the rigid block at a tilting angle θ equal to α, which can be expressed as

$$\int_0^{\eta t_1} M \ddot{x} \, h \, \dot{\theta} \, dt = W R \, (1 - \cos\alpha) \tag{2.21}$$

where η is equal to $(1 - 1/K)$.

When the integration of equation (2.21) is calculated and the resulting

equation is simplified, the following condition is obtained:

$$- \eta t_i \left[\frac{\eta}{2} + \frac{1}{K} \right] + \frac{\sinh(\eta p t_1)}{p} - \frac{\cosh(\eta p t_1)}{p^2 t_1} + \frac{1}{p^2 t_1} = 0 \qquad (2.22)$$

If the angle α is assumed to be small, equation (2.22) can be reduced to:

$$2 p t_1 \sinh(\eta p t_1) - 2 \cosh(\eta p t_1) - p^2 t_1^2 + 2 = 0 \qquad (2.23)$$

Equation (2.23) relates the acceleration term η to the duration term $p t_1$. It is a nonlinear algebraic equation and it can be solved numerically at discrete values of $p t_1$.

2.3.3 Half-Sine Pulse

Using the same technique described in sections (2.3.1) and (2.3.2), the analysis of overturning for the rigid block caused by the half-sine pulse shown in Fig. (2.3.c) is carried out. The base acceleration is expressed as

$$\ddot{x} = a \sin \pi(t/t_1 + \phi) \qquad (2.24)$$

where $\phi = (1/\pi) \sin^{-1}(1/K)$

which will ensure that $\ddot{x}(0) = g\alpha$. The differential equation of motion (2.6), subjected to the initial conditions (2.12), has the following solution:

$$\theta(t) = \alpha(J-1) \cosh(pt) + \frac{\alpha K J \pi}{p t_1} \cos(\pi\phi) \sinh(pt) + \alpha \left[1 - K J \sin \pi(\frac{t}{t_1} + \phi) \right]$$

$$(2.25)$$

Fig. (2.3.a)
Triangular pulse, type 1
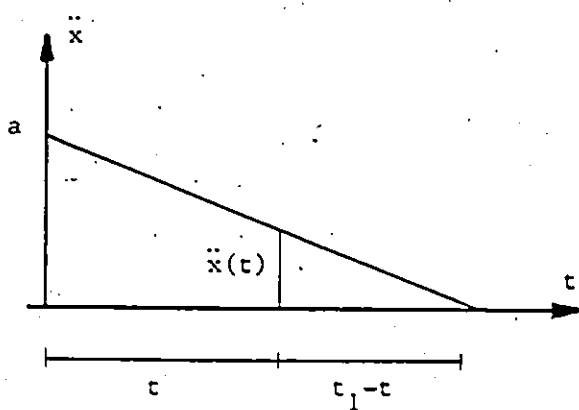
Fig. (2.3.b)
Triangular pulse, type 2
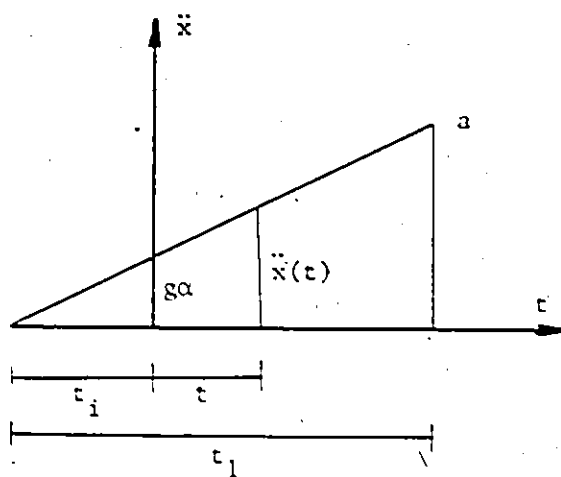
Fig. (2.3.c)
Half-sine pulse
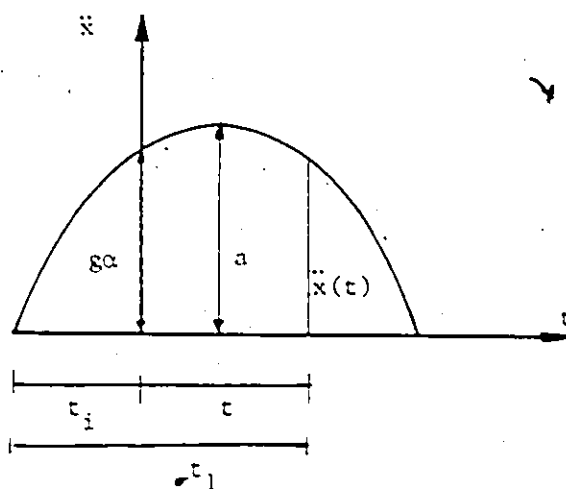
Fig. (2.3) Pulsive excitations

where
$$J = \frac{p^2 t_1^2}{\pi^2 + p^2 t_1^2}$$

The same overturning condition can be written as

$$\int_0^{\sigma t_1} M \times h \, \bar{\dot{\theta}} \, dt = W R (1 - \cos\alpha) \qquad (2.26)$$

where $\sigma = 1 - \phi$

When the integration of equation (2.26) is calculated and the resulting equation is simplified, the following equation is obtained:

$$B_1 \, I_1 + B_2 \, I_2 - \alpha K \, I_3 = \frac{g}{aJ} [\sec(\alpha) - 1] \qquad (2.27)$$

where

$$B_1 = \alpha(J-1)$$

$$B_2 = \alpha K J \pi \cos(\pi\phi)/(pt_1)$$

$$I_1 = \frac{\pi}{pt_1} \sinh(\sigma pt_1) - \frac{1}{K}$$

$$I_2 = \frac{\pi}{pt_1^2} [\cosh(\sigma pt_1) + \cos(\pi\phi)]$$

and

$$I_3 = -\frac{1}{4} [1 - \cos(2\pi\phi)]$$

Equation (2.27) represents the overturning condition. It relates the acceleration terms K and σ to the duration term pt_1.

2.4 Numerical Results

Equations (2.17), (2.23), and (2.27) express K, the maximum base acceleration normalized to gα in terms of the pulse duration pt_1, either explicitly like equation (2.17) or implicitly like equations (2.23) and

(2.27). The implicit equations are solved numerically at discrete values of the pulse duration variable pt_1, ranging from 0.01 to 10.0, using the Regula Falsi iteration method. Figure (2.4) shows the relations derived for the three cases considered. Also, the cases of the rectangular and half-sine pulses, analysed by Housner (1963), are shown for comparison. It should be noted that the half-sine pulse overturning condition described by equation (2.27) is different from that used by Housner. The overturning condition used here implies that when the pulse ends, the block has not yet overturned, but θ continues to increase until overturning occurs. Theoretically, it takes infinite time before θ is equal to α, when all the kinetic energy of the block is turned to potential energy. Under a different assumption, Housner imposed a condition that forces the block to overturn at the end of the half-sine pulse at time t_1. In other words, the angle of rotation θ reaches a value of α at time t_1. Obviously, to attain this requirement, a larger acceleration is required for the same duration t_1, as is evident from Fig. (2.4). To rate the severity of excitations, excluding Housner's half-sine pulse, the other cases can be arranged in a descending order as follows:

1. rectangular pulse,

2. half-sine pulse,

3. triangular pulse with maximum acceleration at the beginning, and

4. triangular pulse with zero acceleration at the beginning.

For a given pulse duration, the rectangular pulse requires the least peak acceleration value to cause overturning. Figure (2.4) shows that for short durations, very large acceleration values are required to
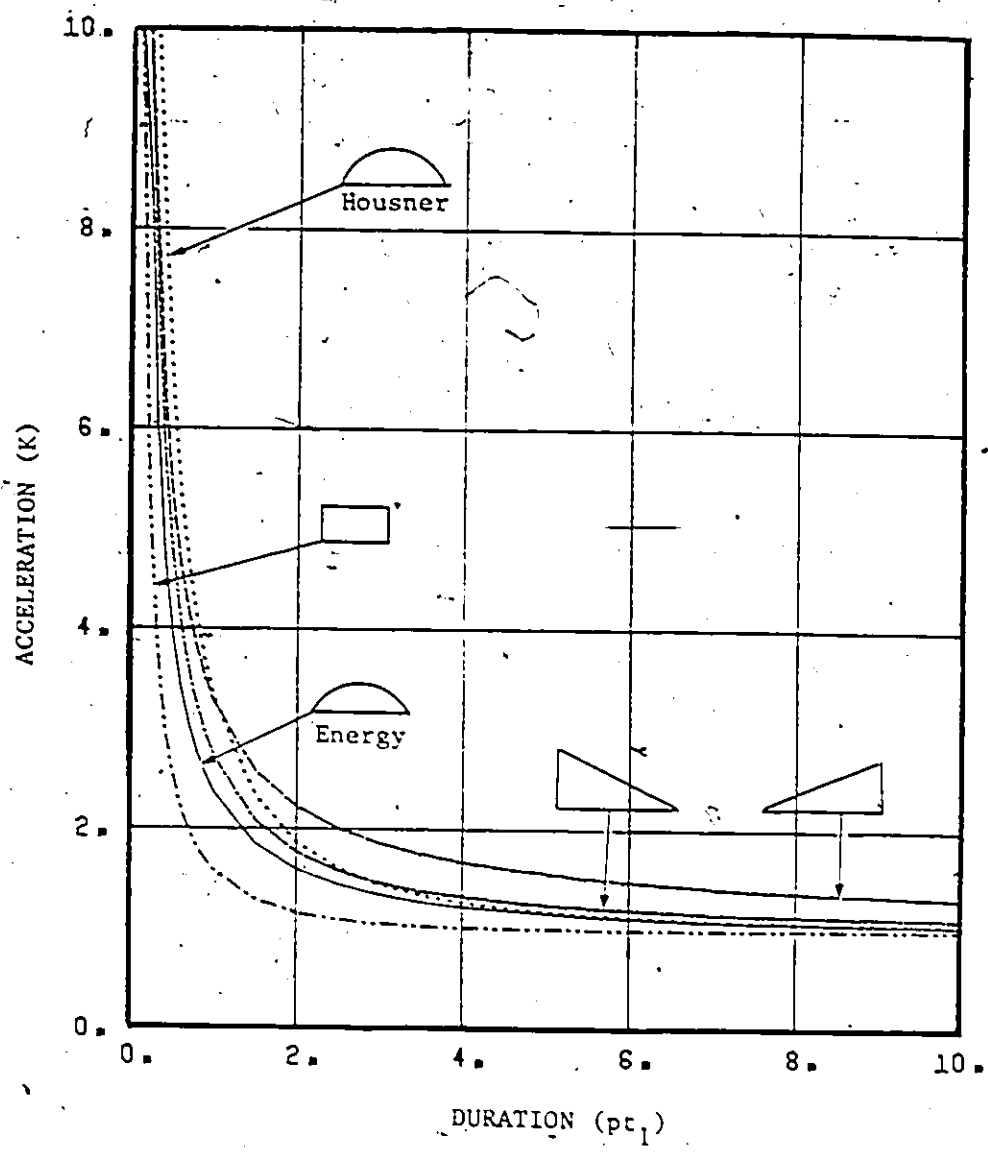
Fig. (2.4)   Peak acceleration of pulsive excitations versus the overturning pulse duration

overturn the block. The normalized acceleration K has nearly constant values for durations larger than 4/p and asymptotically approaches unity.

For durations less than 0.1/p the pulses can be approximated by impulses. The area of the impulse base acceleration-time diagram can be expressed as.

$$\text{Impulse} = \frac{p}{g\alpha} \int_0^{t_1} \ddot{x} \, dt \qquad (2.28)$$

Table (2.1) shows the impulse associated with each shape of pulsive excitation at short durations calculated by equation (2.28). It can be proved (Appendix A) that the limit of the normalized impulse values, when the durations approach zero, is unity. Also, it should be noted that, in calculating the areas of the base acceleration-duration diagrams, the area of the part located before the block starts to move was included.

As was mentioned earlier, the blocks will overturn after an infinite time under the excitations which will satisfy the derived formulas. If at a specified duration pt_1, two values of the acceleration K are chosen, such that one is slightly higher and the other is slightly lower than the theoretical critical value, the block will overturn in a finite time under the first choice of K and will just rock under the second choice. This will provide a verification for the curves shown in Fig. (2.4). To verify the curves, therefore, a pulse duration pt_1 is chosen and the corresponding theoretical maximum base acceleration is calculated. Two values of acceleration, one higher and the other lower than the theoretical value, are applied to a rigid

Table (2.1)

Normalized Impulses

Duration	Normalized Impulse (kpt_1)		
(pt_1)	Half-sine	Triangular-1	Triangular-2
0.05	1.07	1.01	1.03
0.06	1.07	1.02	1.03
0.07	1.08	1.02	1.05
0.08	1.09	1.02	1.05
0.09	1.09	1.02	1.05
0.1	1.1	1.03	1.06

rectangular block with the following properties:

$2b = 500$ mm

$2h = 1200$ mm

$R = 650$ mm

$p \cdot = 3.364$ sec.^{-1}

$\alpha = 0.3948$ rad

$\delta = 0.778$

Figures (2.5) to (2.7) present the response time histories for each of the three pulse shapes considered. The coordinates represent the angle of rotation of the rigid block normalized to α. The data for each case and the corresponding response are summarized in table (2.2). It is shown that the trial values verify well with the theoretical values of acceleration. Also, the time histories presented in Figs. (2.5) to (2.7) indicate that the rocking of the rigid block is sensitive to small changes in the input parameter K. The small differences between the trial acceleration values and the theoretical values lead the block to overturn quickly in one case and rock with a maximum angle of rotation equal to 0.8α in another. In other words, an acceleration below the critical value by less than 1 % results in a decrease of about 20 % in the angle of rotation.
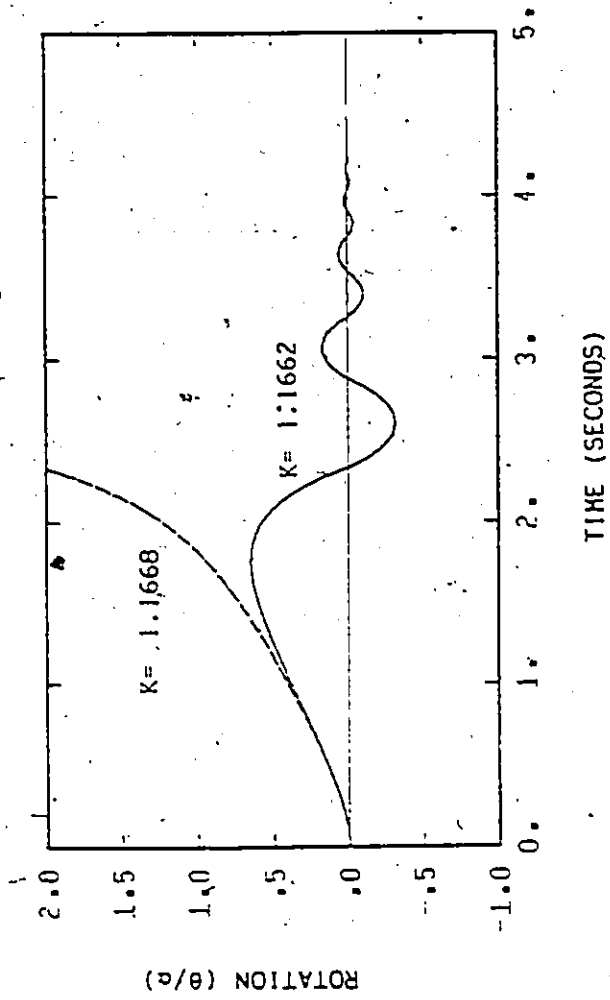
Fig. (2.5)   Response to decreasing triangular pulse (pt₁=7.0)
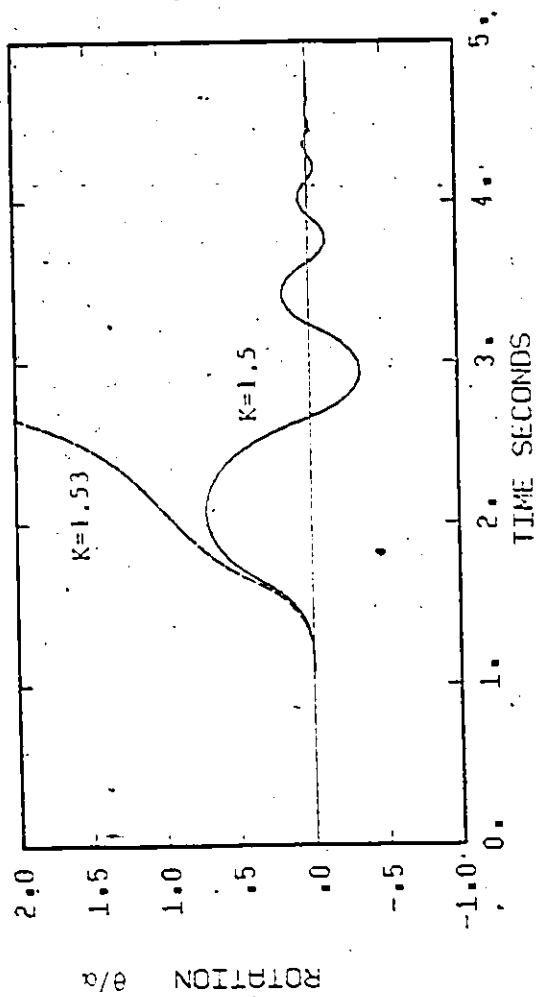
Fig. (2.6)   Response to increasing triangular pulse ($pt_j=5.5$)
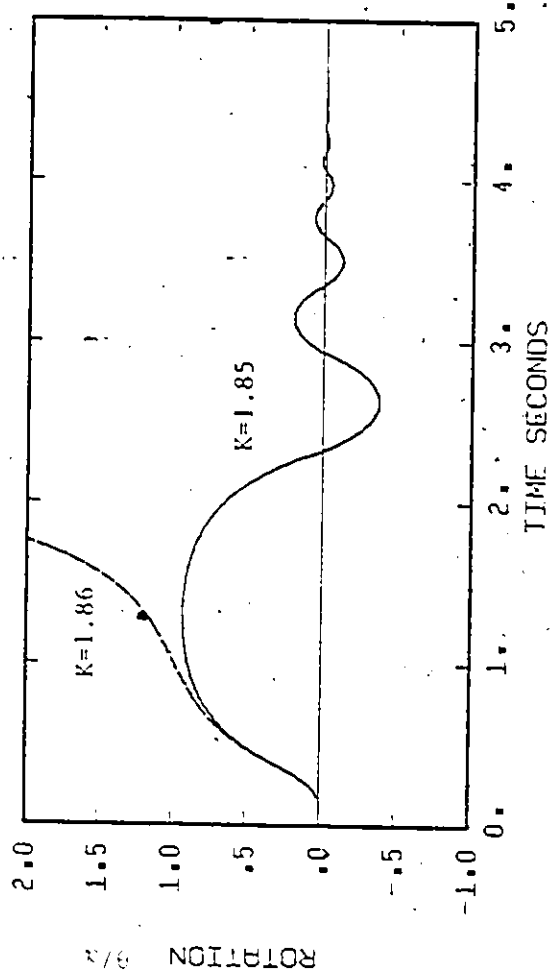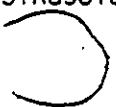
Fig. (2.7)   Response to half-sin pulse (pt₁=1.48)

Table (2.2)

Pulsive Excitations

Overturning Acceleration

Theoretical versus Trial Values

Type of Pulse	Acceleration K			Duration pt_1
	Theoretical values	Lower values	Upper values	
Triangular-1	1.1664	1.1662 Rocking	1.1668 Overturning	7.
Triangular-2	1.52	1.5 Rocking	1.53 Overturning	5.5
Sinusoid	1.855 (energy)	1.85 Rocking	1.86 Overturning	1.48
	2.32 (Housner)			

CHAPTER 3

OVERTURNING OF RIGID BLOCKS

SUBJECTED TO

CRITICAL EXCITATIONS

3.1 Introduction

In the previous chapter, a single pulse was used as the source of excitation and the conditions under which such a pulse will overturn the rigid block were studied. In this chapter, the conditions for overturning are studied when the rigid block is excited by successive pulses of alternate directions. These successive pulses are selected to represent the most severe pulse excitation with regard to the overturning of the rigid block.

If the rigid block is excited by base acceleration, it will not start to tilt until the base acceleration exceeds the minimum value equal to g.tan(α). After the threshold of the base acceleration is exceeded, the rigid block rocks and the amplitude of the angle of rotation may increase or decrease, depending on the excitation time history. If the base acceleration reverses its direction at the instant the angular velocity of the rigid block reverses its sign, energy will continue to be fed into the system. Therefore, the amplitude of the rocking angle will tend to grow rapidly until the block overturns. This type of base excitation will constitute the most critical oscillatory motion to cause the block to overturn.

A rigid block can be overturned by such a critical excitation,

35

which may have a peak acceleration less than g.tan(α), if the rigid block is given an initial angle of tilt θ_1. From the physical point of view, the motion will be amplified when the rate of energy supply to the system exceeds the rate of energy dissipation caused by impact with the floor. For such a condition to exist, a suitable combination of the restitution coefficient δ, the initial angle θ_1 and the normalized acceleration amplitude K is required. The conditions that govern these combinations are derived mathematically for two cases of critical alternate pulsive excitation, namely:

1. rectangular shaped pulses, and

2. triangular shaped pulses.

3.2 Critical Excitation Consisting of Alternate Rectangular Pulses

In this section, the conditions required to overturn the block, when it is subjected to a critical excitation composed of a series of rectangular pulses, are studied. As indicated in the previous section, the base acceleration changes its direction at the instant the angular velocity of the rocking block changes its sign. This implies that the duration of each base acceleration pulse corresponds to a half-cycle of the rocking response of the rigid block. Within each half-cycle of the response, the base acceleration remains constant and the angle of rotation has two peaks, one at the beginning and the other at the end of the half-cycle, as shown in Fig. (3.1.a).

Consider the typical time interval shown in Fig. (3.1.b) which corresponds to one half-cycle of the rocking response. The base acceleration has a constant value "-a". The block starts motion with
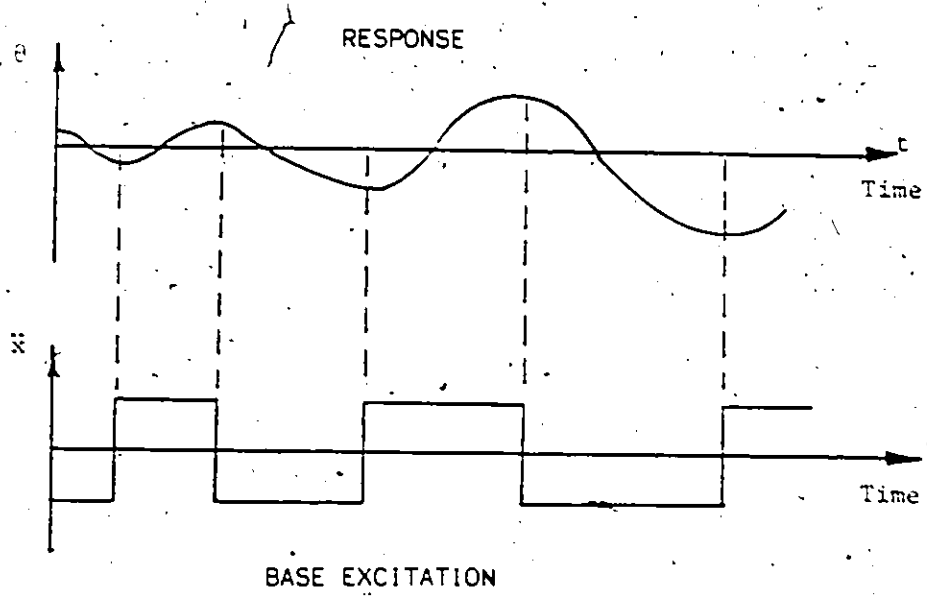
Fig. (3.1.a) Critical rectangular excitation

38
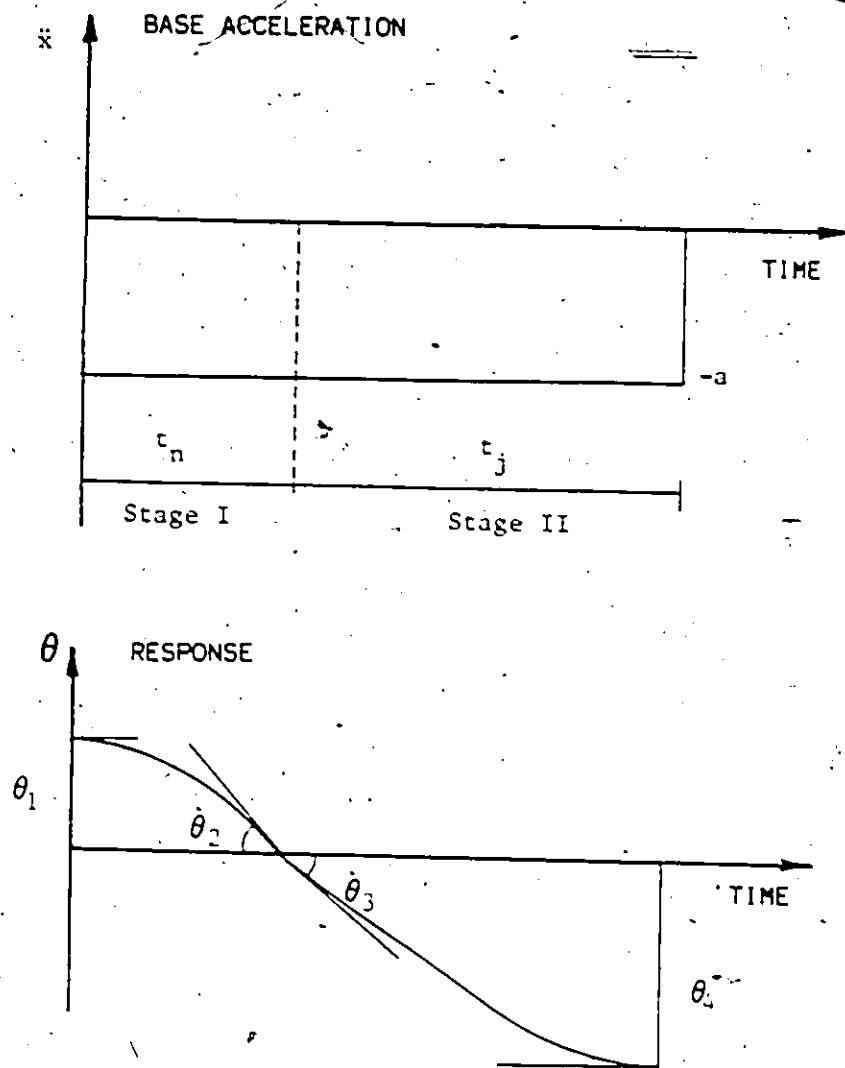
Fig. (3.1.b) Critical rectangular excitation
(half-cycle)

zero angular velocity and with an initial angle of rotation θ_1. The rigid block moves under the force of gravity and the effective force. The angle θ decreases under these forces until the impact with the floor occurs. Then the angle of rotation changes sign while the angular velocity has the same sign. The angle of rotation then increases in the reverse direction until it attains a maximum value θ_4. If $|\theta_4|$ is greater than $|\theta_1|$, then the response amplitude has increased within this half-cycle. With the response growing in each half-cycle, it will ultimately result in the block overturning. Therefore, the problem of overturning in the limit reduces to the condition $(\theta_4 = -\theta_1)$. To arrive at the limiting condition for overturning, the problem is divided into two stages, before and after the impact respectively. The equations of motion of the two stages are solved consecutively. The final conditions of motion at the first stage are considered the initial conditions of motion for the second stage. A comparison of the states of motion at the beginning of the first stage and at the end of the second stage provides a relation between the acceleration "a", the restitution coefficient δ and the initial and final angles of rotation θ_1 and θ_4. The condition of $(\theta_4 = -\theta_1)$ will give the threshold of excitation which will overturn the block.

3.2.1 Derivation

Stage 1

The equation of motion of a rigid block excited by a base acceleration $\ddot{x} = -a$, for a positive angle of rotation, is obtained from equation (2.6) as follows:

$$\ddot{\theta} - p^2\theta = - p^2\alpha \ (\ 1 + K \ ) \qquad \theta > 0 \qquad (3.1)$$

The general solution of the above differential equation, subjected to the initial conditions at t=0 ,

$$\theta(0) = \hat{\theta}_1 \qquad , \qquad \dot{\theta}(0) = 0 \qquad (3.2)$$

can be expressed as

$$v(t) = [\ v_1 - (1+K) \ ] \cosh(pt) + (1+K) \qquad (3.3)$$

where

$$v = \theta/\alpha$$

and

$$v_i = \theta_i/\alpha \qquad , \ i=1, \ 2, \ \ldots$$

The angular velocity of the block during this stage is given by:

$$\dot{v}(t) = p [\ v_1 - (1+K) \ ] \sinh(pt) \qquad (3.4)$$

Stage 1 ends at the instant of impact, at time t_n, which can be determined by setting v=0 in equation (3.3). Thus, the time of impact t_n is found to satisfy:

$$\cosh(pt_n) = \frac{1}{1-f} \qquad (3.5)$$

where

$$\bar{f} = \frac{v_1}{1+K}$$

The angular velocity just before impact, $\dot{v}_2$, is obtained by substituting the value of pt_n given by equation (3.5), in the angular velocity expression (3.4), namely,

$$\dot{v}_2 = \dot{v}(t_n) = - p \ (1+K) \ [f(2-f)]^{1/2} \qquad (3.6)$$

Stage II

This stage starts just after the impact of the block with the floor. The angular velocity of the block just after impact, $\dot{v}_3$, is

related to that just before impact, $\dot{v}_2$, by equation (2.7), giving:

$$\dot{v}_3 = \dot{v}(0) = -\delta p(1+K) \left[f(2-f)\right]^{1/2} \qquad (3.7.a)$$

The initial angle of rotation for this stage is zero, namely,

$$v(0)=0 \qquad (3.7.b)$$

The response of the rigid block in stage II should satisfy the differential equation (2.6) with negative angle of rotation θ. When $(\ddot{x}=-a)$ is substituted into equation (2.6), the following results:

$$\ddot{\theta} - p^2\theta = -p^2\alpha\ (-1 + K\ ) \qquad \theta<0 \qquad (3.8)$$

The general solution of equation (3.8), subjected to the initial conditions given by equations (3.7), becomes:

$$v(t) = (1-K)\ [\cosh(pt) - 1] + \frac{\dot{v}_3}{p}\ \sinh(pt) \qquad (3.9)$$

and the angular velocity at stage II is given by:

$$\dot{v}(t) = p(1-K)\ \sinh(pt) + \dot{v}_3\cosh(pt) \qquad (3.10)$$

At the end of stage II, $t=t_j$, the displacement is maximum while the angular velocity is zero. Mathematically, this is expressed as

$$\dot{v}(t_j) = 0$$

$$v(t_j) = v_4 \qquad (3.11)$$

The time t_j of zero angular velocity is obtained by equating the velocity in equation (3.10) to zero, giving:

$$\tanh(pt_j) = -\frac{\dot{v}_3}{p(1-K)} \qquad (3.12)$$

Equation (3.12) has a solution only if the following inequality is satisfied:

$$0 < \tanh(pt_j) < 1 \qquad (3.13)$$

If the inequality (3.13) is satisfied, the angle of rotation reaches a peak value at the instant of zero angular velocity. If expression (3.13) is not satisfied, the angle of rotation will not have a peak and will continue to grow until the block overturns. The value of $\tanh(pt_j)$ is always greater than zero because the expression given by equation (3.12) is always positive for values of K less than unity. The upper limit of the inequality is analysed by substituting expressions (3.12) and (3.7) into expression (3.13), and solving for K. The following equation results:

$$K = (1+\delta^2 v_1) - \delta (4v_1 + \delta^2 v_1^2 - v_1^2)^{1/2} \qquad (3.14)$$

Equation (3.14) defines the upper limit beyond which the angle of rotation continues to grow without a sign change in the angular velocity. In the following, the case for which equation (3.12) has a solution is considered.

The angle of rotation v_4, at the end of stage II, is obtained by substituting the time expression (3.12) of t_j into the response equation (3.9). The result, after simplification, is written as

$$v_4 = (K-1) \left\{ 1 - \left[1 - \tanh^2(pt_j) \right]^{1/2} \right\} \qquad (3.15)$$

Equation (3.15) can be expressed in terms of the initial angle v_1, using expressions (3.12) and (3.7), giving:

$$v_4^2 + 2 v_4(1-K) = - 2 \delta^2 v_1 (1+K) + \delta^2 v_1^2 \qquad (3.16)$$

If the initial angle of rotation v_1 is assumed to be amplified by a factor r, such that:

$$v_4 = r \ v_1 \qquad , \qquad r < 0 \qquad (3.17)$$

then equation (3.16) becomes:

$$r^2 v_1^2 + 2 \ r \ v_1(1-K) = - 2 \ \delta^2 v_1 \ (1+K) + \delta^2 v_1^2 \qquad (3.18)$$

Solving equation (3.18) for K gives:

$$K = \frac{1}{\delta^2 - r} \left[\frac{v_1(\delta^2 - r^2)}{2} - (r - \delta^2) \right] \qquad (3.19)$$

A special case is the one of periodic motion which is obtained by substituting (r=-1) into equation (3.19), giving:

$$K = \frac{1-\delta^2}{1+\delta^2} \left[1 - \frac{v_1}{2} \right] \qquad (3.20)$$

Equation (3.18) can also be solved for r, giving:

$$r = \frac{K-1}{v_1} + \left[\frac{(1-K)^2}{v_1^2} - \delta^2 \frac{(2-f)}{f} \right]^{1/2} \qquad (3.21)$$

Equation (3.21) implies that, for a given set of normalized base acceleration K, restitution coefficient δ and normalized initial angle v_1, an amplification factor r can be found relating the response amplitudes at the beginning and end of the half-cycle. If the absolute value of r is greater than unity, the amplitude of the angle of rotation increases. If it is less than unity, the response amplitude decreases. A critical value for r equal to (-1) indicates that the response is in a steady-state periodic motion. Alternatively, equation (3.19) gives the

acceleration amplitude K necessary to amplify the angle of rotation r times within a half-cycle. The value of acceleration K obtained from equation (3.20) causes the system to vibrate with a constant amplitude.

It should be noted that neither the response period nor the pulse duration is an independent parameter. The duration of a half-cycle, which will be denoted by T/2, is the sum of the intervals of stages I and II described in equations (3.5) and (3.12), respectively. Thus,

$$pT/2 = pt_n + pt_j$$

$$= \cosh^{-1}(\frac{1}{1-f}) + \tanh^{-1}(\frac{\dot{v}_3}{p(K-1)})$$

$$= pT/2 \ \{v_1, K, \delta\}$$

or

$$= pT/2 \ \{v_1, r, \delta\} \qquad\qquad (3.22)$$

as K and r are related by equation (3.19). There is also a phase angle between the excitation and the response, which is given by:

$$\phi = \frac{2\pi}{T}t_n = \frac{2\pi}{pT}\cosh^{-1}\frac{1}{1-f} \qquad\qquad (3.23)$$

The period calculated by equation (3.22) is dependent on the response amplitude v_1. It increases as v_1 increases. Therefore, to overturn a block using an alternate pulse excitation, the duration of the pulses must increase gradually as the response grows.

3.2.2 Numerical Results

The relationship between the normalized amplitude K of the critical acceleration and the normalized amplitude v_1 of the steady-state periodic motion, as expressed by equation (3.20), is shown in Fig.

(3.2). The figure shows that for a constant restitution coefficient δ, the acceleration amplitude decreases as the response amplitude increases. Within a half-cycle, the work done by the effective force can be expressed by:

$$Work = \int_0^{T/2} Mxh\ddot{\theta}\ dt$$

At the steady-state response, this work is equal to the energy dissipated by the impact with the floor. For a fixed value of the work required to sustain steady-state vibration, a larger value of $\dot{\theta}$ implies a smaller value of $\bar{x}$, as evident from the "work done" expression. As the amplitude v_1 increases, the angular velocity $\dot{\theta}$, also increases. This explains the relationship between the acceleration amplitude K and the response amplitude shown in Fig. (3.2). The limit of applicability defined by equation (3.14) is also shown in the same figure. Beyond that limit, the response will continue to grow without sign change in the angular velocity.

Figure (3.3) shows the variation of the normalized acceleration amplitude K with the restitution coefficient δ, for a given response amplitude and for an amplification factor r equal to (-1). It shows that lower values of δ require higher accelerations to sustain steady-state response. This is a direct consequence of the fact that low restitution coefficients imply high rates of energy dissipation during impact.

Figure (3.4) shows the variation of the amplification factor r with the normalized initial angle v_1. The coefficient of restitution δ
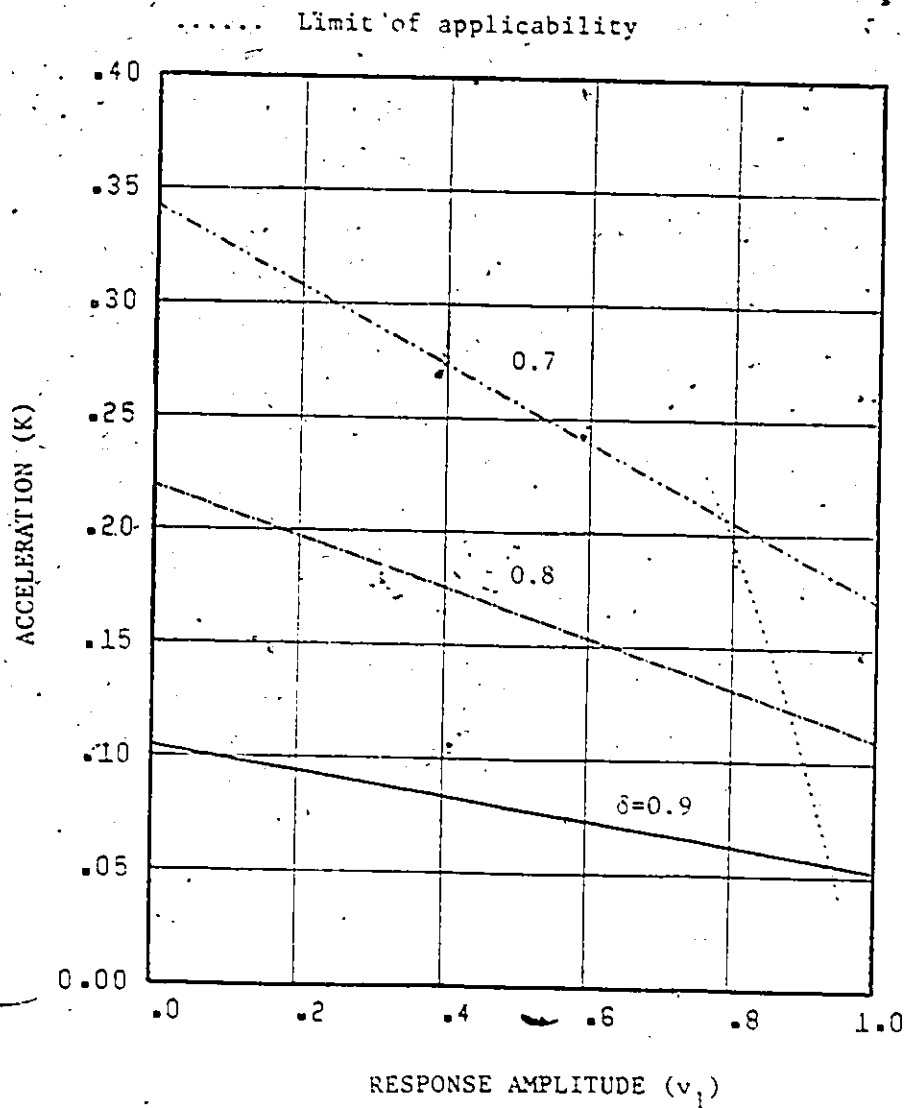
Fig. (3.2)   Critical rectangular acceleration K for steady-state response amplitude v_1
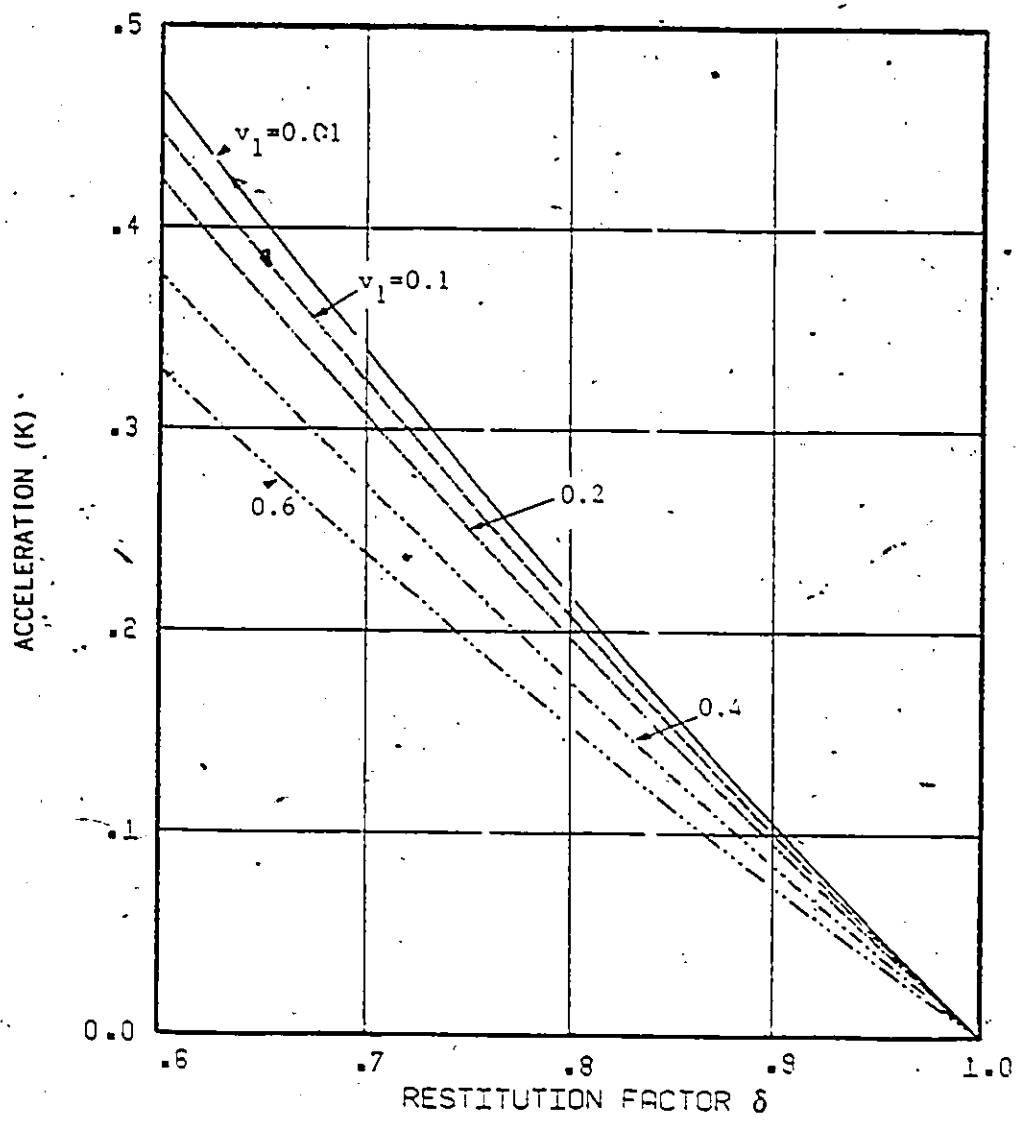
Fig. (3.3) Critical rectangular acceleration K for steady-state
response versus the restitution factor δ
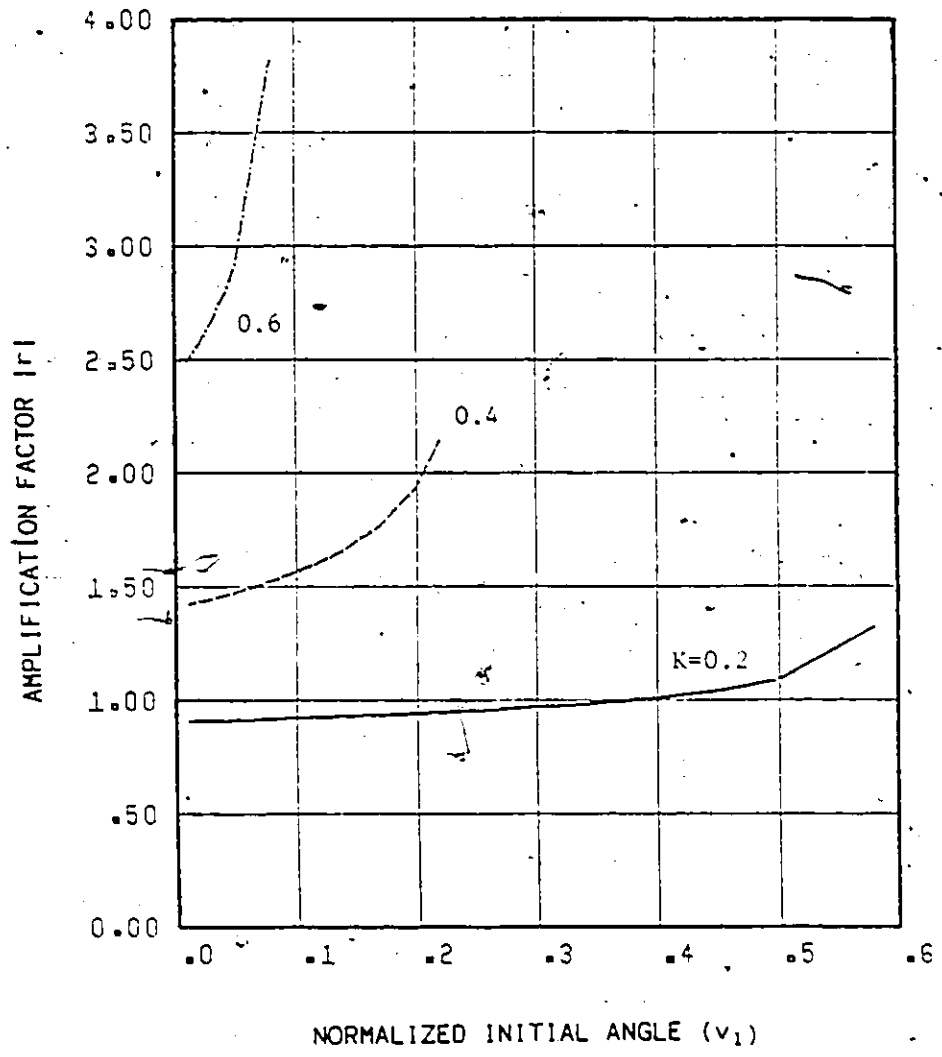
Fig. (3.4)   Aamplification factor r versus the normalized
initial angle v_1 (δ=0.778)

is taken to be equal to 0.778 and different values of acceleration amplitude are used. The results reaffirms that when $|r| > 1$, there are destabilizing consequences. With $|r| > 1$, the amplitude of the subsequent half-cycle of the response will be amplified by $|r|$. This amplified half-cycle response will in turn be amplified by a larger value of $|r|$, since $|r|$ is an increasing variable with v_1. Therefore, the system response will grow rapidly and will lead to the block overturning in a short time.

Figure (3.5) presents the variation of the normalized critical-acceleration amplitude with the normalized initial angle v_1 for different values of the amplification factor r. The envelope given by equation (3.14) is also shown in the same figure. It defines the limit of applicability of equation (3.19). Figure (3.5) shows that the acceleration amplitude K changes more rapidly with the response amplitude v_1 as the amplification factor increases.

To verify the theoretical results, numerical tests were carried out on the response of a rigid rectangular block of size 0.5 m by 1.2 m subjected to critical pulse excitations with constant absolute accelerations. Thirteen cases, using different initial angles and different base acceleration amplitudes, were studied. Table (3.1) shows the combinations of the parameters of the cases studied. To facilitate the dicussion, a case is denoted as C-J when the parameters used in that case can be found in row C and column J in table (3.1). The first row, row A, consists of cases having an acceleration amplitude greater than the minimum acceleration required to start the tilting of the block. The case in the last row, D, has an acceleration amplitude below that
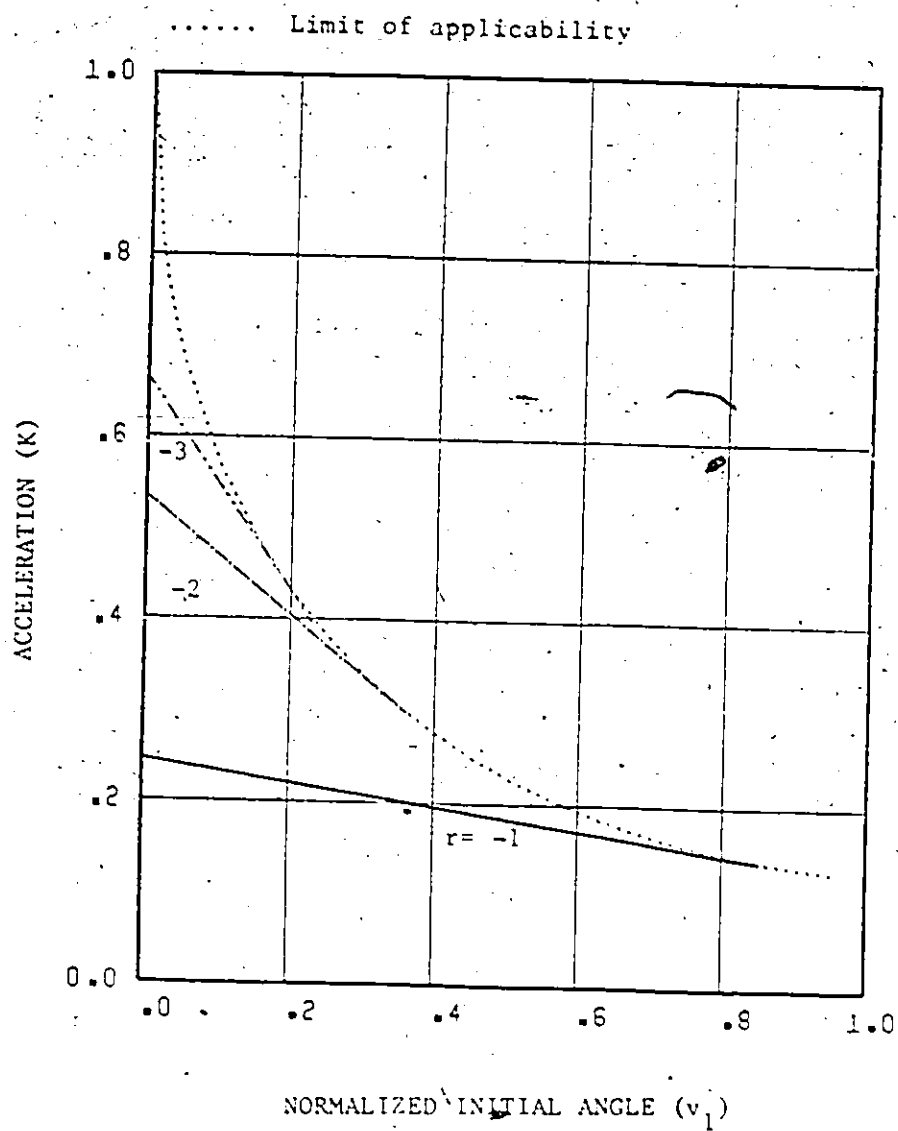
Fig. (3.5)   Critical rectangular acceleration amplitude K versus
the normalized initial angle v_1 ($\delta=0.778$)

Table (3.1)

Critical Rectangular Excitation

Effect of Initial Angle and Base Acceleration

	K	1	2	3	4
			Initial Angle θ/α		
		0.0005	0.005	0.05	0.5
A	1.46	N	N	N	N
B	.74	O	O	N	N
C	.37	O	O	O	N
D	.194			O Decay	
K_O		0.246	0.2455	0.232	0.184

K_O Critical normalized acceleration for steady-state motion

O   Oscillatory case

N   Non-oscillatory case

required for the steady-state periodic motion. Figures (3.6) to (3.9) present the response time histories for these cases. In all cases shown, the rigid block either overturned or the response decayed. If the response reverses its sign several times, the case is denoted as oscillatory "O"; otherwise it is designated non-oscillatory "N". The response of the case denoted D-3 is shown to decay because the acceleration amplitude is less than the critical value necessary for the the steady-state response, as expressed by equation (3.20). Cases A-1 to A-4 have an acceleration amplitude larger than the value required to initiate tilting of the block and the block is overturned rapidly in the first half-cycle of the response. In cases B-1 to B-4 and C-1 to C-4, the acceleration amplitudes are less than g.tan(α), but greater than the values necessary for the steady-state response. If the initial angle v_1 is small, it is amplified several times until the block overturns, as shown by the responses in cases B-1 and B-2 and C-1 to C-3. If the initial angle is large, such that the amplified rotation $|rv_1|$ is greater than unity, the block overturns in the first half-cycle, as shown in cases B-3, B-4, and, C-4.

In the cases presented, the excitations are made to act until the total energy of the rigid block is just sufficient to overturn it. Then the excitations cease and the block continues to rotate under gravity until it overturns. The total duration of the excitation decreases with the increase of either the base acceleration amplitude or the initial angle. All the oscillatory cases have similar responses. Detailed investigations of case C-2 are presented in Figs. (3.10.a) and
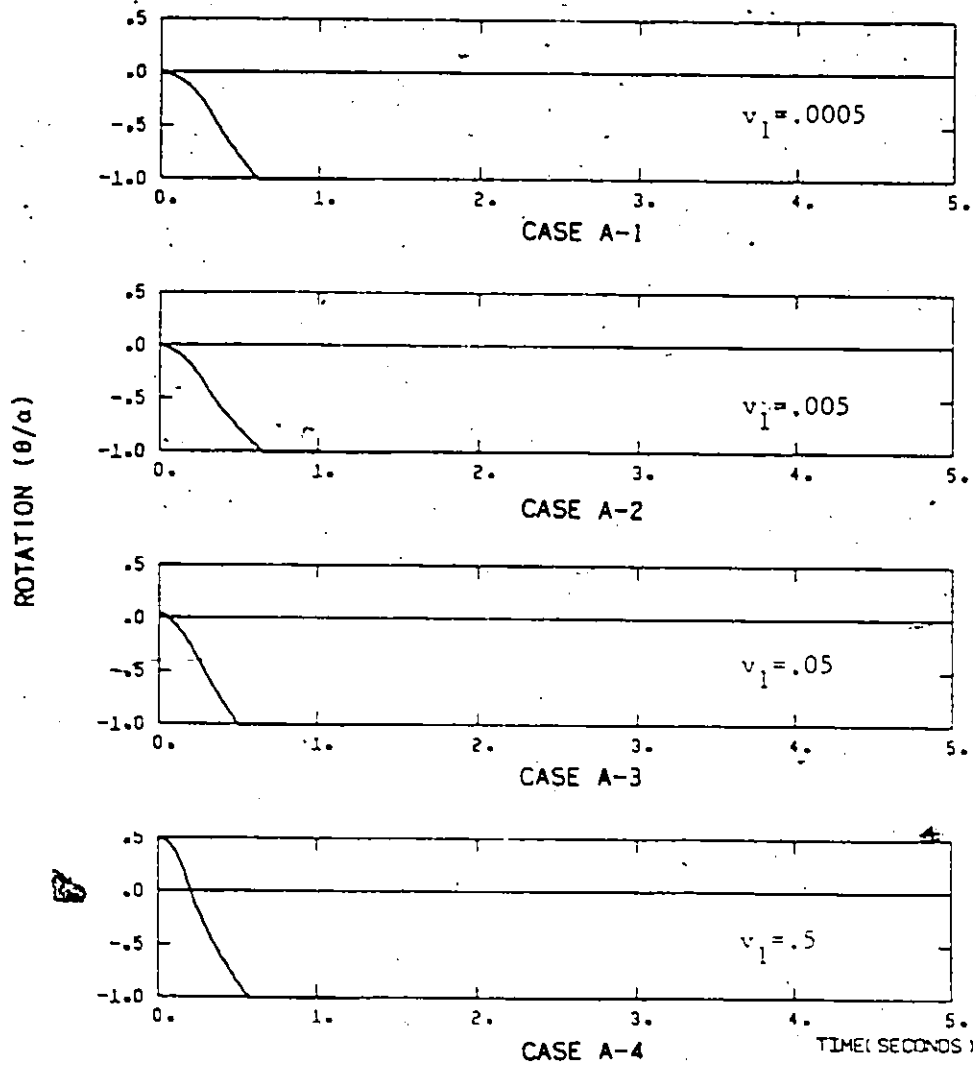
Fig. (3.6)   Response to critical rectangular excitations, cases A-1 to A-4

ROTATION (θ/α)

.5
.0
-.5
0.   1.   2.   3.   4.   5.

$v_1 = .0005$

CASE B-1

.5
.0
-.5
0.   1.   2.   3.   4.   5.

$v_1 = .005$

CASE B-2

.5
.0
-.5
0.   1.   2.   3.   4.   5.

$v_1 = .05$

CASE B-3

.5
.0
-.5
0.   1.   2.   3.   4.   5.

$v_1 = .5$

CASE B-4

TIME(SECONDS)
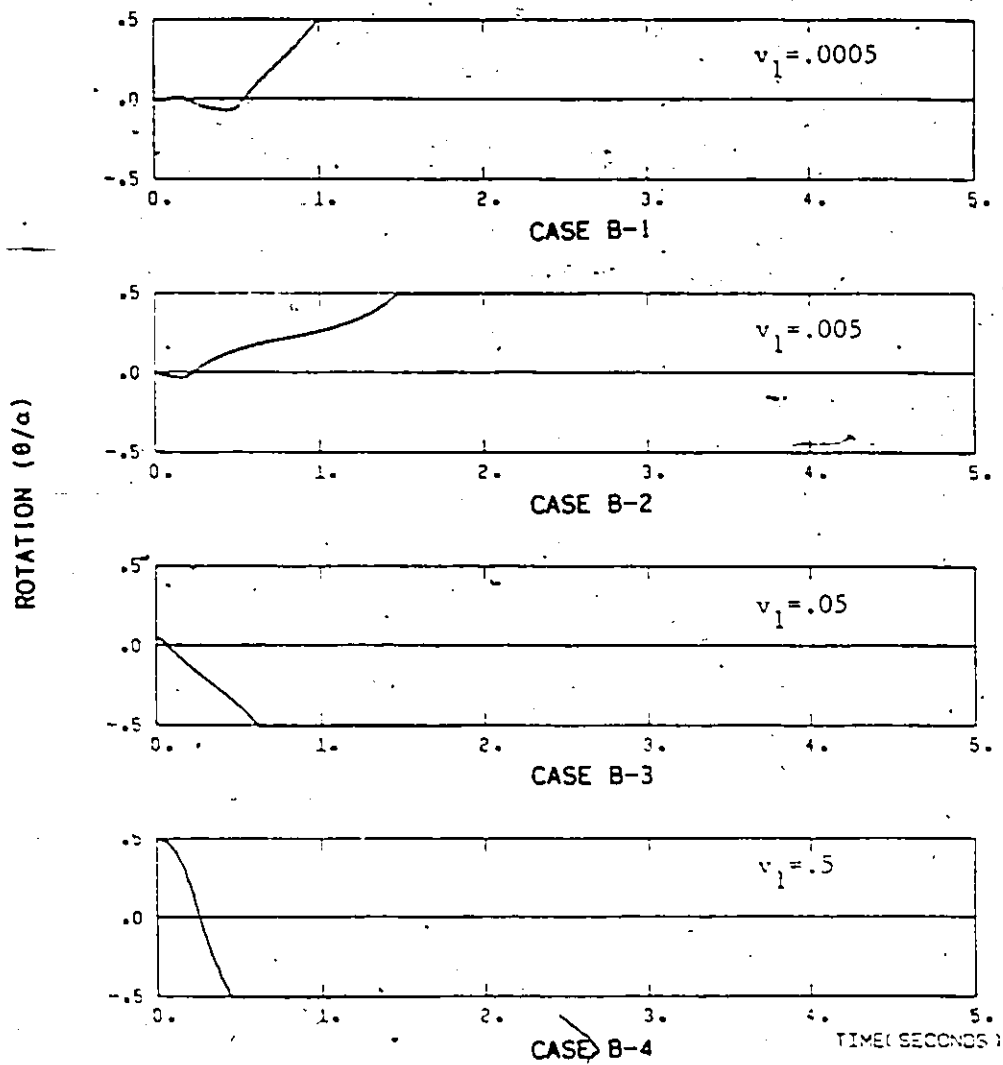
Fig. (3.7)   Response to critical rectangular excitations,
              cases B-1 to B-4
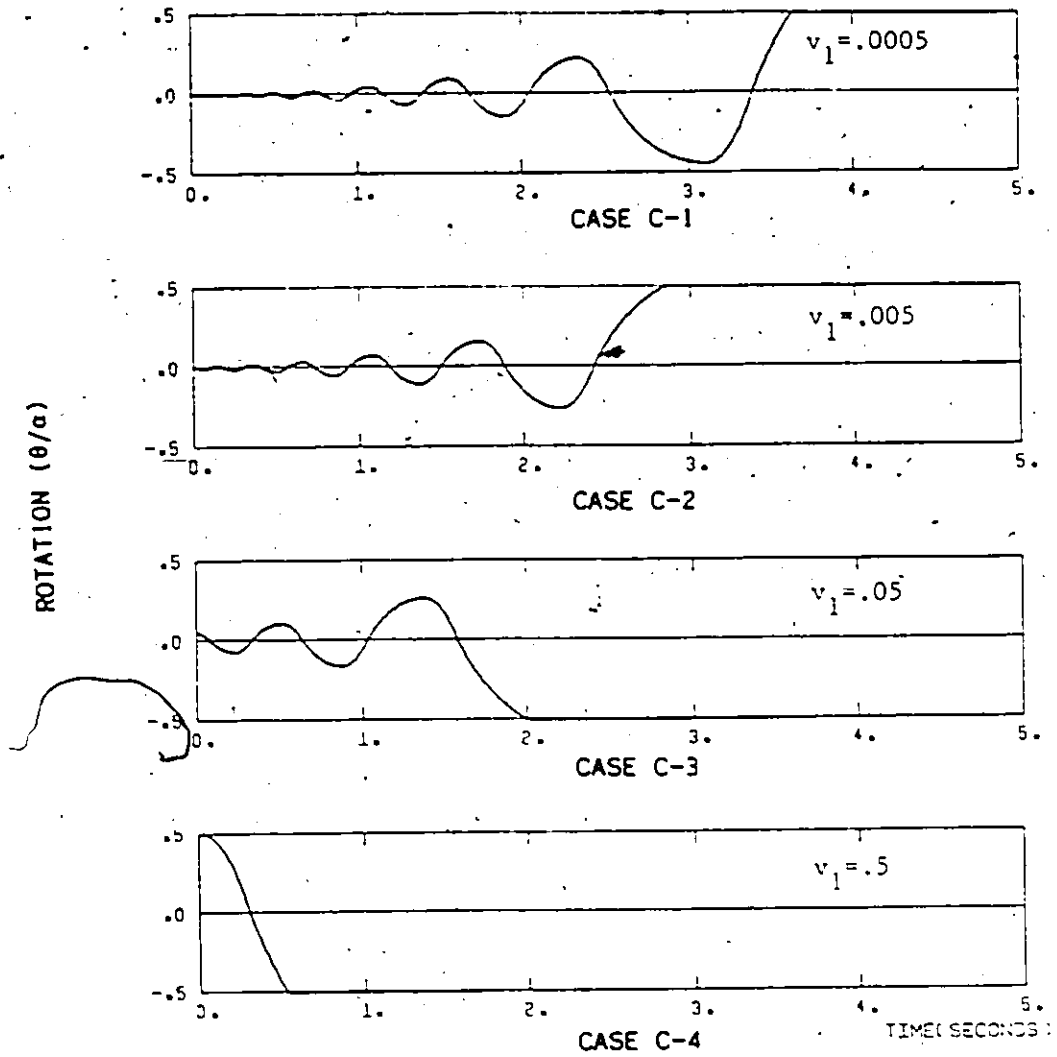
Fig. (3.8)   Response to critical rectangular excitations, cases C-1 to C-4
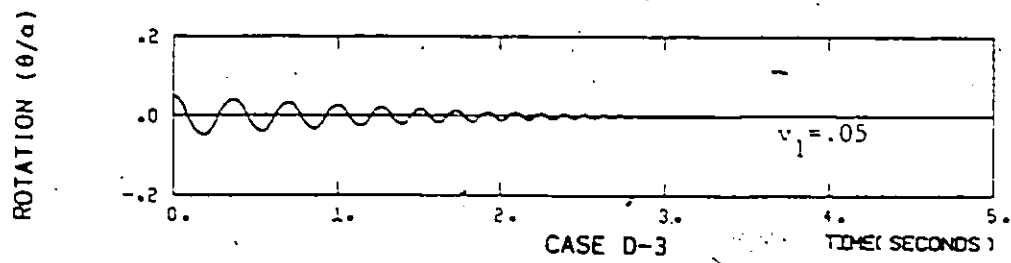
Fig. (3.9)   Response to critical rectangular excitations.
Case D-3

(3.10.b). Figure (3.10.a) shows the variation of the response half-period versus the half-cycle number. The response half-period is calculated as the time between two successive impacts. Figure (3.10.b) presents the variation of the response amplitude versus the half-cycle number. It is shown that as the half-cycle number increases, both the period and the amplitude of the angle of rotation grow more rapidly · until overturning occurs.

3.3 Series of Triangular Pulses

In this section, a critical excitation composed of a series of triangular pulses will be studied. As was done in the case of rectangular pulses, a time interval which corresponds to a half-cycle of the response is considered, as shown in Fig. (3.11). As in the case of rectangular pulses, the block starts to move with an initial angle of rotation θ_1 and with zero angular velocity. The block impacts with the floor after a time t_m. After impact, the angle θ changes sign and tilting increases in the reverse direction. The pulse intensity starts to decrease after a time interval $t_s - t_m$ where $2t_s$ is the total duration of the pulse. Meanwhile, the block continues to rotate in the reverse (negative θ) direction until a peak is reached exactly at the end of the pulse. The problem is solved by dividing the response into these three stages. The equations of motion for the three stages are solved consecutively and the end conditions of one stage are considered the initial conditions of the following stage. The condition of zero angular velocity at the end of the pulse is imposed on the solution, as in the previous study of rocking caused by rectangular pulses.
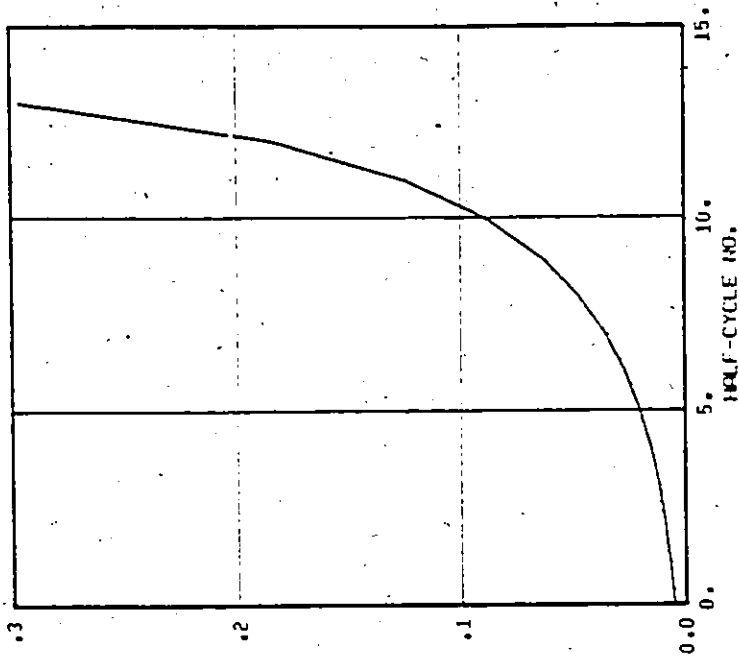
Fig. (3.10.b) Response amplitude growth with the half-cycle number, case C-2
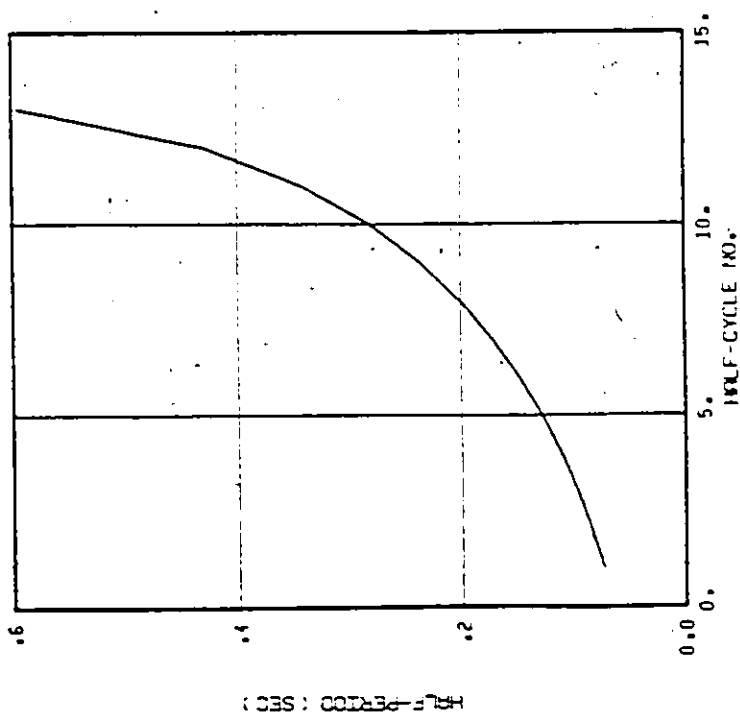
Fig. (3.10.a) Response period growth with the half-cycle number, case C-2
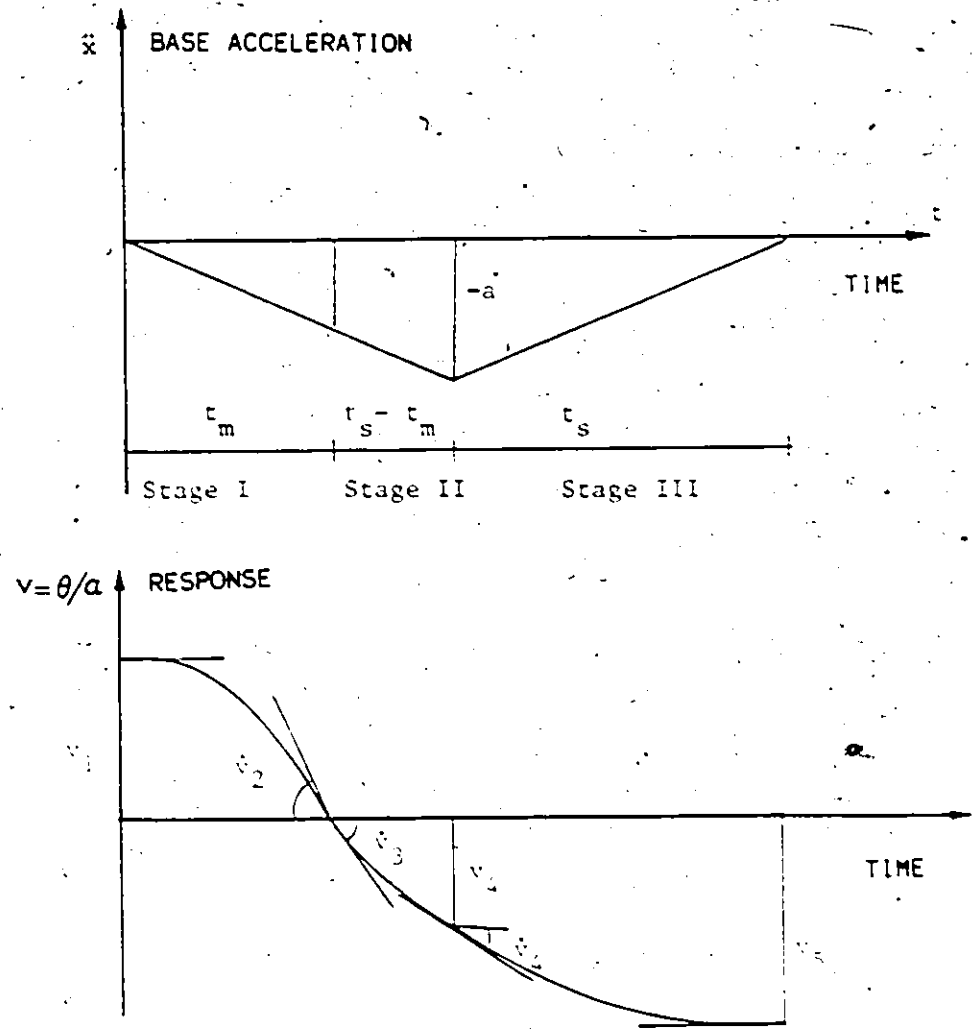
Fig. (3.11) Critical triangular excitation

3.3.1 Derivation

Stage I

The rigid block is assumed to start tilting with zero velocity under the effect of base acceleration, which is expressed as

$$\ddot{x} = a \ t/t_s \qquad (3.24)$$

Then, the equation of motion (2.6), for positive angles of rotation, takes the form:

$$\ddot{\theta} - p^2\theta = - p^2\alpha \ (\ 1 + Kt/t_s) \qquad \theta > 0 \qquad (3.25)$$

The arbitrary constants of the general solution of equation (3.25) are determined using the initial conditions at t=0:

$$\dot{\theta}(0) = \dot{\theta}_1 \qquad , \qquad \theta(0) = 0 \qquad (3.26)$$

Thus the normalized response of the rigid block in stage I can be expressed as

$$v(t) = \frac{\theta(t)}{\alpha} = (v_1-1) \cosh(pt) - \frac{K}{pt_s} \sinh(pt) + \frac{Kt}{t_s} + 1 \qquad (3.27)$$

and the angular velocity $\dot{v}$ takes the form:

$$\dot{v}(t) = p(v_1-1) \sinh(pt) - \frac{K}{t_s} \cosh(pt) + \frac{K}{t_s} \qquad (3.28)$$

Stage I ends at the instant the block impacts with the floor at time t_m. The time t_m can be obtained by setting v=0 in the response equation (3.27), leading to:

$$(v_1-1) \cosh(pt_m) - \frac{K}{pt_s} \sinh(pt_m) + \frac{Kt_m}{t_s} + 1 = 0 \qquad (3.29)$$

The angular velocity of the block just before impact $\dot{v}_2$ is expressed as

$$\dot{v}_2 = \dot{v}(t_m) = p(v_1-1) \sinh(pt_m) - \frac{K}{t_s} \cosh(pt_m) + \frac{K}{t_s} \qquad (3.30)$$

Stage II

This stage starts just after the impact with the floor. The initial conditions for this stage are denoted by v_3 and $\dot{v}_3$. The initial angular velocity $\dot{v}_3$ is related to the angular velocity $\dot{v}_2$ just before impact by equation (2.7), giving:

$$\dot{v}_3 = \delta \left[p(v_1-1) \sinh(pt_m) - \frac{K}{t_s} \cosh(pt_m) + \frac{K}{t_s} \right] \qquad (3.31.a)$$

and

$$v_3 = 0 \qquad (3.31.b)$$

The response of the rigid block in stage II should satisfy the differential equation (2.6) for negative angles of rotation. The variation of excitation with time measured from the beginning of stage II now has the form:

$$\ddot{x} = - \frac{a(t_m+t)}{t_s} \qquad (3.32)$$

which, when substituted in equation (2.6), gives:

$$\ddot{\theta} - p^2\theta = - p^2\alpha - 1 + \frac{K(t_m+t)}{t_s} \qquad \theta > 0 \qquad (3.33)$$

The equation of motion (3.33), when subjected to the initial conditions (3.31), has the following solution:

$$v(t) = \left[1 - \frac{Kt_m}{t_s} \right] \cosh(pt) + \left[\frac{\dot{v}_3}{p} - \frac{K}{pt_s} \right] \sinh(pt) + \left[\frac{K(t_m+t)}{t_s} - 1 \right] \qquad (3.34.a)$$

and the angular velocity is given by:

$$\dot{v}(t) = p\left[1 - \frac{Kt_m}{t_s}\right] \sinh(pt) + \left[\dot{v}_3 - \frac{K}{t_s}\right]\cosh(pt) + \frac{K}{t_s} \qquad (3.34.b)$$

Stage II ends at time $t=t_s-t_m$ when the excitation expression changes. The conditions of rotation and angular velocity at that instant are described by v_4 and $\dot{v}_4$, which are obtained by setting $t=t_s-t_m$ in equations (3.34), thus giving:

$$v_4=v(t_s-t_m)=\left[1 - \frac{Kt_m}{t_s}\right]\cosh p(t_s-t_m)+\left[\frac{\dot{v}_3}{p} - \frac{K}{pt_s}\right]\sinh p(t_s-t_m) + K - 1 \qquad (3.35.a)$$

The angular velocity is given by:

$$\dot{v}_4=\dot{v}(t_s-t_m)=p\left[1 - \frac{Kt_m}{t_s}\right]\sinh p(t_s-t_m) + \left[\dot{v}_3 - \frac{K}{t_s}\right]\cosh p(t_s-t_m) + \frac{K}{t_s} \qquad (3.35.b)$$

Stage III

For this stage, the excitation is expressed by:

$$\ddot{x} = \frac{a(t-t_s)}{t_s} \qquad (3.36)$$

When equation (3.36) is substituted into equation (2.6) for negative rotations and the following initial conditions are used:

$$\dot{v}(0) = \dot{v}_4 \quad , \quad v(0) = v_4$$

the response expressions of stage III are found to be given by:

$$v(t)= [\, v_4 - K + 1 \,]\cosh(pt) + \frac{1}{p}\left[\dot{v}_4 + \frac{K}{t_s}\right]\sinh(pt) - 1 + K(\,1 - \frac{t}{t_s}) \qquad (3.37.a)$$

$$v(t)=p[\ v_4\ -K\ +1\ ]\ \sinh(pt)\ +\ \left[v_4\ +\ \frac{K}{t_s}\right]\cosh(pt)\ -\ \frac{K}{t_s}\qquad J(3.37.b)$$

The state of response at the end of the pulse can be defined by substituting $(t=t_s)$ in equations (3.37) to get the angle of rotation v_s and the angular velocity $\dot{v}_s$. Two end conditions must be satisfied at $t=t_s$. First, the response must have a peak at the end of the pulse. i.e.,

$$\dot{v}(t_s) = \dot{v}_s = 0 \qquad (3.38)$$

Second, the response must be amplified by a factor r, such that:

$$v_s = r\ v_1 \qquad r<0 \qquad (3.39)$$

Substituting the response expressions (3.37) at $t=t_s$ in the end conditions given by equations (3.38) and (3.39), results in the following equations:

$$D_o\ \cosh(pt_s)\ +\ G_o\ \sinh(pt_s)\ -\ 1\ =\ r\ v_1 \qquad (3.40)$$

$$D_o\ \sinh(pt_s)\ +\ G_o\ \cosh(pt_s)\ -\ \frac{K}{pt_s}\ =\ 0 \qquad (3.41)$$

where

$$D_o = v_4 + 1 - K$$

$$= \left[1 - \frac{Kt_m}{t_s}\right]\ \cosh\ p(t_s-t_m)\ +\ C_o\ \sinh\ p(t_s-t_m)$$

$$G_o = \frac{\dot{v}_4}{p} + \frac{K}{pt_s}$$

$$= \left[1 - \frac{Kt_m}{t_s}\right]\ \sinh\ p(t_s-t_m)\ +\ C_o\ \cosh\ p(t_s-t_m)\ +\ \frac{2K}{pt_s}$$

and

$$C_o = \frac{\dot{v}_3}{p} - \frac{K}{pt_s}$$

$$= \delta [v_1-1] \sinh(pt_m) + \frac{K}{pt_s} [\delta - \delta \cosh(pt_m) -1]$$

Equations (3.29), (3.40) and (3.41) are three nonlinear algebraic equations which contain six parameters, namely, K, pt_s, pt_m, δ, v_1 and r, three of which may be considered as independent parameters. If the values of three parameters are assumed to be known, the equations can be solved for the remaining parameters. In the present analysis, the amplification factor r is assumed to be equal to (-1) for steady-state response. Discrete values of the restitution coefficient δ and the normalized response amplitude v_1 are assumed and the nonlinear equations are solved for the normalized base acceleration K, the normalized half-pulse duration pt_s and the normalized impact time pt_m, using a technique based on Newton method (Berezin, Zhidkov, 1965).

3.3.2 Numerical Results

Figure (3.12) presents the variation of the normalized critical triangular acceleration K versus the normalized response amplitude v_1, for the case of steady-state periodic motion. This corresponds to an amplification factor r equal to (-1). In this case, the response-acceleration relationship is similar to that of the rectangular pulse excitation. The base critical acceleration decreases as the response amplitude increases. A higher restitution coefficient, which implies a lower damping in the system, requires a lower acceleration to sustain the steady-state response, as expected. The comparison of Figs. (3.12)
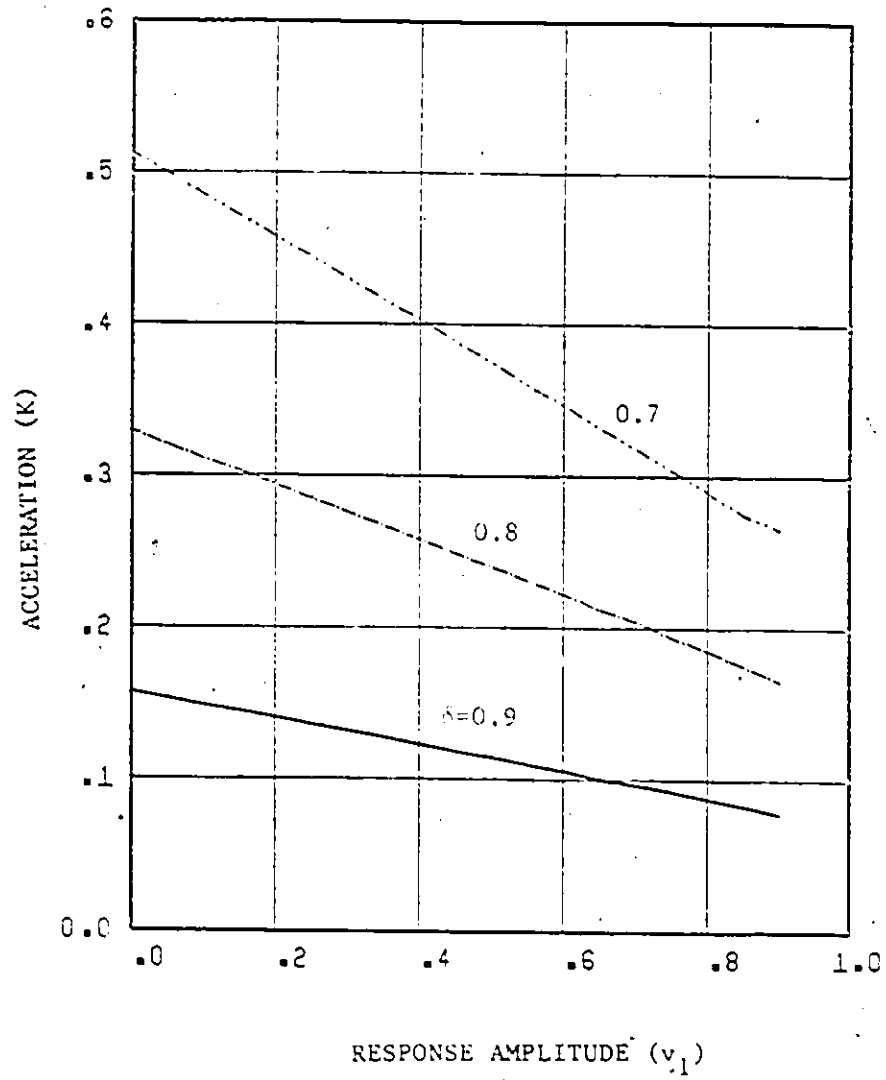
Fig. (3.12) Critical triangular acceleration K for steady—state response amplitude v_1

and (3.2) indicates that a critical excitation of a rectangular pulse shape is more severe than that of a triangular shape. To sustain steady-state responses of the same amplitude, the acceleration amplitude associated with the triangular pulses should be approximately three times that associated with the rectangular pulses. Figure (3.13) shows the normalized pulse duration as a function of the normalized response amplitude. The excitation period increases as the angle of rotation increases. To sustain the steady-state response with a given amplitude, a lower restitution coefficient will require long durations associated with each triangular pulse. Figure (3.13) also illustrates the relationship between the normalized impact time pt_m and the response amplitude. It can be seen that the impact occurs before the triangular pulse reaches its peak, but fairly close to it as shown in Fig. (3.12).

3.4 Linear Response Spectra

A linear response spectrum is a common representation for time history effects on single degree of freedom (SDOF) systems. Time histories of similar effects on SDOF systems will have the same response spectrum. Although the rocking of blocks can be represented by a single degree of freedom (angle of rotation), time histories which have equal effects on linear SDOF systems can have different effects on the rocking response of rigid blocks. Also, time histories which have equal potential to overturn rigid blocks can lead to different responses for linear SDOF systems. In this section, it will be shown that time histories with widely different response spectra can have equal potential for overturning rigid blocks.
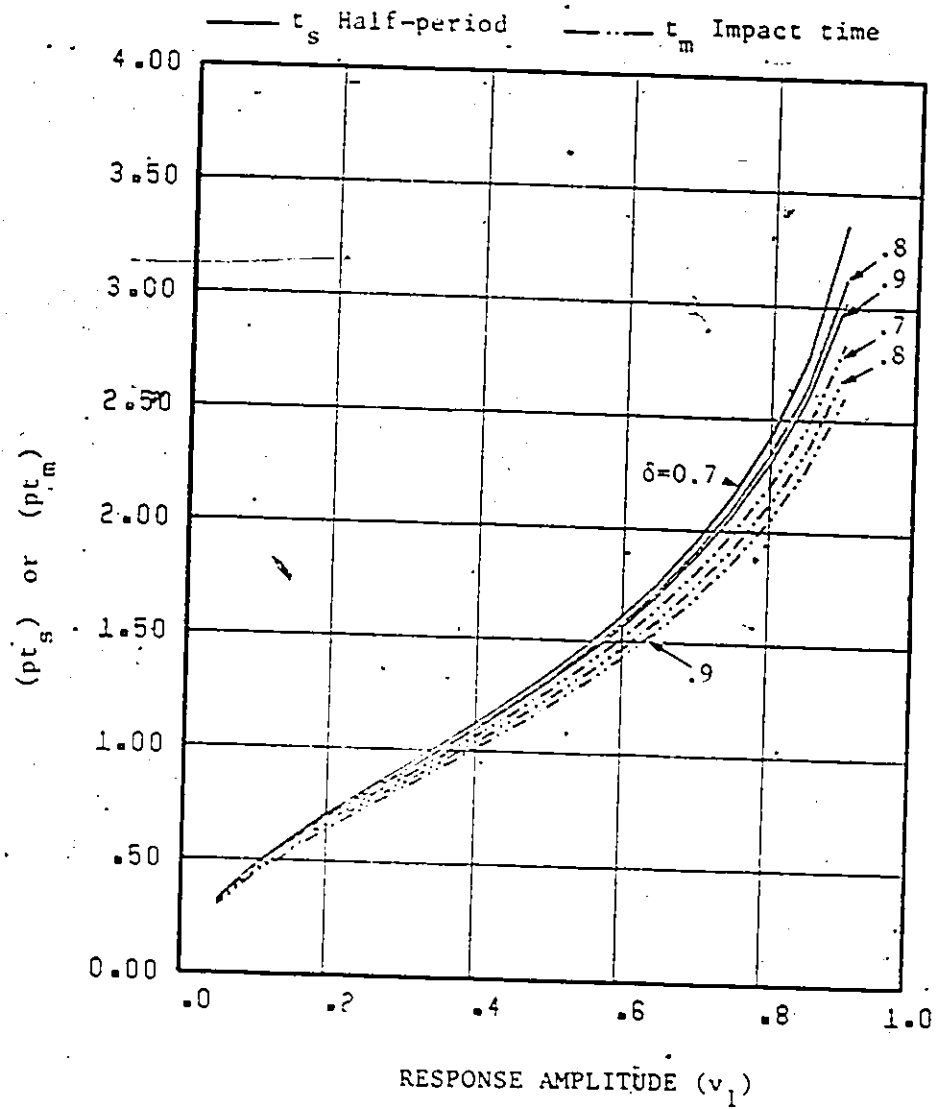
Fig. (3.13) Half-period and impact times for steady-state response under critical triangular excitation

In section (3.2.2), a parametric study was done on the overturning of a rigid block using different levels of base acceleration and different values of the initial angle of tilting. A set of base excitations was used. All of them (except that in the case D-3) caused the rigid block to overturn. If the set of excitations is divided into subgroups, such that each subgroup corresponds to a common initial angle of rotation, then all the time histories within one subgroup can be considered equivalent because they have equal potential for overturning rigid blocks. Within the same subgroup, all the blocks had started from the same initial angle and at the end they had all just overturned.

The response spectrum is calculated for each excitation and the spectra of each subgroup are compared. Figures (3.14.a) to (3.14.d) present the spectra calculated for each subgroup. They show that although the excitations of each subgroup are equivalent in their effects on the rocking block, they have different effects on linear SDOF systems as described by the response spectra. It is shown that time histories with widely different response spectra can lead to the overturning of rigid blocks. In their research, Yim et al (1980) applied several artificial earthquakes with nearly equal spectra to rigid blocks and found that the earthquakes differed in their effects on the rigid blocks. The results presented herein and the results of Yim et al (1980) indicate that an equivalence between excitations, based on either the response of linear SDOF systems or the overturning of rigid blocks, may not result in equal effects on the other system. In other words, the overturning potential of excitations cannot be estimated by using the usual linear response spectrum.
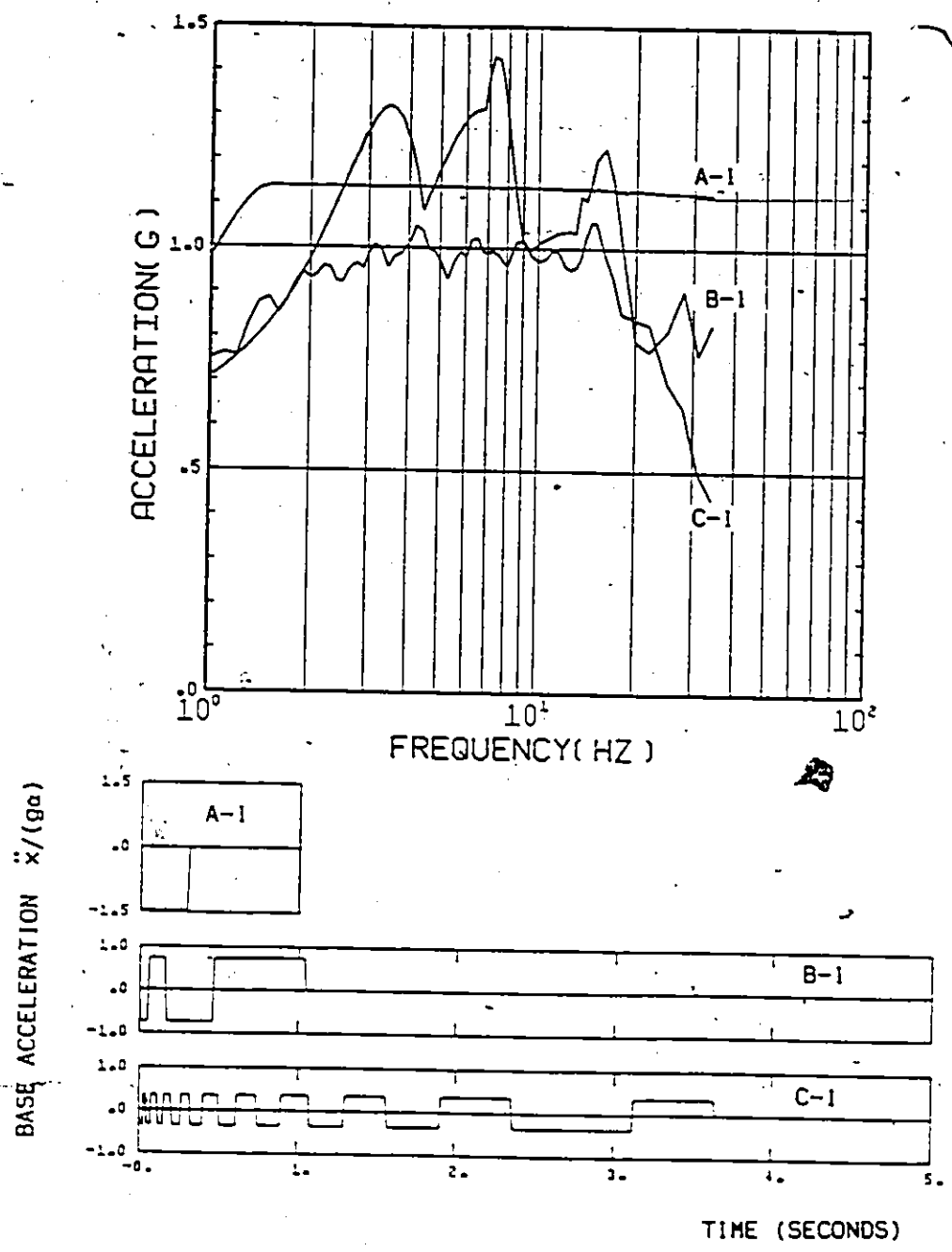
Fig. (3.14.a) Response spectra for critical excitations
A-1, B-1 and C-1 (v_1=0.0005)
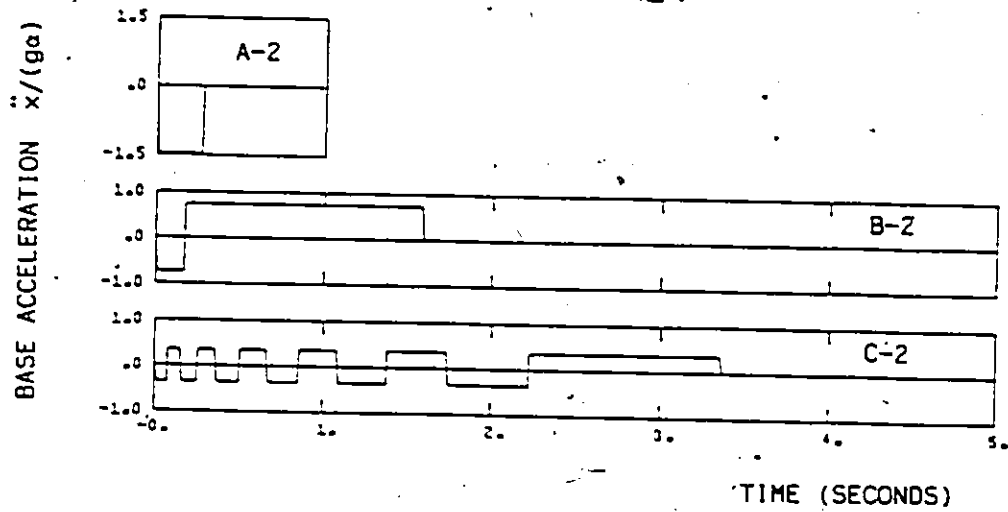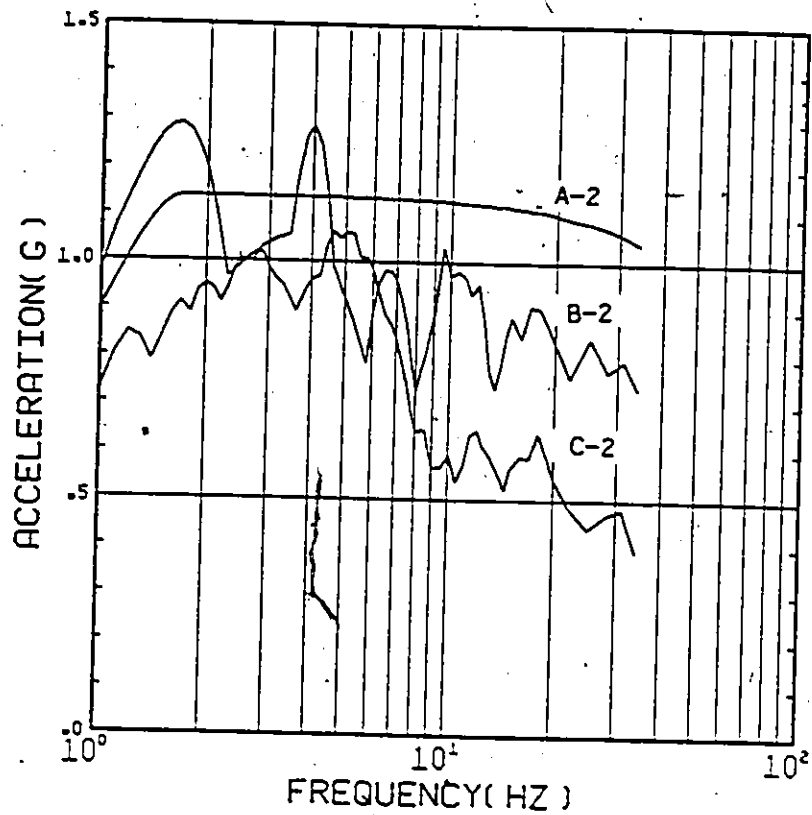
Fig. (3.14.b) Response spectra for critical excitations
A-2, B-2 and C-2 (v_1=0.005)
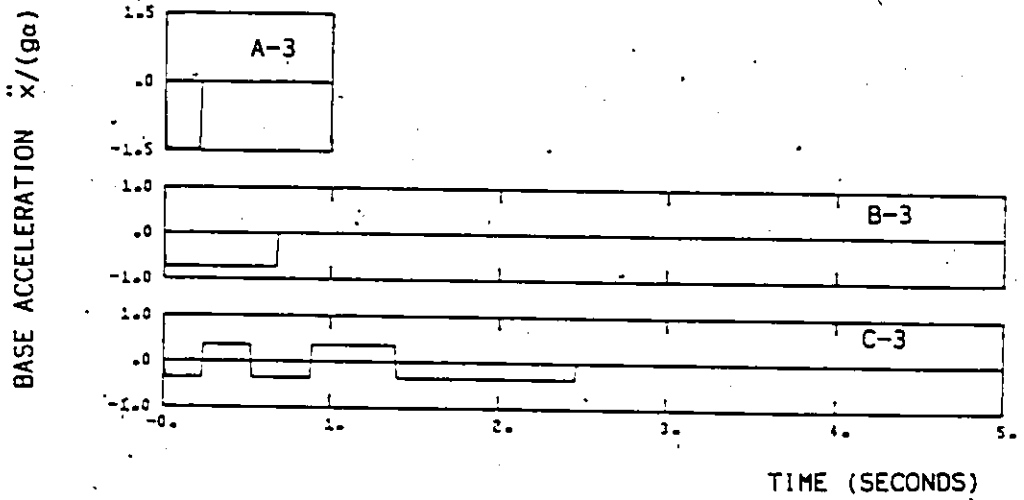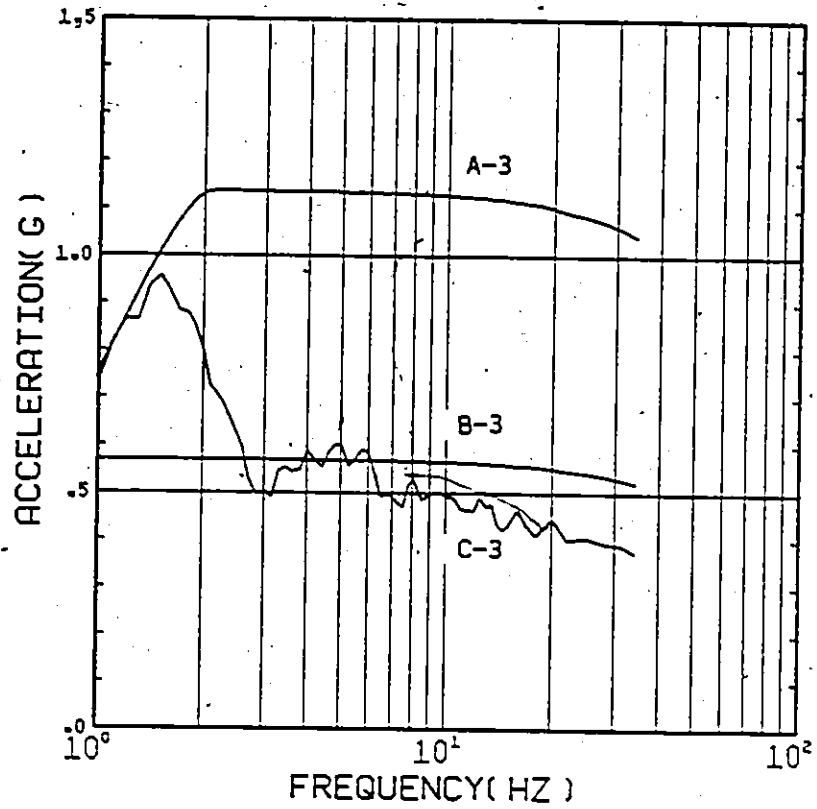
Fig. (3.14.c) Response spectra for critical excitations
A-3, B-3 and C-3 (v_1=0.05)
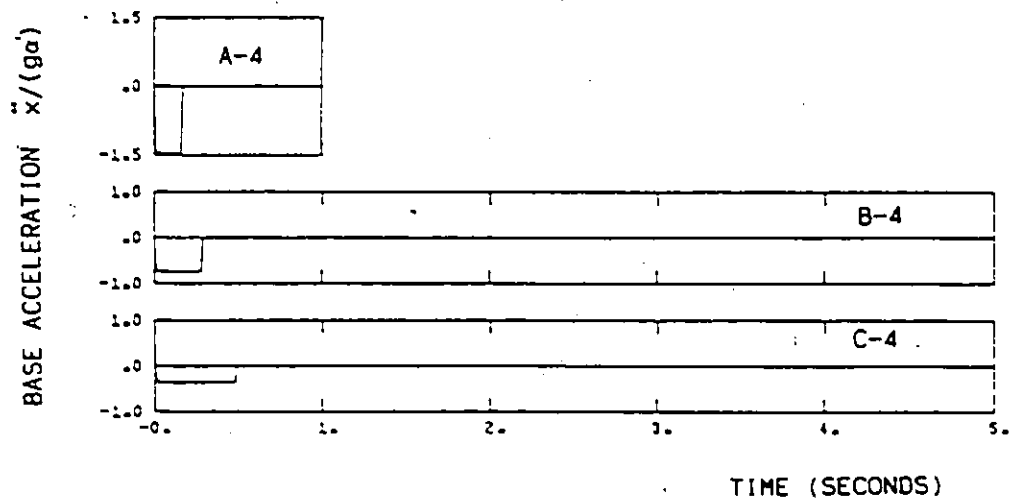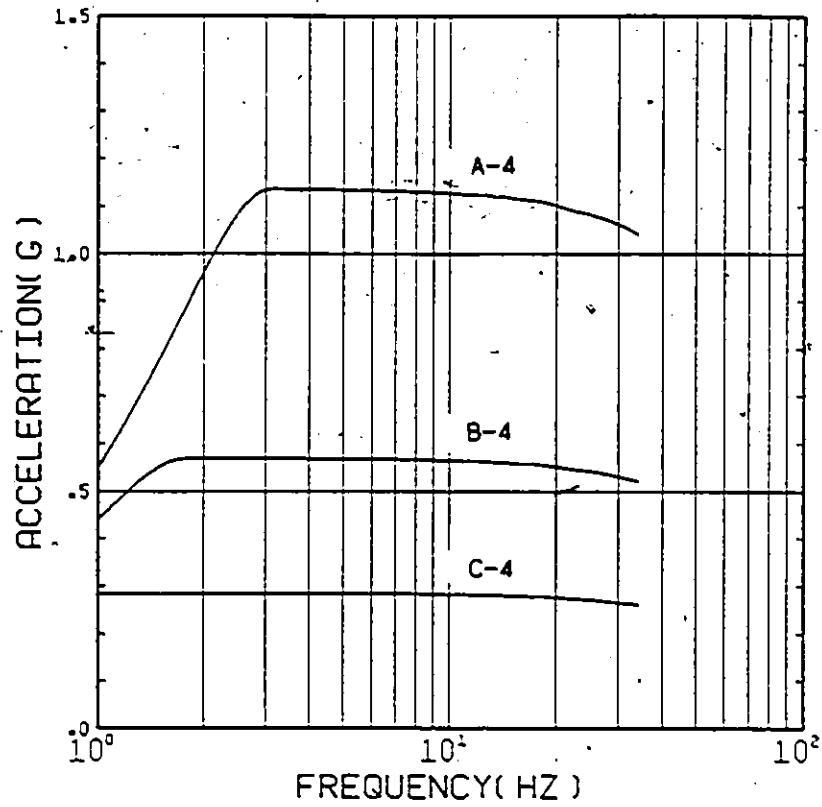
Fig. (3.14.d) Response spectra for critical excitations
A-4, B-4 and C-4 ($v_1=0.5$)

CHAPTER 4

OVERTURNING OF RIGID BLOCKS

BY

HARMONIC EXCITATION

4.1 Introduction

In the previous chapter, the overturning of rigid blocks caused by a series of pulsive excitations was studied. There was a certain phase angle between the response of the rigid block and the excitation, such that the work done by the effective force throughout the time history was positive. A more general case for the periodic response of the rigid block is studied in this chapter. In this case, the work done by the effective force is not always positive. A basic important excitation in the study of any dynamic system is the harmonic excitation. The rocking response of rigid blocks subjected to harmonic excitation differs from the response of linear SDOF systems in two ways. First, the blocks may overturn if the angle of rotation exceeds the angle α during the transient response before the steady state is reached. Second, if the periodic motion is not stable, the rocking response will not attain a steady state.

In this analysis, a rectangular rigid block capable of rocking is subjected to a sinusoidal base excitation and a steady-state periodic response solution is sought. The conditions under which a steady-state response is possible are obtained, and the stability of the resulting steady-state solution is investigated. The approach to the steady-state

rocking problem follows the one used by Ogawa (1980). The work presented herein is an extension of the work done by Ogawa. For completeness, the relevant part of his work will be summarized in sections (4.2) and (4.3).

4.2 Steady-State Response

For harmonic excitation, the total base acceleration $\ddot{x}$ can be expressed as

$$\ddot{x} = a \sin(\Omega t) \tag{4.1}$$

where a and Ω are the acceleration amplitude and the angular frequency respectively. If the contact conditions between the rigid block and the floor, assumed in Chapter 2, are valid and the angle α is small, then the response of the rocking system is governed by the differential equation (2.6). Substituting the base acceleration expression (4.1) into the equation of motion (2.6) results in the following equation:

$$\ddot{\theta} - p^2\theta = \frac{p^2 a}{g} \sin(\Omega t) \mp \alpha p^2 \qquad \theta \gtrless 0 \tag{4.2}$$

If $\tau = \Omega t$

and $\beta = p/\Omega$, where Ω/p is defined as the frequency ratio,

equation (4.2) can be written as

$$\ddot{\theta} - \beta^2\theta = \frac{\beta^2 a}{g} \sin(\tau) \mp \alpha\beta^2 \qquad \theta \gtrless 0 \tag{4.3}$$

where the dots represent differentiation with respect to the normalized time τ.

The arbitrary constants corresponding to the general solution of the differential equation of motion (4.3) are determined using the initial conditions after each impact. Figure (4.1) illustrates the assumed behaviour of the steady-state response in relation to the harmonic excitation. It is assumed that the steady-state response is periodic with a period equal to $2\pi/\Omega$ and that only two impacts with the floor occur within this period. The response is also assumed to have a mean value equal to zero, or

$$\theta(\tau) = - \theta(\tau+\pi)$$

The time origin is chosen in the steady state, such that equation (4.1) is satisfied. The impacts which follow the time origin will be numbered as 0, 1, 2, and so on. The times at which these impacts occur are τ_0, τ_1, τ_2, and so on. The time of zero impact τ_0 is denoted as the phase angle. It is assumed that the zero impact is followed by positive rotation of the block. The state of response between the nth and the (n+1)th impacts is denoted as $\theta_n(\tau)$. If this rotation is normalized to the angle α, it is termed $v_n(\tau)$. The arbitrary constants of the general solution for the differential equation (4.3), corresponding to the state of response v_n, are termed A_n and B_n. Therefore, the nth half-cycle response for the steady-state periodic motion can be expressed by

$$v_n(\tau) = \theta_n(\tau)/\alpha = A_n \, EXP[\beta(\tau-\tau_n)] + B_n \, EXP[-\beta(\tau-\tau_n)] - C \sin(\tau) \pm 1$$

where $\quad\quad\quad\quad\quad\quad\quad\quad\quad\quad\quad\quad\quad\quad\quad\quad\quad\quad\quad \theta \gtrless 0 \quad\quad\quad\quad (4.4)$

$$C = \beta^2 K/(1+\beta^2)$$

$$K = a/(g\alpha)$$

and

$$\tau_n < \tau < \tau_{n+1}$$
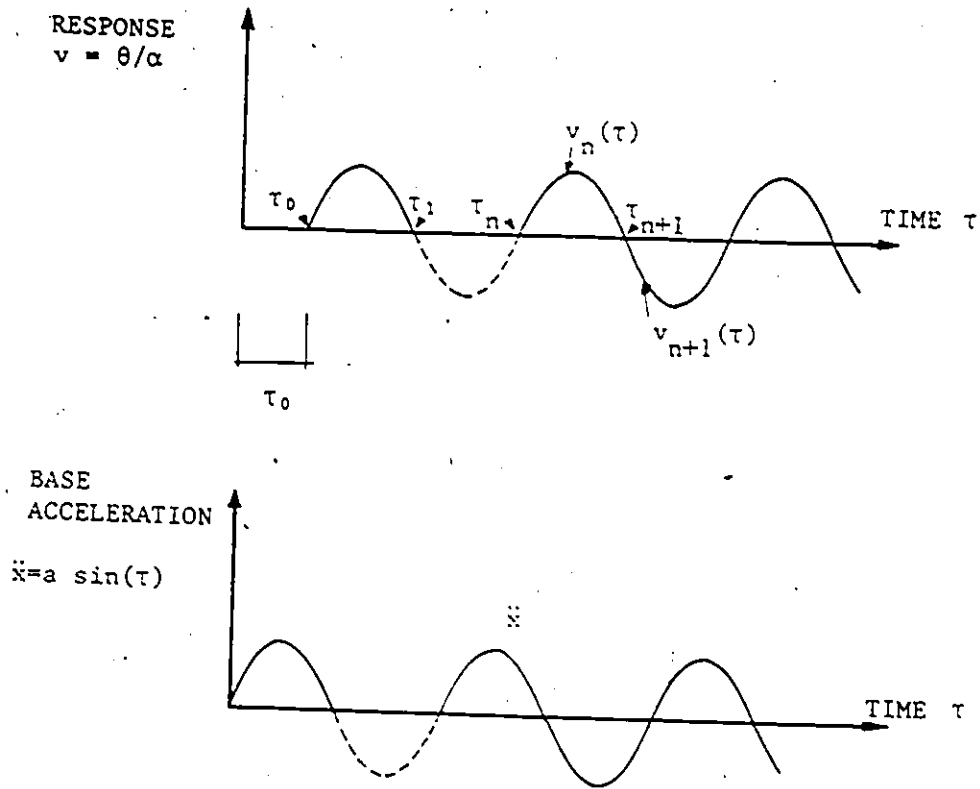
Fig. (4.1)   Periodic motion to sinusoidal excitation

As the response of the rocking system is assumed to be periodic, the arbitrary constants of the response expression (4.4) should be related by:

$$A_n = A_{n+2}$$
$$B_n = B_{n+2} \tag{4.5}$$

The relationship between the arbitrary constants of the nth and (n+1)th half-cycles can also be established by relating their initial conditions as follows:

$$v_n(\tau_n) = v_{n+1}(\tau_{n+1}) = 0 \tag{4.6}$$

$$\dot{v}_n(\tau_n) = -\dot{v}_{n+1}(\tau_{n+1}) \tag{4.7}$$

The expressions of the rotation and the angular velocity of the (n+1)th half-cycle are readily obtained by substituting (n+1) for n in the corresponding expressions. Equations (4.6) and (4.7) can be solved for A_n and B_n to give:

$$A_n = -A_{n+1}$$
$$B_n = -B_{n+1} \tag{4.8}$$

Equations (4.5) and (4.8) indicate that the arbitrary constants of the response expression (4.4) only reverse sign after each impact. Thus it is possible to express them as

$$A_n = (-1)^n A_0$$
$$B_n = (-1)^n B_0 \tag{4.9}$$

where A_0 and B_0 are constants. In this case, the response parameters are reduced to three constants, namely, A_0, B_0 and τ_0. They can be obtained as follows. For the nth half-cycle, the angle of rotation is

zero at the beginning and at the end. These conditions are expressed as

$$v_n(\tau_n) = 0 \tag{4.10}$$

$$v_n(\tau_{n+1}) = 0 \tag{4.11}$$

At the instant of impact with the floor, according to equation (2.7), the angular velocity of the rigid block after impact is δ times the angular velocity before impact. At the (n+1)th impact, therefore, this can be expressed as

$$\dot{v}_{n+1}(\tau_{n+1}) = \delta \; \dot{v}_n(\tau_{n+1}) \tag{4.12}$$

Since the response is assumed to have a period $T=2\pi/\Omega$, during which two impacts occur, the time of the nth impact is related to the phase angle by:

$$\tau_n = \tau_0 + n\pi \qquad\qquad n = 0, 1, 2,\ldots \tag{4.13}$$

By substituting the response expressions of the angle of rotation and the angular velocity in the three conditions expressed in equations (4.10) to (4.12) and using equation (4.13), the following equations are obtained. Equation (4.10) gives:

$$A_0 + B_0 - C \sin(\tau_0) + 1 = 0 \tag{4.14}$$

and equation (4.11) gives:

$$A_0 \; EXP(\beta\pi) + B_0 \; EXP(-\beta\pi) + C.\sin(\tau_0) + 1 = 0 \tag{4.15}$$

The third condition (4.12) gives:

$$A_O \ [1 + \delta \ EXP(\beta\pi)] - B_O \ [1 + \delta \ EXP(-\beta\pi)] - \frac{C}{8} \ (1-\delta) \ \cos(\tau_O) = 0 \tag{4.16}$$

The unknown parameters in the general solution for the steady-state response A_O, B_O and τ_O can now be obtained using equations (4.14) to (4.16). The three algebraic equations can be solved for A_O, B_O and $\sin(\tau_O)$, leading to:

$$A_O = \frac{q-1}{2} \left[\frac{C \ [\ X \pm \ H \ (1+H^2-X^2)^{1/2}]}{q(1+H^2)} + 1 \right]$$

$$B_O = \frac{q+1}{2} \left[\frac{C \ [\ X \pm \ H \ (1+H^2-X^2)^{1/2}]}{q(1+H^2)} - 1 \right]$$

$$\sin(\tau_O) = \frac{X \pm \ H \ (1+H^2-X^2)^{1/2}}{(1+H^2)} \tag{4.17}$$

where

$q=\tanh(\beta\pi/2)$

$H=Dq/\beta$

$X=Dq^2/C$

and

$D=(1-\delta)/(1+\delta)$ \hfill (4.18)

The variable D represents the damping in the system. Large values for D indicate high damping. The variable q is a frequency parameter and it decreases as the excitation frequency increases. The variable H depends on the damping in the system and the excitation frequency. The .variable X depends on the damping, the excitation frequency and the input acceleration.

Now it is possible to express the steady-state response in terms of the parameters A_O, B_O and τ_O as

$$v_n(\tau) = (-1)^n + (-1)^n \, \text{EXP}[\, \beta(\tau-\tau_n)\,] \, \frac{q-1}{2} \left[\frac{C \,[\, X \pm H \,(1+H^2-X^2)^{1/2}\,]}{q(1+H^2)} + 1 \right]$$

$$+ (-1)^n \, \text{EXP}[-\beta(\tau-\tau_n)] \, \frac{q+1}{2} \left[\frac{C \,[\, X \pm H \,(1+H^2-X^2)^{1/2}\,]}{q(1+H^2)} - 1 \right]$$

$$-C \sin(\tau)$$

$$n=0, 1, 2,\ldots \qquad \tau_n < \tau < \tau_{n+1} \qquad (4.19)$$

Equation (4.19) expresses the normalized rotation of the block during the steady state and is valid between two impacts which occur at times τ_n and (τ_{n+1}).

There are two solutions for the problem corresponding to two possible phase angles as shown in equation (4.17). Numerical values for the phase angles show that one of them is nearly zero, indicating that the corresponding response is almost in phase with the excitation. On the other hand, the other phase angle is slightly less than π, denoting that the corresponding steady-state response is out of phase with the base motion. The negative sign in front of the square root in equations (4.17) and (4.19) corresponds to the in-phase solution, while the positive sign corresponds to the out-of-phase solution.

4.3 Boundaries of the Periodic Solution

Investigation of equation (4.17) shows that real values for the phase angle can exist only if the quantity under the square root is positive, namely,

$$1 + H^2 - X^2 > 0 \qquad (4.20)$$

Substituting the expressions of H and X, given by equation (4.18), into the condition (4.20) and solving for K results in the following:

$$K > \frac{Dq^2(1+\beta^2)}{\beta(\beta^2+D^2q^2)^{1/2}} \qquad (4.21)$$

For acceleration amplitudes less than the value specified by expression (4.21), no periodic motion can occur. Numerical values indicate that the acceleration calculated by expression (4.21) is less than unity, which is the minimum value required to initiate the rocking motion from rest. Thus, for the range of excitation amplitude K less than unity but greater than the value given by expression (4.21), some initial tilting of the rectangular block is necessary to achieve the steady-state response.

In the derivation of the periodic response expression (4.19), conditions at the beginning and at the end of the response half-cycle were imposed such that the angle of rotation was zero at those instants. No constraints were set on the response between the two ends. Thus, there is no guarantee that the angle of rotation calculated by equation (4.19) will not change sign at intermediate points between the two ends of the half-cycle considered. From numerical examples, it appears that for the out-of-phase solution, this change of sign does not occur. For the in-phase solution, however, this change of sign is quite probable, particularly for large input acceleration. The occurrence of such impacts will contradict the assumption that there are no intermediate impacts within the half-cycle of interest. Accordingly, the response

expression (4.4) does not govern the response of the rocking block within the half-cycle considered. An exact way to find the condition required for no intermediate impacts is to set the response expression (4.19) greater than zero at the time τ. Because the resulting inequality is difficult to solve, an approximate solution can be obtained by satisfying the inequality at a specified time $\tau_m = \tau_n + \pi/2$, i.e., at the mid-point of the half-cycle to which the response peak is very close. Thus, for the in-phase solution we set

$$v_{mid} = v_n(\tau_n + \pi/2) > 0 \qquad (4.22)$$

When the response equation (4.19) is used to express the response at the time τ_m, and the resulting expression is then substituted into the inequality (4.22), the following expression is obtained:

$$v_n(\tau_n + \pi/2) = 1 - \mathrm{sech}(\beta\pi/2) - C\cos(\tau_o) > 0 \qquad (4.23)$$

Inequality (4.23) represents an upper limit for the range of the input acceleration in the frequency-acceleration domain, above which no in-phase solution can exist.

4.4 Stability of the Periodic Motion

• In the previous sections, the expressions which calculate the response corresponding to the assumed periodic motion were derived. In additions, some bounds were found for the range of input parameters which can produce this periodic motion. However, as will be seen later, the response calculated which satisfies these limits may only be conditionally stable, depending on the input and system parameters. To

study the stability of the solution given by equation (4.19), small deviations are given to the parameters of the solution (A_o, B_o and τ_o). The growth or decay of such small disturbances will determine the stability of the solution obtained.

If the parameters of the nth half-cycle are disturbed such that:

$$A_n = (-1)^n A_o + \Delta A_n$$

$$B_n = (-1)^n B_o + \Delta B_n$$

$$\tau_n = \tau_o + n\pi + \Delta\tau_n$$

The disturbances will change (either decay or grow) in the next half-cycle. Thus, the disturbed parameters in the next half-cycle become:

$$A_{n+1} = (-1)^{n+1} A_o + \Delta A_{n+1}$$

$$B_{n+1} = (-1)^{n+1} B_o + \Delta B_{n+1}$$

$$\tau_{n+1} = \tau_o + (n+1)\pi + \Delta\tau_{n+1} \qquad (4.24)$$

where ΔA_n, ΔB_n, and $\Delta\tau_n$, and ΔA_{n+1}, ΔB_{n+1} and $\Delta\tau_{n+1}$ are the deviations associated with the nth and (n+1)th half-cycles, respectively. Now, substituting the disturbed parameters in the conditions described by equations (4.10) to (4.12), we obtain the conditions relating the disturbances in successive half-cycles. Substituting equations (4.24) into equation (4.10), then reducing we have:

$$\Delta A_n + \Delta B_n - (-1)^n C \cos(\tau_o) \Delta\tau_n = 0 \qquad (4.25)$$

The second condition is obtained by substituting equations (4.24) into equation (4.11). After this is reduced, the following expression is

obtained:

$$(-1)^n A_0 \beta (\Delta\tau_{n+1} - \Delta\tau_n) \, EXP(\beta\pi) - (-1)^n B_0 \beta (\Delta\tau_{n+1} - \Delta\tau_n) \, EXP(-\beta\pi)$$

$$+ \Delta A_n \, EXP(\beta\pi) + \Delta B_n \, EXP(-\beta\pi) + (-1)^n C \cos(\tau_n) \, \Delta\tau_{n+1} = 0 \qquad (4.26)$$

When equations (4.24) are substituted into the third condition given by equation (4.12), and the resulting equation is reduced, the following expression is obtained:

$$\beta\Delta A_{n+1} - \beta\Delta B_{n+1} - (-1)^n C \sin(\tau_0) \, \Delta\tau_{n+1}$$

$$\delta[\, (-1)^n A_0 \beta^2 \, EXP(\beta\pi) \, (\Delta\tau_{n+1} - \Delta\tau_n) + (-1)^n B_0 \beta^2 \, EXP(-\beta\pi) \, (\Delta\tau_{n+1} - \Delta\tau_n)$$

$$+ \beta \, EXP(\beta\pi) \, \Delta A_n - \beta \, EXP(-\beta\pi) \, \Delta B_n - (-1)^n C \sin(\tau_0) \, \Delta\tau_{n+1} \,] \qquad (4.27)$$

The conditions described by equations (4.25) to (4.27) relate the disturbances which occur in the nth and the (n+1)th successive half-cycles. If the disturbances are assumed to vary with time in an exponent form, the disturbances at the nth half-cycle can be expressed in terms of a parameter λ as

$$\Delta A_n = \Delta_a \, \lambda^n$$

$$\Delta B_n = \Delta_b \, \lambda^n$$

$$\Delta\tau_n = (-1)^n \, \Delta_t \, \lambda^n \qquad (4.28)$$

where Δ_a, Δ_b and Δ_t are the disturbances in the system parameters at the zero half-cycle. The variable λ defines the growth or the decay of the disturbances according to its modulus value. If it is larger than unity, the disturbances will grow after each impact with the floor and the periodic motion is not stable. If it is less than unity, the disturbances will diminish gradually and the periodic motion is

considered stable. Equations (4.25) to (4.27), relating the disturbances at successive half-cycles, can be reduced using equation (4.28) and are expressed in a matrix form as

$$
\begin{bmatrix}
-1 & 1 & -\cos(\tau_0) \\
\lambda - EXP(\beta\pi) & \lambda - EXP(-\beta\pi) & Q_1 \\
\lambda - \delta EXP(\beta\pi) & -\lambda + \delta EXP(-\beta\pi) & Q_2
\end{bmatrix}
\begin{bmatrix}
\Delta_a \\
\Delta_b \\
\Delta_t
\end{bmatrix}
= 0
$$

(4.29)

where

and
$$Q_1 = \beta(\lambda+1) [A_0 EXP(\beta\pi) - B_0 EXP(-\beta\pi)]$$

$$Q_2 = \delta\beta(\lambda+1) [A_0 EXP(\beta\pi) + B_0 EXP(-\beta\pi)] + (C/\beta) \lambda (1-\delta) \sin(\tau_0)$$

Equations (4.19), (4.21) and (4.29) are the same equations derived by Ogawa (1980). Ogawa, however, obtained an expansion for the determinant of equation (4.29) which is different from the one obtained in this research, as will be shown later.

The characteristic equation of the system, obtained by equating the determinant of equation (4.29) to zero, can be written as

$$a_2 \lambda^2 + a_1 \lambda + a_0 = 0$$

(4.30)

where

$$a_0 = - 2 C \delta \cos(\tau_0) + 2 \beta \delta (A_0 - B_0)$$

$$a_1 = 2 C (1+\delta) \cos(\tau_0) \cosh(\beta\pi) - 2 C \beta (1-\delta) \sin(\tau_0) \sinh(\beta\pi)$$

and
$$- 2 \beta [A_0 EXP(\beta\pi) - B_0 EXP(-\beta\pi)] + 2 \beta \delta (A_0-B_0)$$

$$a_2 = - 2 C \cos(\tau_0) - 2 \beta [A_0 EXP(\beta\pi) - B_0 EXP(-\beta\pi)]$$

For stable periodic motion, both roots of the characteristic equation (4.30) must have absolute values less than unity, namely,

$$\text{or,} \qquad |\ \lambda_i\ | < 1 \qquad\qquad i=1,\ 2$$

$$\left|\ \frac{-a_1 \pm (a_1{}^2 - 4a_2a_0)^{1/2}}{2a_2}\ \right| < 1 \qquad\qquad (4.31)$$

Expression (4.31) defines an upper limit in the frequency-acceleration domain for the input parameters required for stable periodic motion. If the disturbance is imposed on a periodic motion excited by an acceleration and a frequency which are represented by a point in the stable region, the disturbance will decay gradually. Later, a comparison of the results obtained by equation (4.31) and the results of Ogawa will be presented. It must be noted that equation (4.31) is valid for both the in-phase and out-of-phase types of periodic motion. The type of motion is accounted for by substituting the corresponding phase angle, found by using equation (4.17), in the coefficients of equation (4.31).

4.5 Numerical Results

Figure (4.2) shows the different regions of the frequency-acceleration domain characterizing the periodic response caused by harmonic excitation. The input frequency is represented by the quantity Ω/p, while the acceleration amplitude is represented by K. Different curves are presented in Fig. (4.2). The N curve represents the minimum acceleration required to start the rocking motion. In this case, K=1. The Z curve is given by equation (4.21) and represents the minimum conditions for the periodic motion caused by harmonic excitation. The I
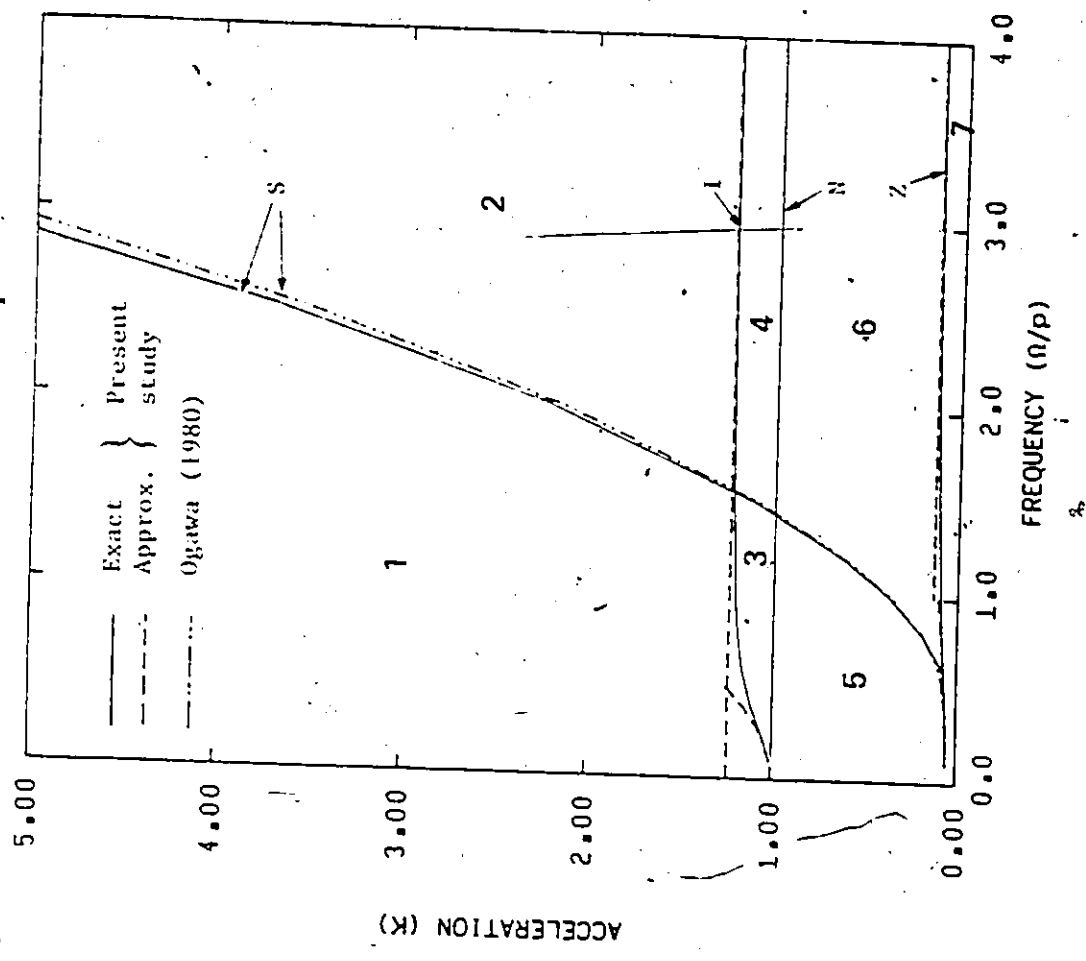
Region

1 Unstable out-of-phase motion
2 Stable out-of-phase motion
3 Both motions are unstable
4 Stable out-of-phase motion/
   Unstable in-phase motion
5 Both motions are unstable
6 Stable out-of-phase motion/
   Unstable in-phase motion/
   (Initial conditions required)
7 No periodic motion

Fig. (4.2) Regions of existence and
            stability of periodic
            motion

curve is given by equation (4.23) and represents the upper limit for the range of input parameters which produce the in-phase periodic motion. The S curve is given by equation (4.31) and represents the upper limit for the range of stability of the out-of-phase periodic motion. The curves shown are calculated for a restitution coefficient δ equal to (0.9).

If a block is to have a steady-state periodic motion under the effect of a harmonic excitation which has a normalized acceleration amplitude less than unity, some non-zero initial conditions for the angle of rotation are necessary. As the Z curve represents the minimum conditions for the periodic motion, no such motion is possible with the combinations of frequency and acceleration represented by points below this curve. The periodic motion resulting from excitations represented by the points below the I curve has a period equal to $2\pi/\Omega$ and there are two impacts within this period. Above the I curve, this assumption does not hold and more than two impacts can occur within one period. As for stability, it is found that the in-phase solution is always unstable. The out-of-phase solution is stable for the range of input parameters below the S curve. The results for the S curve obtained by Ogawa are also shown in Fig. (4.2). The difference between the results presented here and Ogawa's results is not large in the range shown of the frequency-acceleration domain for $\delta=0.9$. Larger differences are observed, however, for lower values of δ, as shown in Fig. (4.3). These are due to the different values of the coefficients of the characteristic equation obtained by Ogawa. The differences increase as the restitution coefficient decreases.
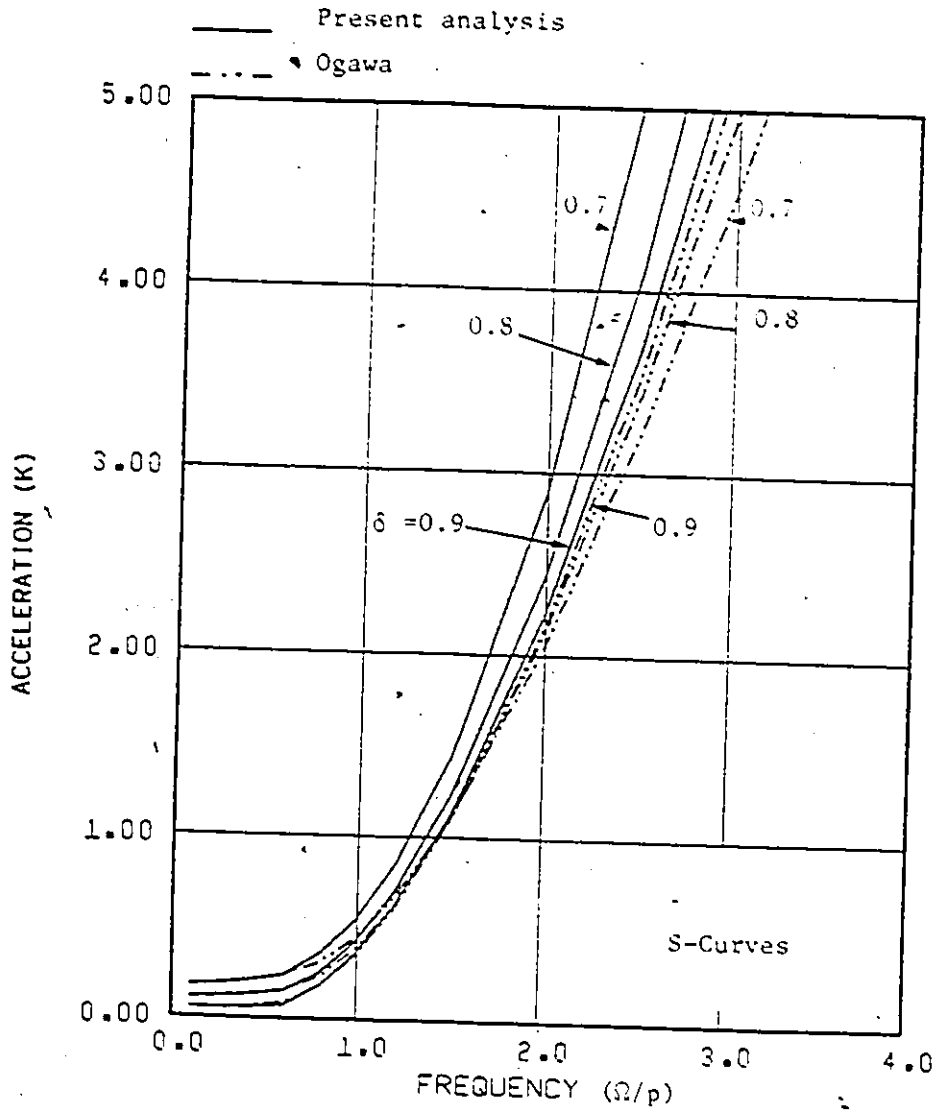
Fig. (4.3) Upper limit for stability of the out-of-phase periodic motion

The effect of the restitution coefficient on each of the limiting cases shown in Fig. (4.2) is described in Figs. (4.3) to (4.5). Figure (4.4) shows that lower restitution coefficients require higher levels of the minimum acceleration for the steady-state response presented by the Z curve. This is explained by the fact that lower restitution coefficients cause more energy to dissipate from the system through impact and, accordingly, higher accelerations are required to increase the energy supply to the system. For frequency ratios Ω/p larger than three, the function representing the minimum conditions for the periodic motion has nearly a constant value depending on the restitution coefficient.

The restitution coefficient has the same effect on the I curve as on the Z curve. Figure (4.5) shows that the restitution coefficient has in this case less effect on this limit and the function has nearly a constant value even for different values of δ.

Figure (4.3) demonstrates the effect of the coefficient of restitution on the upper limit of stability of the out-of-phase periodic motion represented by the S curve. The increase of δ lowers the upper limit of stability for the out-of-phase periodic motion. This is explained by fact that increasing the restitution coefficient decreases the rate of energy dissipation from the system. Accordingly, large input acceleration can feed more energy into the system than can be dissipated by impact and overturning can occur. Ogawa's results, however, indicate that an increase in the restitution coefficient causes an increase in the acceleration upper limit.
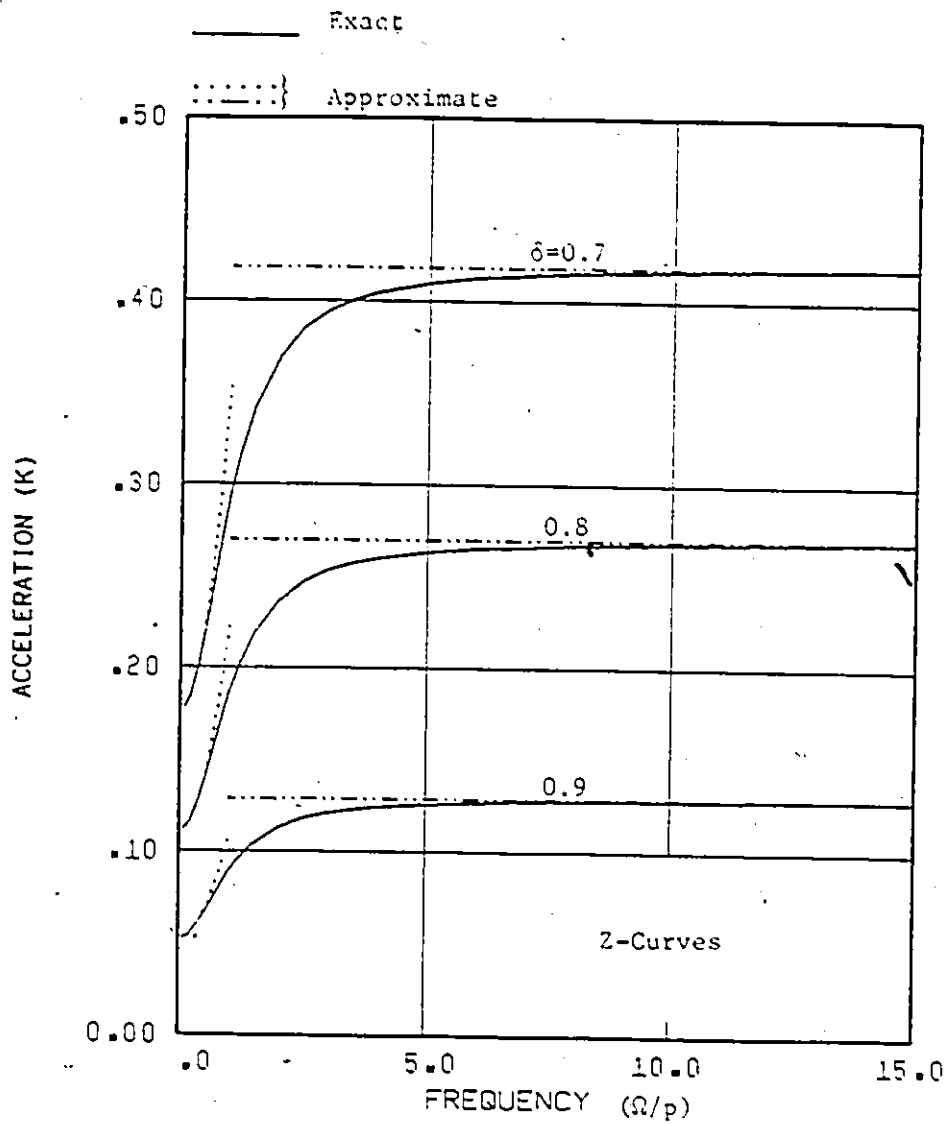
Fig. (4.4)   Lower limit of existence of the periodic motion
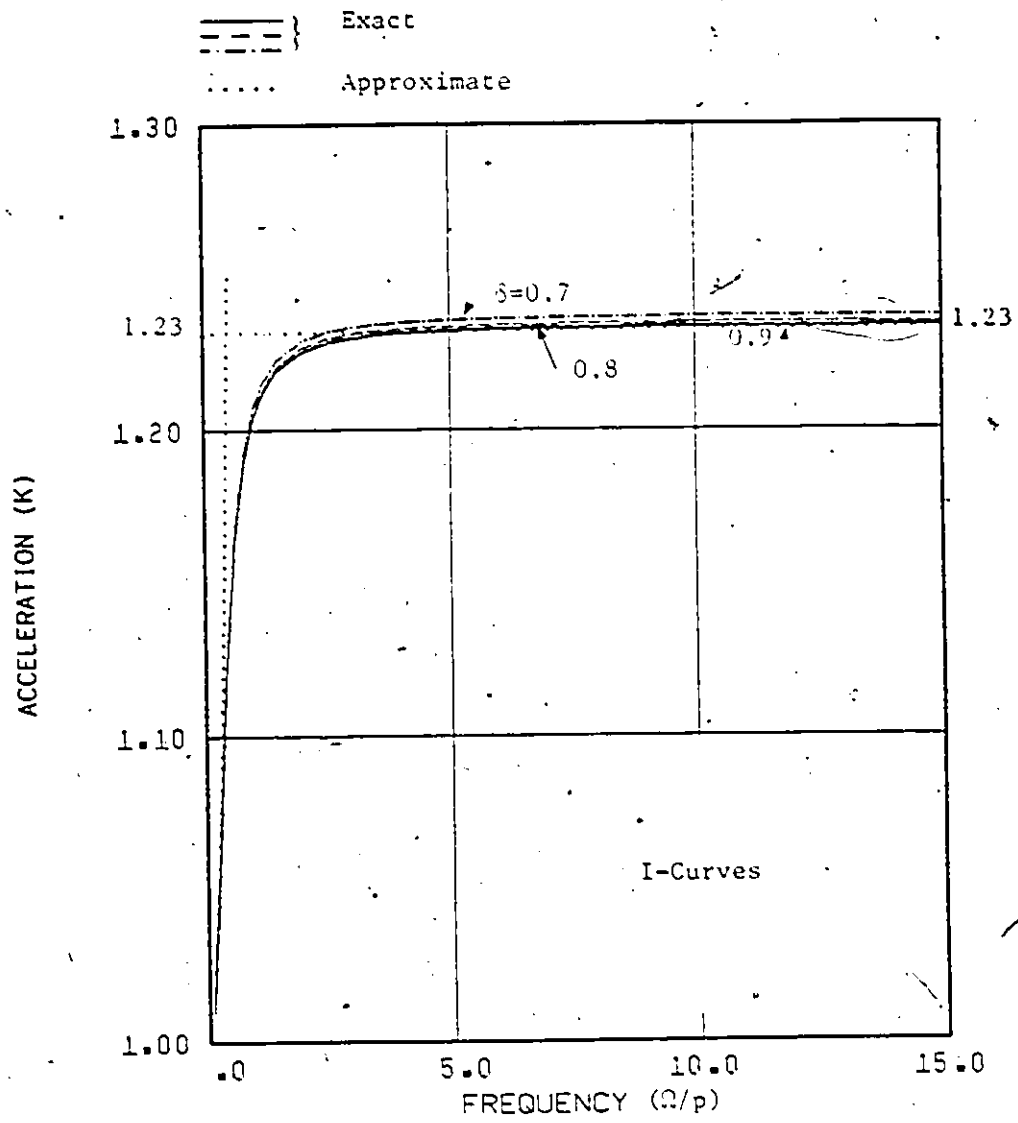
Fig. (4.5)   Upper limit for existence of the in-phase periodic motion

In summary, it is found that decreasing the restitution coefficient will raise the upper limit of the stable out-of-phase periodic motion and also will raise the lower limit of existence of the periodic motion. The increase in the upper limit, however, is larger than the increase in the lower limit. Accordingly, the range of possible stable periodic motion increases as the restitution factor decreases.

4.6 Response Curves of Periodic Motion

Figure (4.6) shows the response curves for the out-of-phase periodic motion of the blocks. The system was assumed to have a restitution coefficient equal to 0.925 . The Figure shows the response curves that correspond to different acceleration amplitudes. The vertical axis represents the maximum angle of rotation normalized to the angle α. For a constant acceleration K, the amplitude of the periodic motion has its maximum value at a low frequency. As the frequency increases, the response amplitude decreases less rapidly. At a constant frequency, larger accelerations induce higher response amplitudes, although the increase is not proportional to the increase of the input acceleration. The response curves are bounded by upper and lower envelope curves. The upper envelope curve corresponds to the response of the cases excited by base motions with input parameters represented by the points on the S curve. This envelope limits the maximum response in the low frequency range. The lower envelope curve corresponds to the points located on the Z curve. The curves marked by circles "●" represent the results obtained by Spanos (1984).
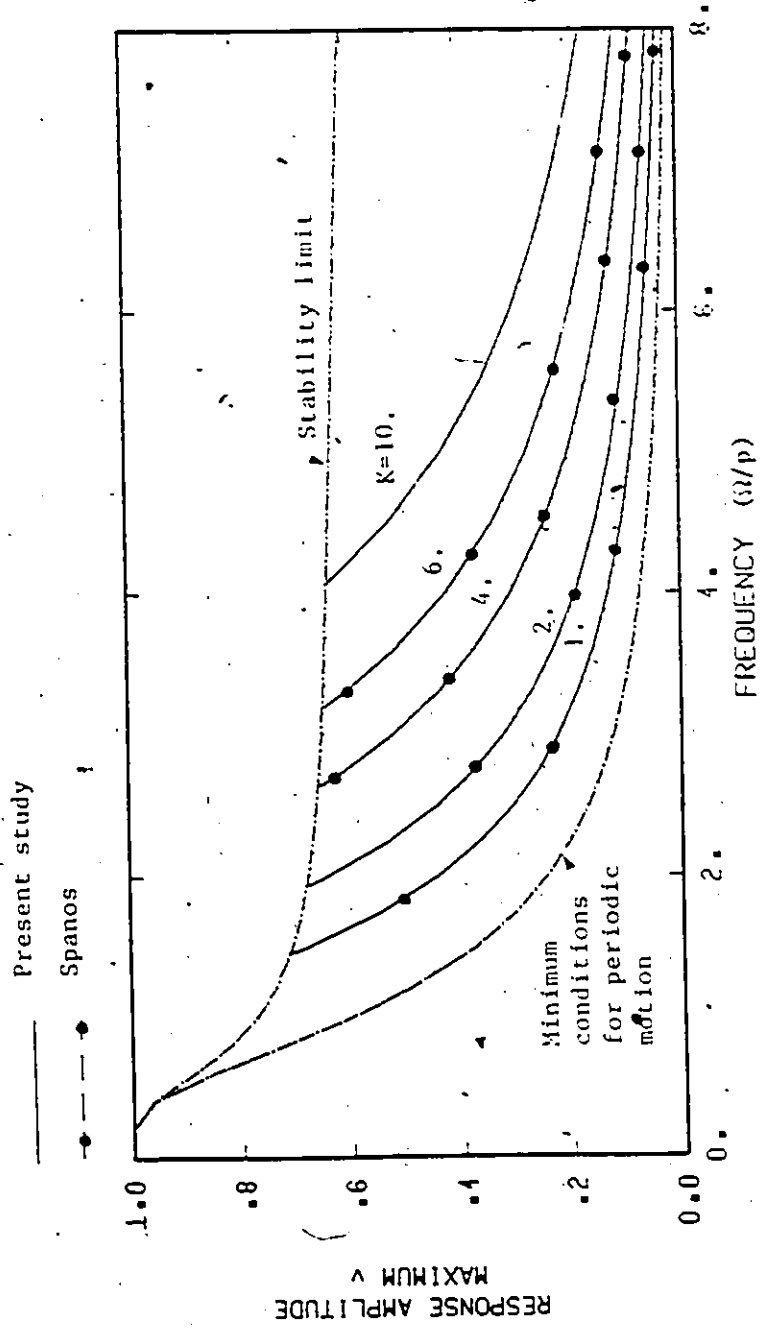
Fig. (4.6)   Frequency response curves for the normalized angle of
rotation v   (δ= 0.925)

Figure (4.7) illustrates the variation of the phase angle for different values of the normalized acceleration amplitude K as a function of the exciting frequency, for the out-of-phase solution. The same Figure also shows the envelopes corresponding to the Z and the S curves. The values of the phase angle presented in Fig. (4.7) are normalized to π. The phase angle attains nearly constant values through most of the frequency range shown. Although larger acceleration values lead to slightly higher phase angles, the phase angle can be considered almost independent of the exciting acceleration and frequency in most of the frequency range shown.

4.7 Transient Response

In the previous analysis, it was assumed that the rigid block will reach the steady state, and the derived formulas gave the steady-state response of the system. The ability of the system to reach the steady state will depend on the initial conditions. It may happen that the rigid block will overturn during the transient response before it reaches the steady state. Figure (4.8) shows, as examples, two cases with the same frequency and with a small difference in the acceleration amplitude. Both motions started from rest. In the first case, the steady state was reached, but in the second case, the system was overturned during the transient phase of the response. In these cases, the frequency and acceleration are far enough from the boundary of stability for the out-of-phase motion represented by the S curve. The first case shows that the maximum angle of tilting during the transient response is considerably larger than the steady-state response
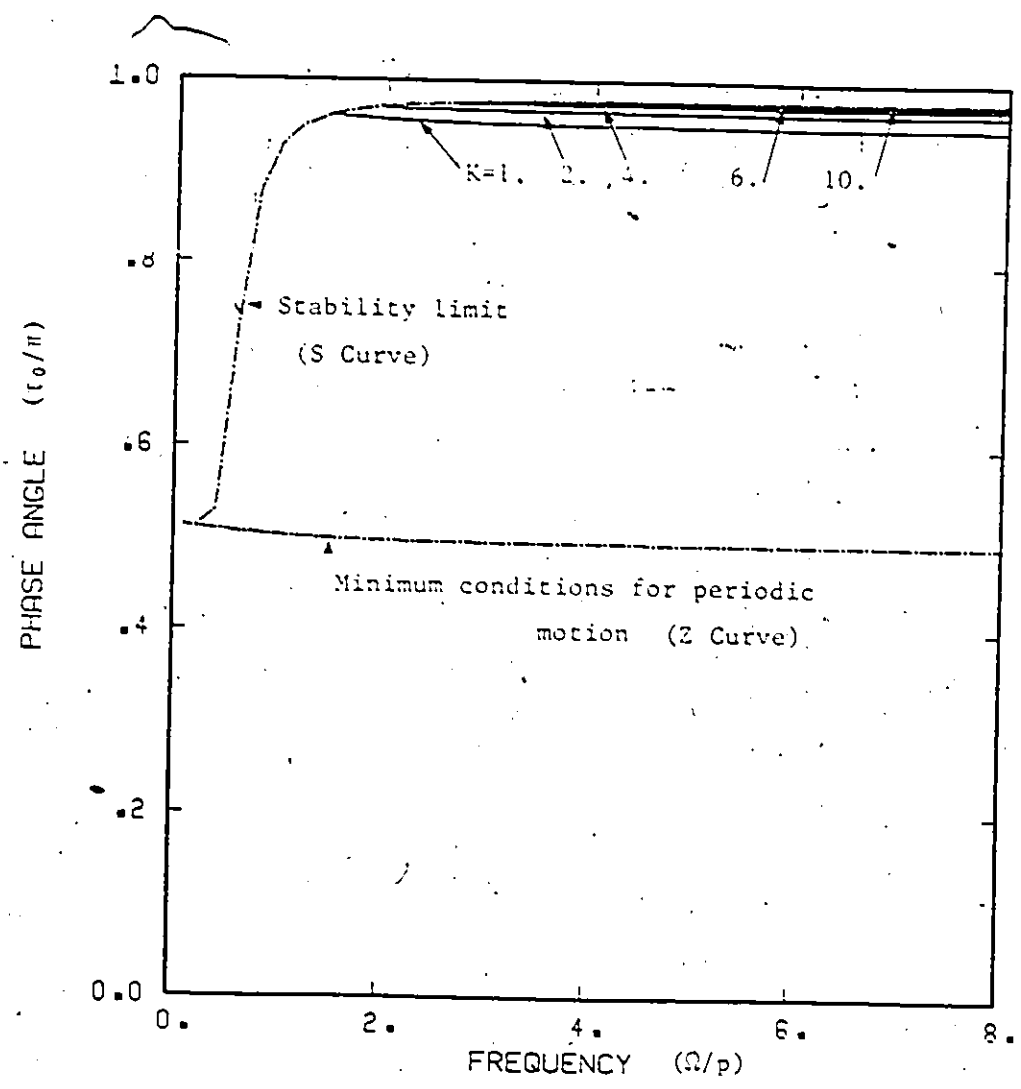
Fig. (4.7) Frequency response curves for the normalized phase angle
τ_0/π. ($\delta = 0.925$)
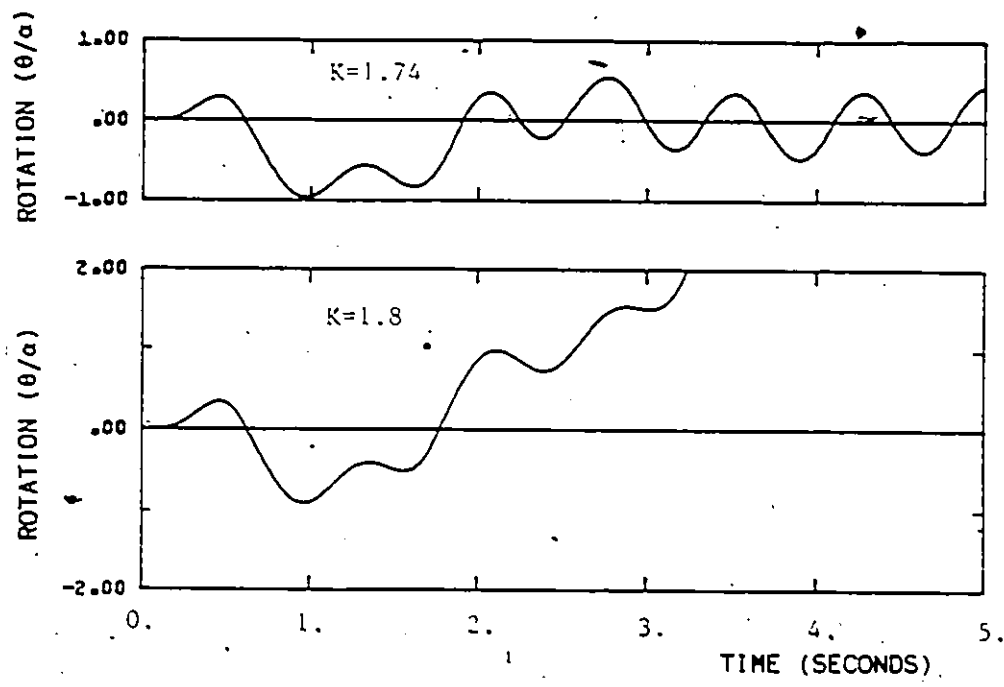
Fig. (4.8)   Transient response (Ω/ω=2.5)

amplitude. As a result, when the acceleration amplitude is increased by a small amount, the system overturned, as shown in the second case.

The purpose of this section is to introduce another boundary for stability of rigid blocks in the frequency-acceleration domain. This boundary will define the range of input parameters (K and Ω/p) which will cause the rigid block to overturn during the transient response before reaching the steady state. A trial and error method is adopted to define such a boundary. At a constant frequency, small accelerations are tried at the beginning, then increased gradually until the system overturns. This value of acceleration is defined as the required overturning acceleration for this frequency. The process is repeated at discrete points covering the frequency range of interest. Figure (4.9) shows the results obtained for different values of the restitution coefficient. It is shown that the overturning acceleration increases as the frequency increases and as the restitution coefficient decreases. The increase in the overturning acceleration with the decrease of δ is explained by the fact that the decrease of δ causes higher rates of energy dissipation from the system. In other words, decreasing δ increases the stability of rigid blocks against overturning.

Spanos (1984), in a recently published research work, analysed the problem of periodic rocking under the effect of harmonic excitation. He calculated the corresponding frequency-response curves. He also investigated the overturning of initially quiescent rigid blocks in the frequency-acceleration domain and examined the stability of the periodic solution obtained.
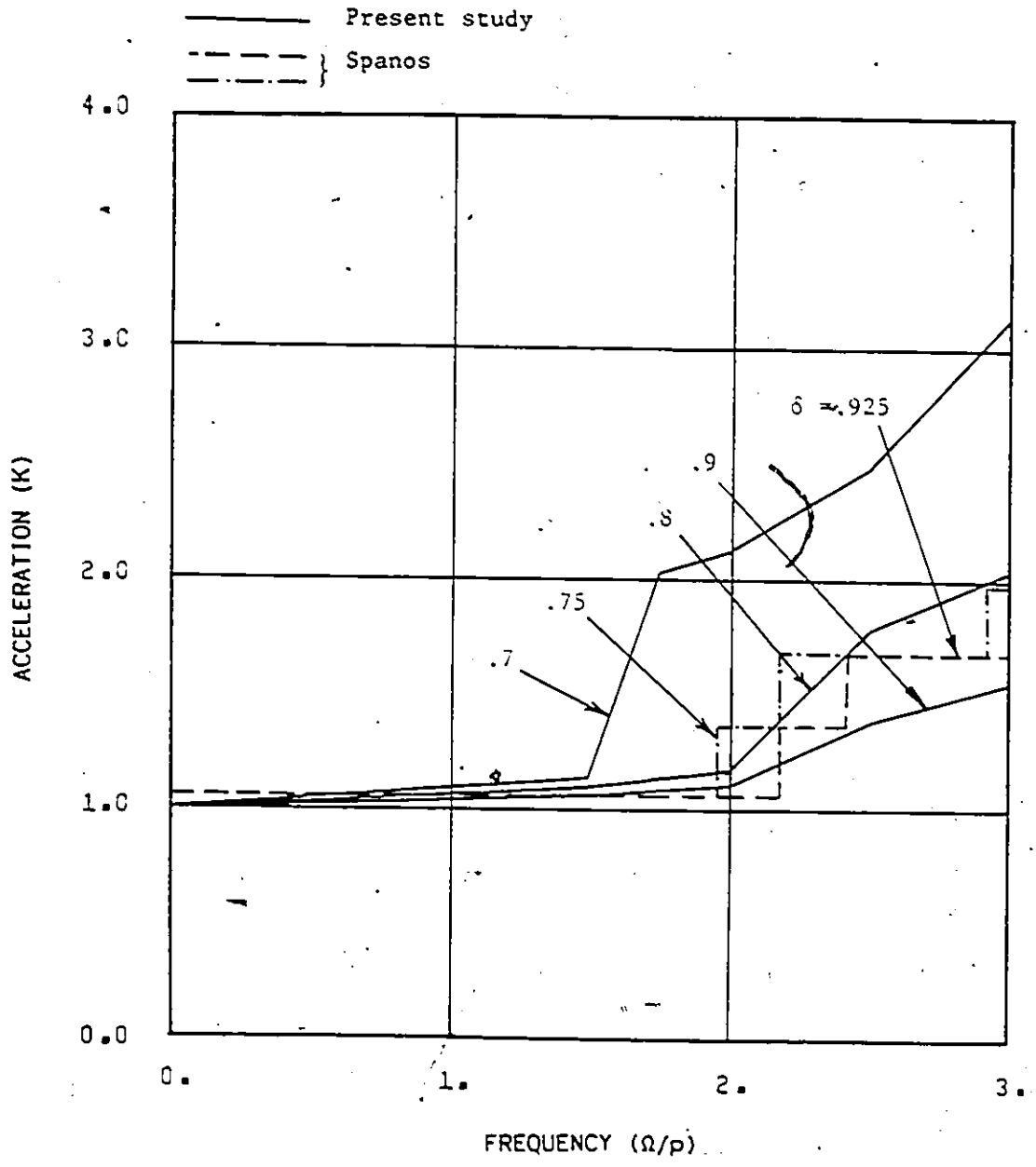
Fig. (4.9)   Lower limit of base acceleration for overturning during transient response phase

A comparison of Spanos' results and the results obtained in this research is presented in Figs. (4.6), (4.9) and (4.10). The response curves shown in Fig. (4.6) indicate agreement between the two sets of results. Figure (4.9) compares the lower limit of overturning for blocks starting from rest. It should be noted that each set of results was calculated using different values of the restitution coefficient. The comparison leads to the following observations. In general, both studies found the effect of δ on the block stability to be the same, i.e., decreasing δ increases the stability of the block against overturning. Spanos' boundaries, however, intersect with the boundaries found by this study in some zones in the frequency-acceleration domain. This behaviour can perhaps be explained as follows. First, Spanos represented the stability regions by stepped boundaries, which are not accurate except at discrete points. Second, the interval of acceleration between the points checked by Spanos is relatively large. Third, although the stability of the rigid block increases in general by the decrease of δ, exceptions may be found, as can be seen in Spanos' results, where the curves of different restitution coefficients coincided in some parts. Figure (4.10) presents the comparison for the upper and lower limits for stable steady-state periodic motion. The lower limits of existence of the periodic motion agree with the results of Spanos. However, the effect of the restitution coefficient on the upper limit of stability for the out-of-phase periodic motion found by Spanos is different from the effect found in this research. Spanos stated that decreasing the restitution coefficient of the system will
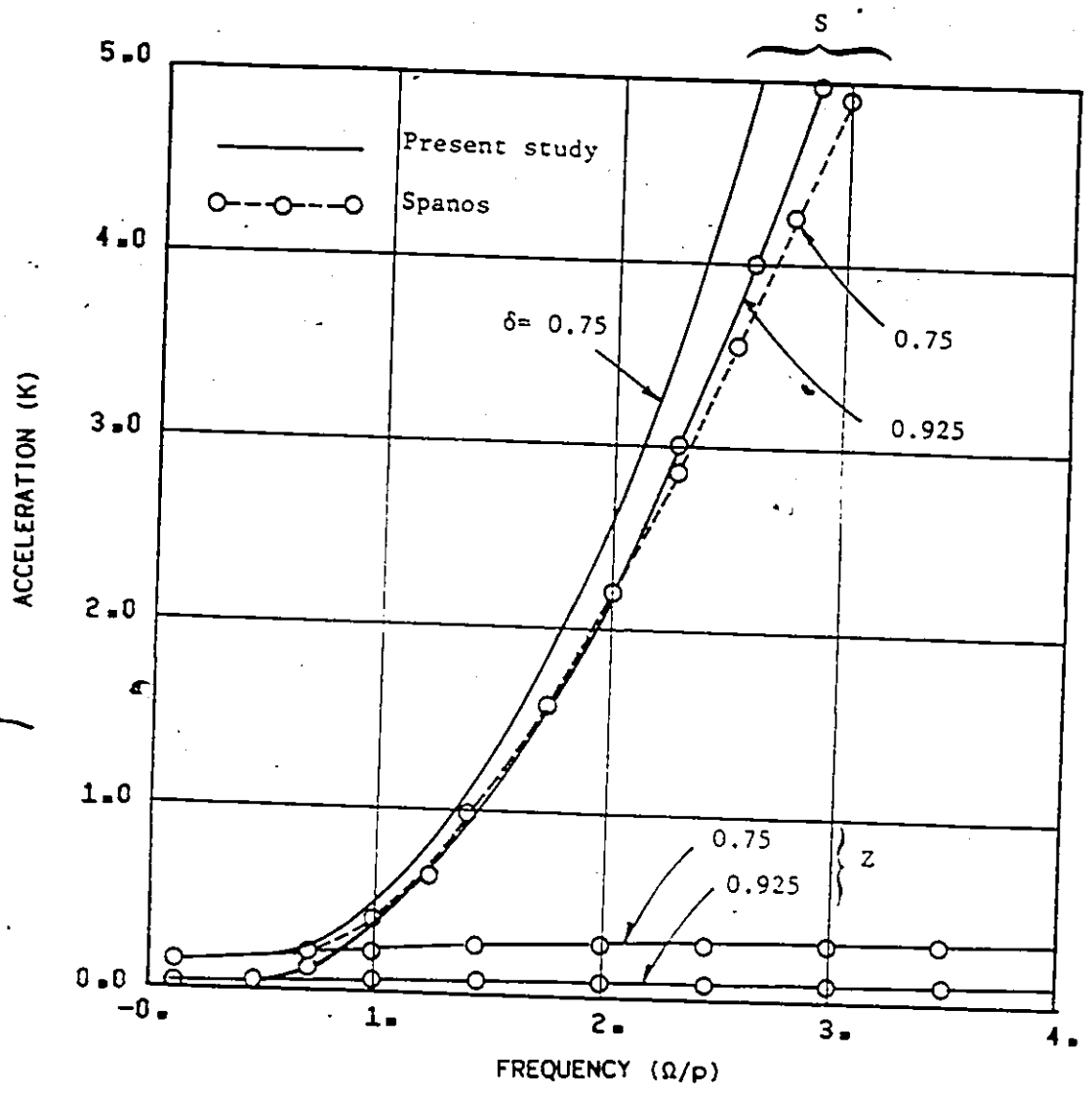
Fig. (4.10)   Regions of possible steady—state periodic motion

lower the upper limit of stability region for the out-of-phase motion. This is different from the findings of this research which indicate that decreasing the restitution coefficient raises the stability limit.

4.8 Approximate Formulas

As was shown in Figs. (4.4), (4.5) and (4.8), several response functions have an asymptotic behaviour, or they have nearly a constant value with the frequency ratio Ω/p. Such behaviour is seen in the minimum condition of existence for the periodic motion represented by the Z curve, the upper limit of existence for the in-phase periodic motion represented by the I curve, or the phase angle. As a first approximation, it is possible to eliminate the frequency dependence from these curves. This simplification will leave δ as the only independent variable. In case δ also is not an important parameter, such as in the case of the I curve, a constant value for the curve can be obtained.

In the following, the limits of certain functions, used in this analysis, are calculated. The function q can be expanded in the form:

$$q = \tanh(\beta\pi/2) = \beta\pi/2 - \beta^3\pi^3/4 + \ldots$$

Therefore

$$q/\beta = \pi/2 - \beta^2\pi^3/4 + \ldots$$

and

$$\lim_{\beta\to 0} (q/\beta) = \pi/2 \tag{4.32}$$

Also

$$\lim_{\beta\to 0} q^2(1+1/\beta^2) = \lim_{\beta\to 0} (q^2/\beta^2) = \pi^2/4 \tag{4.33}$$

The function $\mathrm{sech}(\beta\pi/2)$ is also expanded to:

$$\text{sech}(\beta\pi/2) = 1 - \beta^2\pi^2/8 + \ldots.$$

This leads to the following expression:

$$\text{Limit}_{\beta\to0} (1+1/\beta^2)[1-\text{sech}(\beta\pi/2)] = \text{Limit}_{\beta\to0} (1/\beta^2)(\beta^2\pi^2/8) = \pi^2/8 \tag{4.34}$$

Using equations (4.32), (4.33) and (4.34), the Z, I and $\sin(\tau_0)$ functions, given by equations (4.21), (4.23), and (4.17) respectively, can be approximated at large frequencies as follows. For the minimum condition of periodic motion represented by the Z curve, we obtain:

$$K > \frac{\pi^2 D}{(16 + 4\pi^2 D^2)^{1/2}} \tag{4.35}$$

For the upper limit of existence of the in-phase periodic motion represented by the I curve, equation (4.23) can be rearranged as follows:

$$K \cos(\tau_0) < (1 + 1/\beta^2)[1 - \text{sech}(\pi\beta/2)] \tag{4.36}$$

Since the phase angle corresponding to the in-phase type of motion is small, it can be assumed that $\cos(\tau_0)=1.0$. Therefore, using the limit given by equation (4.34); equation (4.23) can be reduced to the form:

$$K < \pi^2/8 \tag{4.37}$$

The phase angle is expressed using the variables H and X, which can be reduced, using the limits obtained at high frequencies, to the following forms:

$$H = \pi D/2$$

$$X = \pi^2 D/(4K) \tag{4.38}$$

When the simplified expressions (4.38) are substituted into the phase

angle expression given by equation (4.17), the following equation results:

$$\sin(\tau_o) = \frac{- 4\pi^2 D + 2\pi D [16 K^2 + \pi^2 D^2 (4 K^2 + \pi^2)]^{1/2}}{4 + \pi^2 D^2} \qquad (4.39)$$

The simplified expressions given by equations (4.35) to (4.39) were calculated for large frequency values. For small frequency values, other approximations can be made to simplify the expressions of the Z and I curves. At small frequencies, the parameter q is nearly equal to unity. Therefore, for the minimum condition of periodic motion given by the Z curve, equation (4.21) is reduced to:

$$K > \frac{D (\beta^2 + 1)}{\beta^2 + D^2} \qquad (4.40)$$

For the upper limit of existence for the in-phase periodic motion given by the I curve, equation (4.23) is reduced to:

$$K < 1 + 1/\beta^2 \qquad (4.41)$$

The results obtained using the approximate relations for large and small frequencies are compared with the exact results in Figs. (4.2), (4.4), and (4.5). It is shown that the results of the approximate formulas for large frequencies are acceptable for frequency ratios Ω/p greater than two. However, for small frequencies, the results of the approximate relations are acceptable for frequency ratios less than nearly (0.7).

4.9 Summary and Conclusions

Under the effect of harmonic excitation, the rigid block may vibrate periodically, overturn, or remain stationary. Considering the frequency-acceleration domain for the excitation, steady-state periodic motion is possible within a wedge in the domain. As the restitution coefficient decreases, the upper and lower limits for this wedge shift upwards. For a specified acceleration amplitude, the maximum steady-state response amplitude occurs at a low frequency and the response amplitude decreases monotonically as the excitation frequency increases. If the periodic motion is unstable, overturning of the rigid block can occur. For situations with stable steady-state periodic motion, overturning can still occur if the transient phase of the response exhibits excessive rotations. From the results obtained, it is found that, as the restitution coefficient decreases, the system becomes more stable against overturning and can withstand higher accelerations. In this study, simpler approximate relations governing the existence of the steady-state periodic motion are derived and applied. The approximate relations are found to be accurate for practice.

CHAPTER 5

RESPONSE OF PARTIALLY FIXED EQUIPMENT

WITH

RIGID BOLTS

5.1 Introduction

It has been shown before by many researchers that systems which are allowed to rock on their foundations may have a better chance of surviving a severe earthquake than systems with fixed bases, because, there can be considerable reductions in the deformations of the systems allowed to rock, compared to those whose bases are fixed. This is due to the energy dissipation between the foundation and the ground during rocking. Unfortunately, rocking involves the risk of overturning if the response built up exceeds a certain level. Furthermore, overturning potential is a highly complex phenomenon which depends to a great extent on the time history of the base excitation. If the system is fastened loosely to the foundation, however, the advantages of rocking can be gained without the risk of overturning. In this case, the system is allowed to rock up to a maximum angle, but is restrained from rocking beyond the allowable angle of tilt by an anchor system. A system loosely mounted on the floor cannot overturn unless the anchor system fails. Partially fixed systems belong to an intermediate category between the two extremes for mounting equipment on floors, i.e., complete fixation and no attachment at all.

106

In this chapter, the behaviour of partially-fixed systems subjected to harmonic excitation and earthquake-induced floor motions is investigated. It is intended in this research to provide a clear understanding of the behaviour of these systems under base excitations. The response will be presented in the form of either frequency-response curves or response time histories, for each of the parameters governing the response.

5.2 Model and Assumptions

In this analysis, the model considered is assumed to be constrained so that only displacements in the plane parallel to the direction of floor excitation are possible. Also, it is assumed that the deformations of the equipment frame are small. The equipment is represented by a continuous linear system which has distributed parameters for mass, damping and cross-sectional area; m, c and A, respectively. To simplify the analysis, the continuous system is assumed to respond in a single prescribed mode. Thus, the total number of deformation degrees of freedom is reduced to one. The system is considered non-deformable in the direction normal to the base and the mode of response corresponds to the first lateral-vibration mode of a shear beam. The system is assumed to be welded to a rigid massless rectangular plate of width 2b, as illustrated in Fig. (5.1). The rigid plate is fastened to a rigid floor by an anchor system represented in the model by two identical bolts placed at equal distances from the edges of the base plate. The bolts are not fastened tightly to the base plate, and gaps are left between their heads and the base plate so that

the base plate can uplift above the rigid floor, allowing the entire system to rock. The force-displacement relationship of the bolts is assumed to be of a rigid-plastic type. The coefficient of friction between the base plate and the rigid floor is assumed to be sufficiently large to prevent the system sliding along the floor. Figure (5.2) illustrates the force-displacement relationship of one of the bolts. The displacement Δ_p., represented by the horizontal axis, is the displacement of point p' on the plate in the axial direction of the bolt. The initial gap size is termed g_o, while the gap size after the stretching of bolts occurs is termed g_t. It is assumed that the bolts are subjected only to tensile forces, produced when the base plate uplifts with a sufficient amplitude to touch the bolts. At any instant, the configuration is determined by the following two degrees of freedom: the rotation of the base plate relative to the floor $\theta(t)$, and the lateral deformation of the continuous system relative to the base plate. The lateral deformation is measured by a displacement function $u(y,t)$, where u is the lateral displacement of the equipment system parallel to the base plate at height y and time t. The system is assumed to be excited by a horizontal total floor acceleration $\ddot{x}$. During such an excitation, five stages of response can occur. These stages, shown in Fig. (5.3.a), are described below.

Stage 1

At the beginning, the base plate is at rest. The equipment system vibrates laterally under the effect of the lateral floor acceleration. The deformation of the continuous system, relative to the
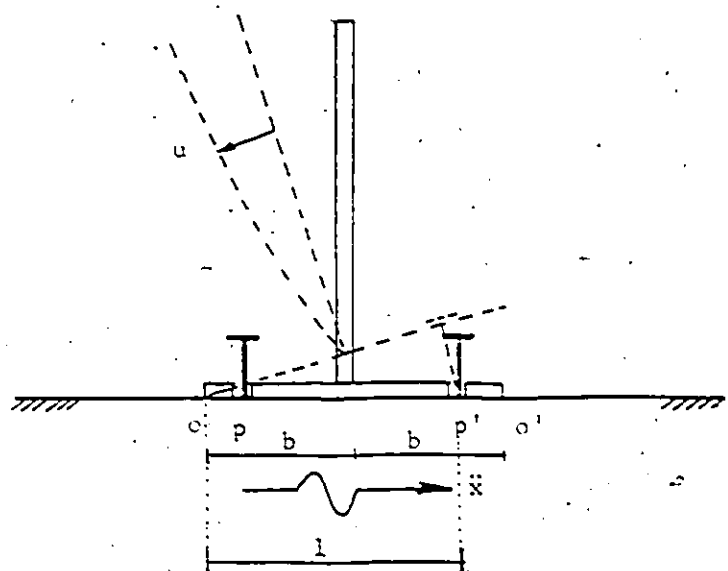
Fig. (5.1)   Partially fixed system
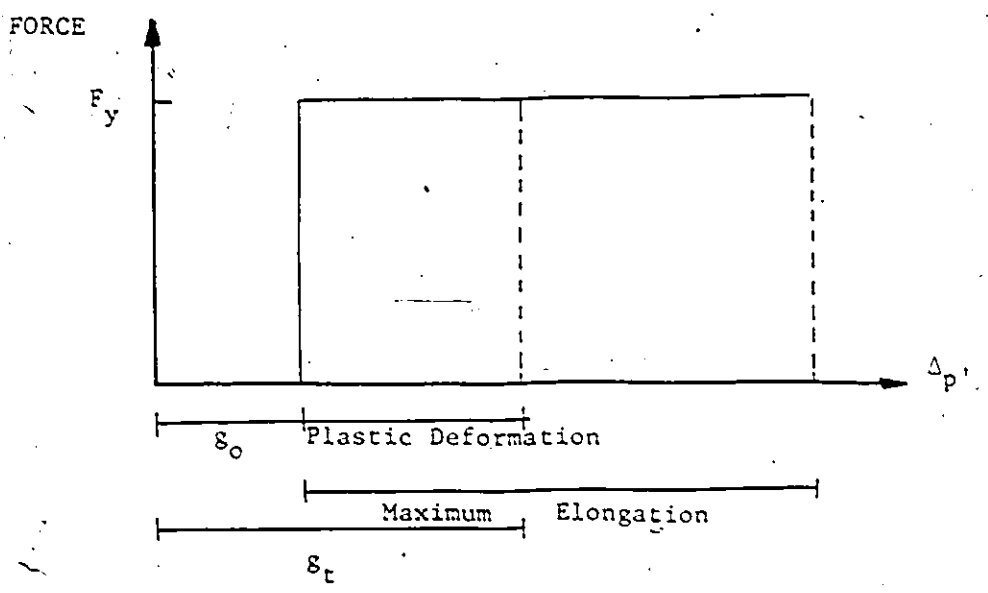
Fig. (5.2)   Force-displacement relationship of a rigid-plastic bolt
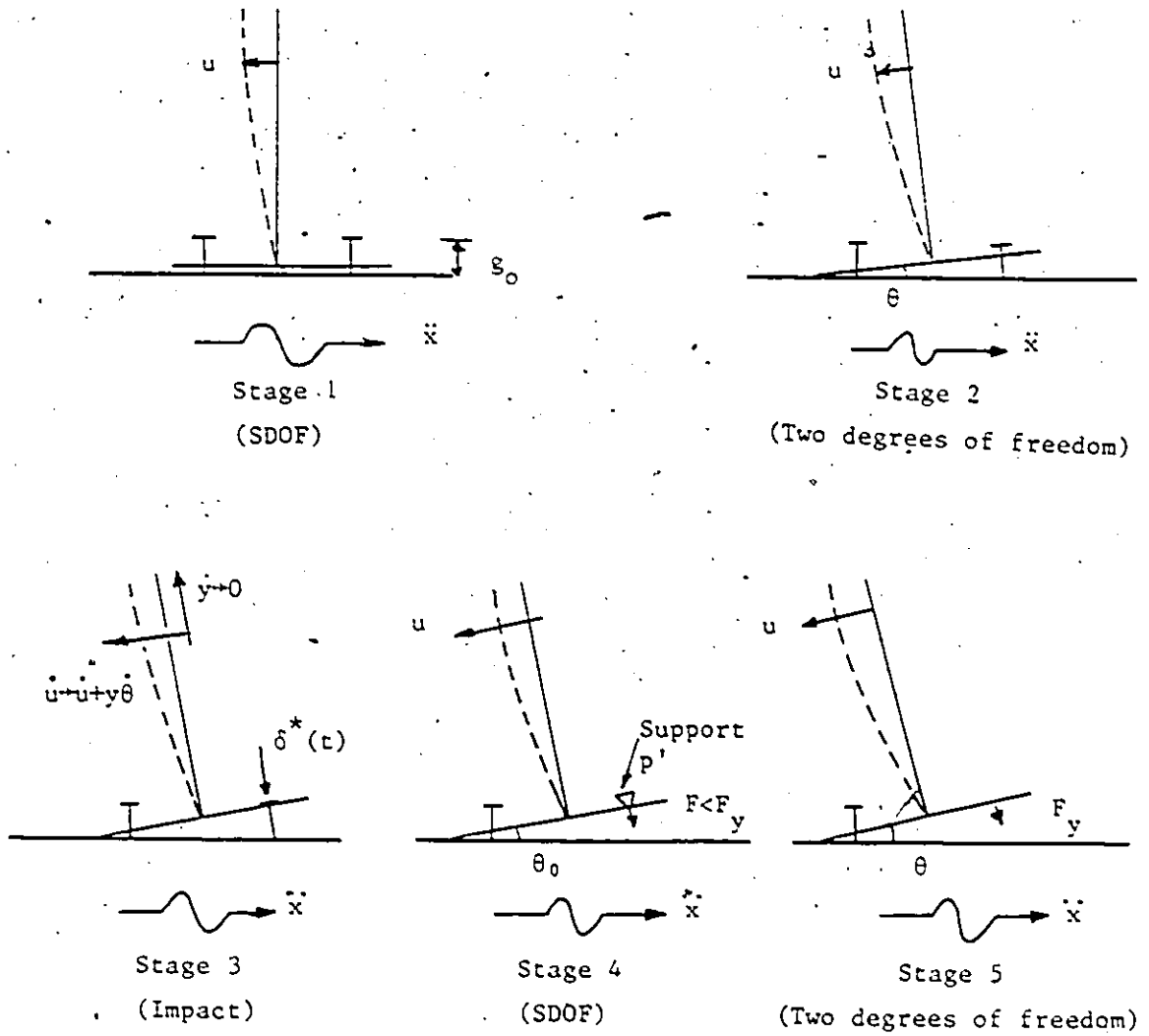
Fig. (5.3.a) Response stages

base plate, is expressed by a single prescribed mode. Therefore, the system vibrates as a single degree of freedom (SDOF) system on a fixed base. This stage will continue as long as the conditions of uplift are not satisfied. Once these conditions are fulfilled, stage 1 will end, uplift will occur and stage 2 will start.

Stage 2

In this stage, the base plate is uplifted from the rigid floor. The system has two degrees of freedom. These degrees of freedom are the rotation of the base plate relative to the floor $\theta(t)$ and the deformation $u(y,t)$ of the continuous system relative to the base plate. In this stage, no bolt forces are applied to the base plate, because the axial displacement of point p' is less than the total gap g_t at that point. The total gap g_t may have a constant or an increasing value depending on the response of the system. If the bolt is non-yielding, the total gap will remain the same as the initial gap g_o. If it yields, the total gap will be equal to the sum of the initial gap plus the permanent deformation of the bolt. Stage 2 will continue as long as the axial displacement of point p' does not exceed the total gap and will end in either of two ways. If the axial displacement of point p' exceeds the total gap g_t, the system will enter stage 3 of the response behaviour. If the rocking amplitude of the base plate decays, rocking will stop after a number of high-frequency impacts with the floor and the response will return to stage 1.

Stage 3

This stage represents the impact between the base plate and the

bolt head. The impact is assumed to be instantaneous and the impact force is represented by a Dirac delta-function, $\delta^*(t)$. It is assumed that the dynamic stresses during the impact with the bolt will not cause the bolt to yield or break. It is also assumed that the impact will stop the angular velocity $\dot{\theta}$ of the base plate instantaneously, and the velocity component of the equipment elements in the direction normal to the base plate will become zero. After the impact, the response will enter stage 4.

Stage 4

In this stage, the base plate is supported at two points, .o and p'. The reaction at o is upward while the reaction at p' is downward, restraining further rotational motion of the plate. During this stage, the restraining bolt is in tension. The system again responds as a SDOF system. Assuming that the reaction in the bolt at this stage is less than its yield strength, the rigid-plastic bolt will not stretch. This stage will end in one of two ways. If the bolt force exceeds its yield strength, the response will enter stage 5. If the bolt reaction reduces to zero, then the base plate separates from the bolt head and the response will return to stage 2.

Stage 5

In this stage, the system has two degrees of freedom again. These degrees of freedom are the rotation of the base plate and the lateral deformation of the continuous system. The base plate is acted upon by a tensile force equal to the bolt's yield strength. Yielding

causes the bolt to elongate and to absorb some energy. This stage will end in one of two ways. If the tensile force in the bolt decreases to below the bolt's yield strength then the response will return to stage 4. If the criterion of failure is satisfied, the bolt will break, the base plate will no longer be restrained by the bolt force, and the response will return to stage 2.

The second half of the rocking cycle starts when the base plate impacts with the floor, and the rocking of the system will take place about o' instead of o. Then the angle of rotation θ changes sign and a similar set of the five response stages are followed, with the left bolt providing the restraining force. Figure (5.3.a) shows the different stages of response discussed above. Figure (5.3.b) presents a flow-chart which describes the response transition from one stage to another.

5.3 Failure Criterion

In this study, the bolts are subjected to repeated loading causing uniaxial tension forces. Figure (5.4) illustrates the possible bolt force-deformation paths. If the number of repetitions is large, fatigue of the bolts can be a problem. In earthquake engineering, however, where the duration of excitation is generally limited, fatigue failure may not be a serious problem. Therefore, fatigue failure of the bolts is not considered in this investigation. Excessive yielding of the bolts, however, can lead to failure. A simple failure criterion is used herein by assuming that a bolt will fail in the same way it fails under a uniaxial monotonic increasing static tension test. This criterion is based on either of two concepts: a) the bolt will fail

Negative. | Positive
Rotation | Rotation

```
                              ┌─────────────────────────────────┐
                              │          Stage 1                │
                              │  SDOF system on a fixed base     │
                              └─────────────────────────────────┘
                                    ↑                │
                                  High            Uplift
                                frequency        condition
                                 impact          satisfied
                                    │                ↓
  ┌────────┐              ┌─────────────────────────────────┐
  │Stage 2 │  Floor impact│          Stage 2                │
  │        │ ←──────────→ │  Two degree of freedom system    │
  │        │   ───────────→│        Δp'<gt'                  │
  └────────┘              │       No bolts forces            │
                          └─────────────────────────────────┘
                                                      │ Λp'=St
                                   Bolt               ↓
                                 tension=0.  ┌─────────────────────┐
                                    │        │      Stage 3        │
                                    │        │  Base plate impacts │
                                    ↑        │    with the bolt    │
                                             └─────────────────────┘
           Bolt               ┌─────────────────────────────────┐
           breaks             │         Stage-4                 │
                              │ SDOF system on a fixed base     │ ←──
                              │        Δp'=gt                    │
                              │  Bolt tension less than          │
                              │      yield strength              │
                              └─────────────────────────────────┘
                                    ↑                │
                               Bolt force          Bolt
                               less than           yields
                                 yield               │
                                    │                ↓
                              ┌─────────────────────────────────┐
                              │         Stage 5                 │
                              │  Two degree of freedom system    │
                              │       Bolt yields                │
                              └─────────────────────────────────┘
```

Fig. (5.3.b)
Transition between
different stages

BOLT FORCE
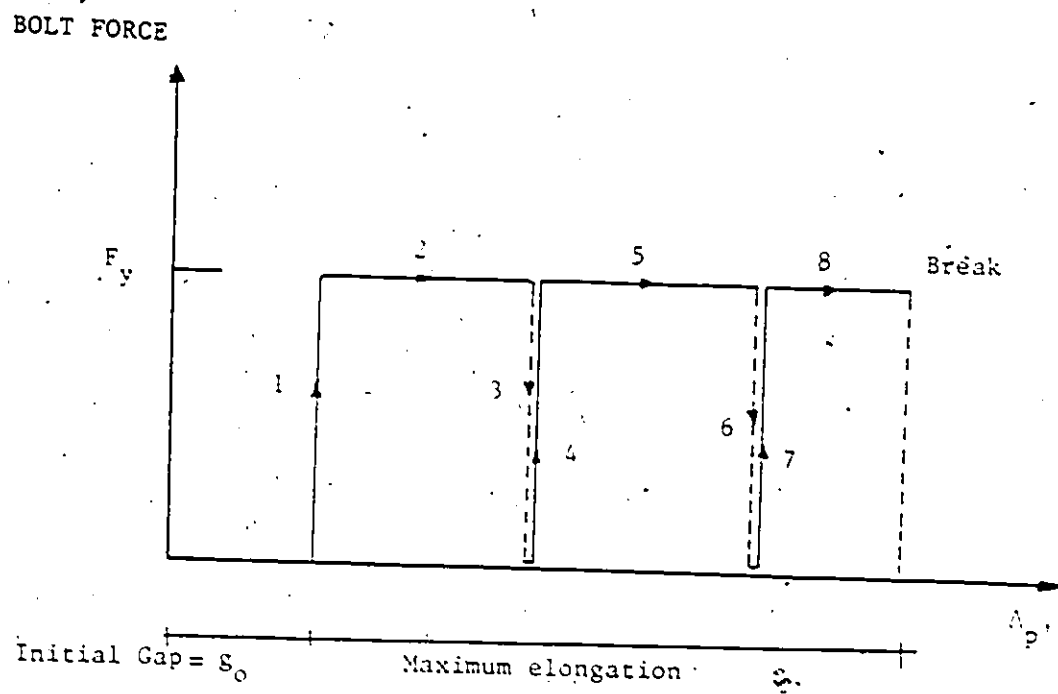
Fig. (5.4)   Stress loops in a rigid-plastic bolt

when the energy absorbed through yielding reaches a maximum limit, or
b) it will fail at a maximum strain. In this analysis, if the
accumulated absorbed energy of the bolt exceeds the toughness of the
material multiplied by its volume, the bolt is assumed to break. Also,
if either the left or the right anchor bolt breaks, the equipment system
is considered to have failed (overturned).

5.4 Equations of Motion

The differential equations governing the system motion are
obtained by considering the dynamic equilibrium of:

    a) the forces acting on the system in the lateral direction parallel

       to the base plate, and

    b) the moment of forces about the center of rotation of the base

       plate.

In the following subsections, the equations of motion for each stage are
derived.

5.4.1 Equations of Motion for Stage 1

Figure (5.5) shows the forces acting on a differential mass
element during stage 1. The system response is governed, in this stage,
by the differential equation of a damped shear beam,

$$m \left(\frac{\partial^2 u}{\partial t^2} - \frac{d^2 x}{dt^2} \right) - GA \frac{\partial^2 u}{\partial y^2} + c \frac{\partial u}{\partial t} = 0 \tag{5.1}$$

where u is the lateral displacement of the shear beam parallel to the
base plate at height y and time t, x is the total floor displacement in
the horizontal direction and m, G and A are, respectively, the beam mass
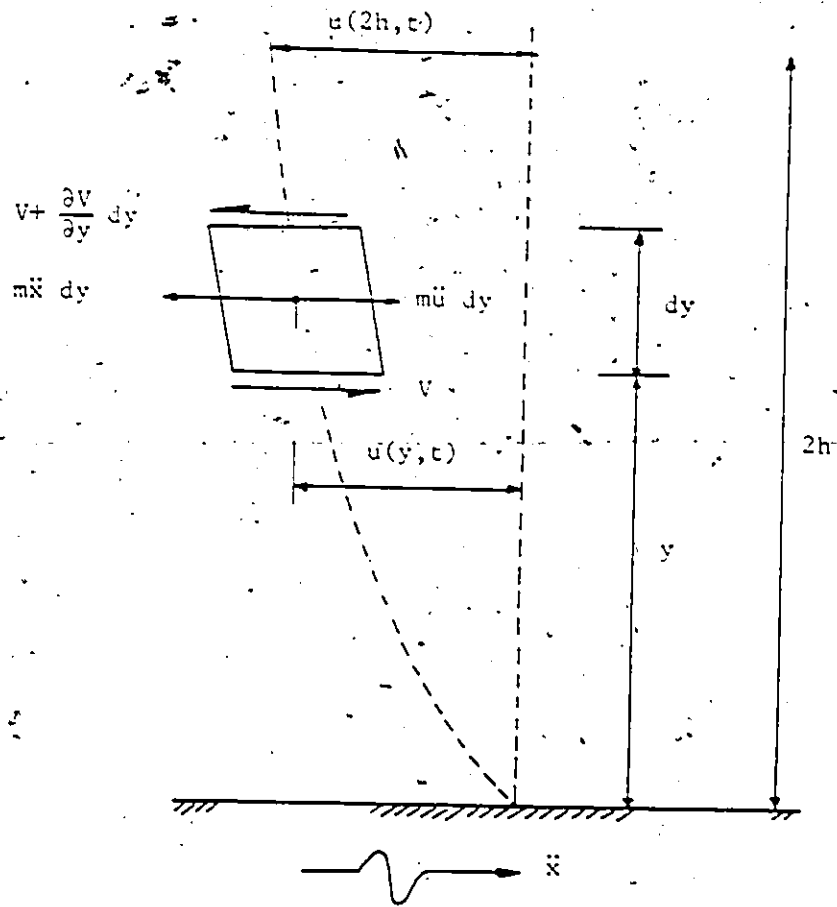
Fig. (5.5)   Forces equilibrium during stage 1

per unit length, the shear modulus and the shear cross-sectional area.

If the beam is assumed to deform in a prescribed mode $\phi(y)$, such that

$$u(y,t) = U(t) \cdot \phi(y) \qquad (5.2)$$

the differential equation (5.1) is reduced to

$$M^* \ddot{U} + C^* \cdot \dot{U} + K^* U = N^* \ddot{x} \qquad (5.3.a)$$

The dots, in the above equation, represent ordinary differentiation with respect to time and

$$M^* = \int_0^{2h} m \phi^2 \, dy$$

$$C^* = \int_0^{2h} c \phi^2 \, dy$$

$$K^* = - \int_0^{2h} GA \, \phi \cdot \phi`` \, dy$$

and

$$N^* = \int_0^{2h} m \phi \, dy$$

$2h$ is the total length of the shear beam, and the dashes represent ordinary differentiation with respect to the spatial variable y.

Equation (5.3.a) can be written in the standard form

$$\ddot{U} + 2 \xi \omega \dot{U} + \omega^2 U = \frac{N^*}{M^*} \ddot{x} \qquad (5.3.c)$$

where ω is the natural frequency of the system on a fixed base and ξ is

the percentage of critical damping.

When an assumed mode shape identified with the first free vibration mode of a uniform shear beam is used, i.e.,

$$\phi(y) = \sin\left[\frac{\pi y}{4h}\right]$$

the generalized coordinate $U(t)$ then has the physical interpretation as the lateral displacement at the top of the equipment frame, or

$$U(t) = u(2h,t)$$

5.4.2 Condition for Uplift

As stated previously, the system will remain in stage 1 until the condition of uplift is satisfied. Mathematically, uplift occurs when the overturning moment about the base plate edge exceeds the counteracting moment due to the weight of the system, namely

$$\left| \int_0^{2h} m \left[\frac{d^2x}{dt^2} - \frac{\partial^2 u}{\partial t^2} \right] y \, dy \right| > Wb \tag{5.3.d}$$

where W is the weight of the equipment and b is the half-width of the base plate.

5.4.3 Equations of Motion for Stage 2

In this stage, the equipment is vibrating while the base plate is uplifting from the floor, as shown in Fig. (5.6). The bolts are not stressed. Two conditions of dynamic equilibrium are considered, namely, the equilibrium of forces in the lateral direction of a differential

Total equilibrium

$m\ddot{u}\ dy$

$M\ddot{x}$

CG

w

α

θ

$I_o\ddot{\theta}$

$ms\dot{\theta}^2\ dy$

$V + \dfrac{\partial V}{\partial y}\ dy$

$m\ddot{u}\ dy$

$m\ddot{x}\ dy$

V

$ms\ddot{\theta}\ dy$

$c\dot{u}\ dy$

s

θ

$\ddot{x}$

dy

$2h$

y

Element equilibrium
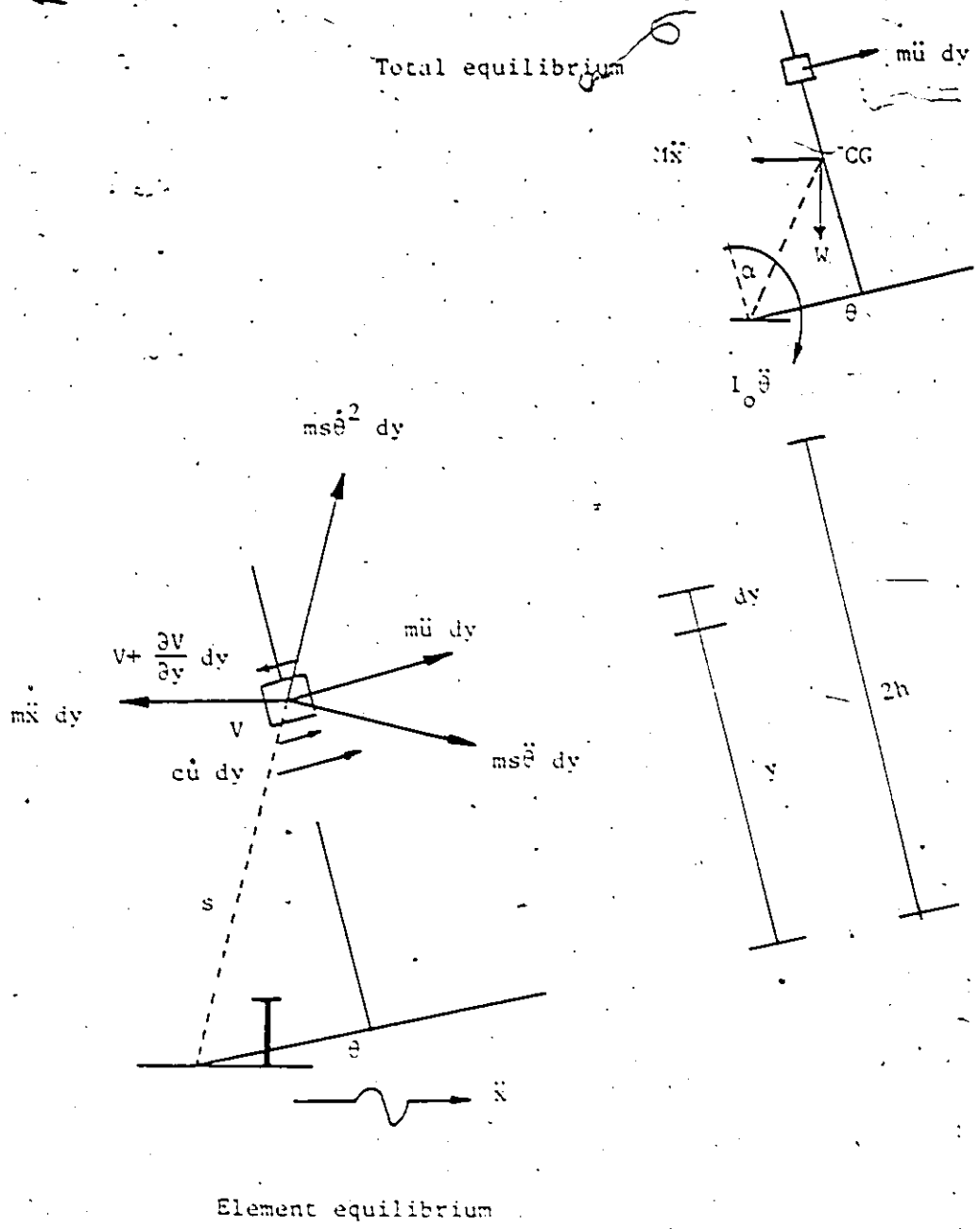
Fig. (5.6)   Forces equilibrium during stage 2

mass element, and the equilibrium of moments about the center of rotation o. It should be noted that during the rotation of the base plate, two additional components of acceleration should be taken into account when considering the equilibrium conditions for the differential mass element. The first component is radial and equal to $s\dot{\theta}^2$, where s is the radial distance between the differential element and the center of rotation. The second component is tangential and equal to $s\ddot{\theta}$. The equilibrium condition in the lateral direction, parallel to the base plate, can be expressed as

$$m \frac{\partial^2 u}{\partial t^2} + my \frac{d^2\theta}{dt^2} = m \frac{d^2 x}{dt^2} \cos(\theta) - mb \left[\frac{d\theta}{dt}\right]^2 - GA \frac{\partial^2 u}{\partial y^2} - c \frac{\partial u}{\partial t} + mg \sin(\theta)$$

(5.4)

The transformation given by equation (5.2) can then be used to account for the spatial variation of forces. By substituting equation (5.2) into equation (5.4), multiplying the resulting equation by ϕ and integrating over the beam length, the following equation is obtained:

$$M^* \ddot{U} + F^* \ddot{\theta} = N^* [\ddot{x} \cos(\theta) - b\dot{\theta}^2 + g \sin(\theta)] - K^* U - C^* \dot{U}$$

(5.5)

where M^*, K^*, C^* and N^* are defined in equation (5.3.b) and

$$F^* = \int_0^{2h} my\phi \, dy$$

Equating the moment of all forces about the center of rotation o to zero gives the following equation:

$$I_o \ddot{\theta} + WR \sin(\alpha-\theta) - MR \ddot{x} \cos(\alpha-\theta) = -F^* \ddot{U}$$

(5.6)

where I_o is the equipment mass moment of inertia about point o. W is the equipment weight and M is its mass. R is the distance between the center of mass and the center of rotation of the system o. The angle α is the angle between the line connecting the center of mass and point o, and the normal to the base plate.

The initial conditions of any (stage j) depend on the immediately preceding (stage i) as shown in Fig. (5.3.b). Define

θ_{ei} as the angle of rotation at the end of stage i.

θ_{sj} as the angle of rotation at the start of stage j.

U_{ei} as the generalized displacement of the equipment at the end of stage i, and

U_{sj} as the generalized displacement of the equipment at the start of stage j.

In general,

$$\theta_{sj} = \theta_{ei}$$

$$\dot{\theta}_{sj} = \dot{\theta}_{ei}$$

$$U_{sj} = U_{ei}$$

and

$$\dot{U}_{sj} = \dot{U}_{ei} \tag{5.7}$$

where stage j follows stage i. There are special cases, however, which will be mentioned. For the case of transition from stage 1 to stage 2,

$$\theta_{s2} = \dot{\theta}_{s2} = 0 \tag{5.8}$$

For the case of transition from stage 4 to stage 2,

$$\theta_{s2} = \theta_o$$

and

$$\dot{\theta}_{s2} = 0 \tag{5.9.a}$$

where θ_o is the angle of rotation at which the base plate is just in touch with the bolt and is defined by

$$\sin \frac{\theta_o}{2} = \frac{g_t}{2l} \qquad\qquad (5.9.b)$$

where g_t is the total gap size and l is the distance between the point p' and the center of rotation o.

5.4.4 Stage 3 (Base Plate-Bolt Impact)

This stage occurs instantaneously, and can be considered a transition stage between two stages of motion. In this stage, the base plate hits the bolt and is acted upon by an impulsive force expressed by a Dirac delta-function. It is assumed that, at the end of this stage, the velocity of the system elements in the direction normal to the base plate vanishes, and the angular velocity of the base plate becomes zero.

5.4.5 Equations of Motion for Stage 4

This stage is similar to stage 1 with the difference that the system is now offset by an angle θ_o with the rest position, as shown in Fig. (5.7). The angle θ_o is defined by equation (5.9.b). Therefore, the equation of motion obtained from the equilibrium of a differential element in the lateral direction has the form:

$$m \frac{\partial^2 u}{\partial t^2} - m \frac{d^2 x}{dt^2} \cos(\theta_o) - GA \frac{\partial^2 u}{\partial t^2} + c \frac{\partial u}{\partial t} - mg \sin(\theta_o)=0 \qquad (5.10)$$

Using the transformation given by equation (5.2), equation (5.10) can be

124
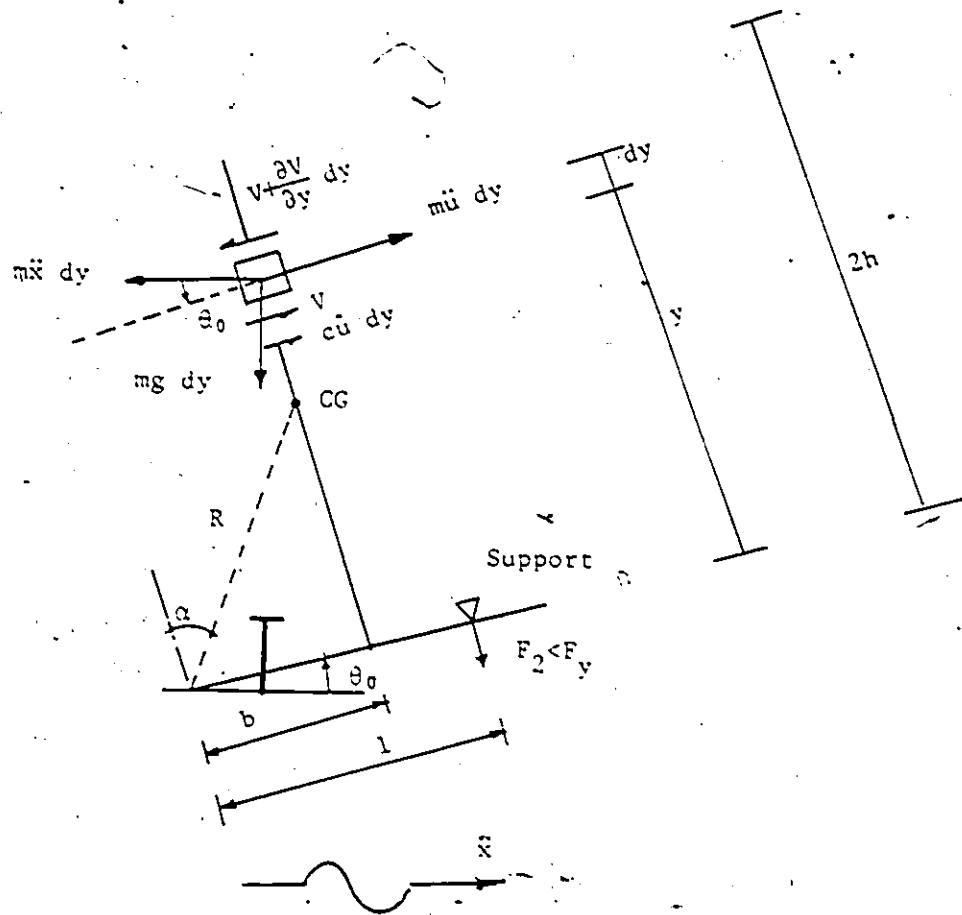
Fig. (5.7)   Forces equilibrium during stage 4

put in the form:

$$\ddot{U} + 2\xi\omega\,\dot{U} + \omega^2\,U = \frac{N^*}{M^*}\,\ddot{x}\,\cos(\theta_o) + \frac{N^*}{M^*}\,g\,\sin(\theta_o) \qquad (5.11)$$

This stage will continue as long as the bolt force (the reaction) is tension and is less than its yield strength. Mathematically, this condition can be expressed as

$$0 < F_2 < F_y \qquad (5.12)$$

where F_2 is the tension force in the right bolt and F_y is its yield strength. The bolt force can be defined from the moment equation

$$F_2 \; l \; \cos\frac{\theta_o}{2} = MR\,\frac{d^2x}{dt^2}\,\cos(\alpha-\theta_o) - \int_0^{2h} my\,\frac{\partial^2 u}{\partial t^2}\,dy - WR\,\sin(\alpha-\theta_o)$$

$$(5.13)$$

For the initial conditions, if stage 4 follows stage 3,

$$\theta_{s4} = \theta_o$$

$$\dot{\theta}_{s4} = 0$$

and

$$\frac{\partial u}{\partial t}\Bigg|_{s4}^{t_b} = \frac{\partial u}{\partial t}\Bigg|_{e2}^{t_b} + y\,\frac{d\theta}{dt}\Bigg|^{t_b} \qquad (5.14.a)$$

where the derivatives of u and θ are calculated at the time t_b of impact between the base plate and the bolt. The subscripts s4 and e2 refer to the corresponding variables at the start of stage 4 and the end of stage 2, respectively. The last condition of equation (5.14.a) should be satisfied at every point through the entire height of the system.

However, the single mode representation of the field displacement u cannot satisfy this condition. An approximate way to satisfy it is by integrating the equation over the whole system height, giving

$$\int_0^{2h} \left. \frac{\partial u}{\partial t} \right|_{s4}^{tb} dy = \int_0^{2h} \left. \frac{\partial u}{\partial t} \right|_{e2}^{tb} dy + \int_0^{2h} y \left. \frac{d\theta}{dt} \right|^{tb} dy$$

(5.14.b)

Equation (5.14.b) implies that the total momentum in the lateral direction is kept constant during the impact between the base plate and the bolt. Using the transformation given by equation (5.2), equation (5.14.b) can be expressed as

$$\dot{U}_{s4} = \dot{U}_{e2} + \frac{\pi h}{2} \dot{\theta}$$

(5.14.c)

For the case of transition from stage 5 to stage 4,

$$\dot{\theta}_{s4} = 0$$

(5.14.d)

5.4.6 Equations of Motion for Stage 5

The response behaviour in stage 5 is similar to that in stage 2, i.e., the system is vibrating laterally while the base plate is rotating, as shown in Fig. (5.8). The difference between these two stages is that, while the bolt is not stressed in stage 2, the bolt is stressed at the yield level in stage 5, and some energy of the system is absorbed due to the yielding of the bolt. The two conditions of dynamic equilibrium applied for stage 2, will be applied again for stage 5. First, there is the equilibrium of forces in the lateral direction of a differential element of mass, and the resulting equation is the same as

Total equilibrium
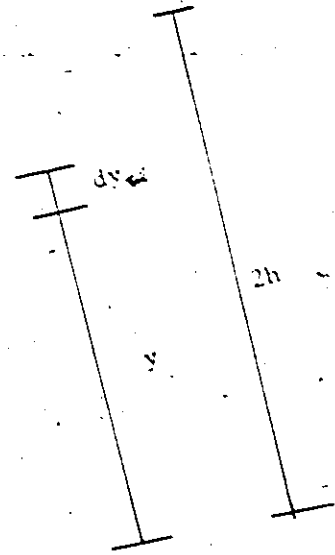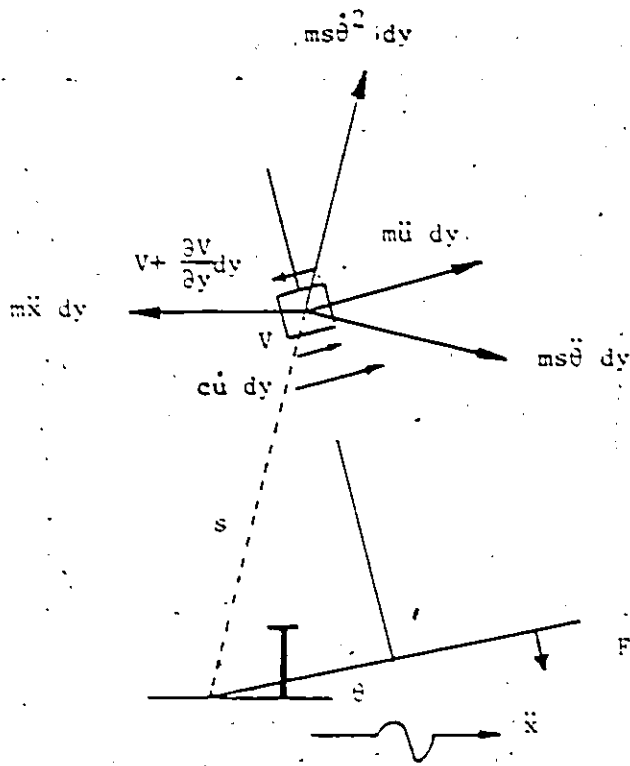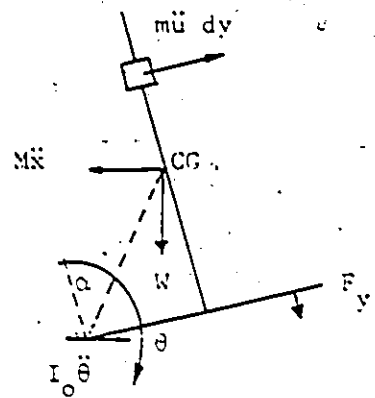
Element equilibrium

Fig. (5.8)   Forces equilibrium during stage 5

equation (5.4). Second, there is the equilibrium of moments about the center of rotation o, and this gives

$$I_o \ddot{\theta} - MR \ddot{x} \cos(\alpha-\theta) + WR \sin(\alpha-\theta) + F_y l \cos(\frac{\theta}{2}) = -F^* \ddot{U} \tag{5.15}$$

The initial conditions of stage 5 are

$$\theta_{ss} = \theta_o$$

and

$$\dot{\theta}_{ss} = 0 \tag{5.16}$$

It is noted that equation (5.6), derived for stage 2, is a special case of equation (5.15) and can be obtained by omitting the bolt force term from equation (5.15).

5.4.7 Equations of Motion for Negative Rotations

Equations (5.5, 5.6, 5.11 and 5.15) were derived for positive angles of rotation, i.e., the base plate rotates about the left edge o. Similar equations can be derived when the base plate rotates about the right edge o'. In this case, the corresponding equations are as follows.

Stage 2

Equation (5.5) becomes

$$M^* \ddot{U} + F^* \ddot{\theta} = N^* [\ddot{x} \cos(\theta) + b \dot{\theta}^2 + g \sin(\theta)] - K^* U - C^* \dot{U} \tag{5.5}^*$$

and equation (5.6) takes the form:

$$I_o \ddot{\theta} - WR \sin(\alpha+\theta) - MR \ddot{x} \cos(\alpha+\theta) = - F^* \ddot{U} \tag{5.6}^*$$

Stage 4

Equation (5.11) becomes

$$\ddot{U} + 2\xi\omega\,\dot{U} + \omega^2\,U = \frac{N^*}{M^*}\,\ddot{x}\,\cos(\theta_0) - \frac{N^*}{M^*}\,g\,\sin(\theta_0)\,. \tag{5.11}^*$$

Stage 5

Equation (5.15) becomes .

$$I_0\,\ddot{\theta} - MR\,\ddot{x}\,\cos(\alpha+\theta) + WR\,\sin(\alpha+\theta) + F_y l\,\cos\frac{\theta}{2} = -F^*\,\ddot{U} \tag{5.15}^*$$

It is noted that, for negative rotation of the base plate, the following terms change signs:

	$(\alpha-\theta)$	becomes	$(\alpha+\theta)$
	$-b\,\dot{\theta}^2$	becomes	$+b\,\dot{\theta}^2$
and			
	$+g\,\sin(\theta_0)$	becomes	$-g\,\sin(\theta_0)$

5.4.8 Impact Between the Base Plate and the Floor

At the instant of impact with the floor, the kinetic energy reduction is accounted for by assuming that the angular velocity $\dot{\theta}(t)$ is reduced from $\dot{\theta}_b$ (just before impact) to $\dot{\theta}_a$ (just after impact) such that

$$\dot{\theta}_a = \delta\,\dot{\theta}_b \quad , \qquad 0 < \delta < 1 \tag{5.17}$$

For rigid blocks rocking on rigid floors, a restitution coefficient δ could be estimated (Housner, 1963) by assuming that the angular momentum about the edge of impact with the floor is conserved during the impact. In this analysis, if it is assumed that the angular momentum is also conserved for the flexible system, and if the transformation given by equation (5.2) is used, the following equation is obtained:

$$I_o \dot{\theta}_a + \dot{U}_a \int_o^{2h} m\phi y \, dy = I_o \dot{\theta}_b - 2Mb^2 \dot{\theta}_b + \dot{U}_b \int_o^{2h} m\phi y \, dy \qquad (5.18)$$

where u_b and u_a are, respectively, the velocities of the differential mass element just before and after the impact. If it is assumed that the restitution coefficient has the same expression derived by Housner (1963) for rocking of rigid blocks, δ will be expressed as

$$\delta = \frac{I_o - 2Mb^2}{I_o} \qquad (5.19)$$

If equations (5.17) and (5.19) are substituted into equation (5.18), then solving leads to

$$\dot{U}_a = \dot{U}_b \qquad (5.20)$$

In other words, after the impact with the floor, there is a reduction in the angular velocity of the base plate, but there is no reduction in the lateral relative velocity of the system.

5.4.9 Equations of Motion for Small Angle of Rotation

Equations of motion for stages 2, 3, 4 and 5 were derived for a large angle of rotation. Simplification is possible if the angles θ, β_o and α are assumed to be small. In this case, the equations of motion for these stages will be as follows.

Stage 2

Equations (5.5) and (5.5)* become

$$M^* \ddot{U} + F^* \ddot{\theta} = N^*[\ddot{x} \mp b \dot{\theta}^2 + g \theta] - K^* U - C^* \dot{U} \qquad \theta \gtrless 0 \tag{5.21}$$

and equations (5.6) and (5.6)* take the form:

$$I_o \ddot{\theta} - WR (\theta \mp \alpha) - MR \ddot{x} = - F^* \ddot{U} \qquad \theta \gtrless 0 \tag{5.22}$$

Stage 4

Equations (5.11) and (5.11)* become

$$\ddot{U} + 2\xi\omega \dot{U} + \omega^2 U = \frac{N^*}{M^*} \ddot{x} \pm \frac{N^*}{M^*} g \theta_o \qquad \theta \gtrless 0 \tag{5.23}$$

Stage 5

Equations (5.15) and (5.15)* are reduced to

$$I_o \ddot{\theta} - MR\ddot{x} + WR(\theta \mp \alpha) + F_y l = -F^* \ddot{U} \qquad \theta \gtrless 0 \tag{5.24}$$

Further reduction is also possible if the horizontal floor acceleration $\ddot{x}$ is considerably larger than $g\theta$. In this case, equation (5.21) is simplified to

$$M^* \ddot{U} + F^* \ddot{\theta} = N^*[\ddot{x} \mp b \dot{\theta}^2] - K^* U - C^* \dot{U} \qquad \theta \gtrless 0 \tag{5.25}$$

and equation (5.23) takes the standard form

$$\ddot{U} + 2\xi\omega \dot{U} + \omega^2 U = \frac{N^*}{M^*} \ddot{x} \tag{5.26}$$

5.5 Floor Motion

In general, equipment installed inside a structure is fixed to a

floor which vibrates when the structure is subjected to an earthquake ground motion. If it is assumed that the mass of the equipment is small relative to the mass of the structure, then the equipment will be subjected to an excitation which is equivalent to the motion of the floor to which it is mounted, as shown in Fig. (5.9). The frequency content of the floor motion will be different from that of the actual earthquake ground motion in that the frequencies which differ from the natural frequency of the structure tend to be filtered out. In this study, the response of the equipment subjected to floor motions caused by the occurrence of earthquakes is investigated.

To generate these floor motions, two different earthquake excitations are examined, the El Centro (1940) N-S component and the Taft (1952) S69E component. Each of these components is applied to a symmetric single-storey structure with a rigid floor. The structure is assumed to have a damping ratio equal to 0.05, and a natural frequency equal to the natural frequency of the equipment on a fixed base. This situation would provide a severe excitation to the equipment placed on the floor. In the present case, the equipment (as will be shown later) has a natural frequency of 5 Hz when it is mounted on a fixed base. Therefore, the structure is assumed to have a natural frequency of 5 Hz.

If the structure is assumed to be linear, the equation of motion will be

$$\ddot{x}^r + 2\xi_s\omega_s \; \dot{x}^r + \omega_s^2 \; x^r = - \; \ddot{x}_g \qquad (5.27)$$

where x^r is the displacement of the floor relative to the foundation system in the horizontal direction, ω_s and ξ_s are the natural frequency
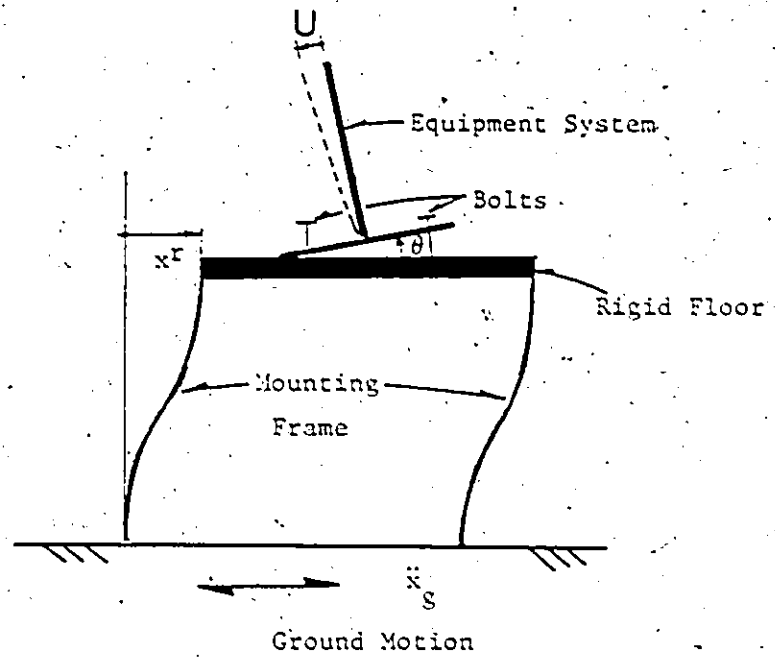
Fig. (5.9)   Equipment mounted on a SDOF structure

and the percentage of critical damping of the structure, respectively, and $\bar{x}_g$ is the ground acceleration.

The total floor acceleration $\bar{x}$ is expressed as

$$\bar{x} = \bar{x}^r + \bar{x}_g \tag{5.28}$$

To find out the response of the equipment system to the transient floor motion, the total floor acceleration $\bar{x}$ is calculated first using equation (5.28). Then it is substituted in the governing equations of rocking (5.1) to (5.26). Figures (5.10) and (5.11) present the floor response (total acceleration) calculated by equations (5.27) and (5.28) for the two earthquake components.

5.6 Verification of the Computer Program

The mathematical model which describes the equipment response was coded in a Fortran-iv program called BOLT. This computer program is used to compute the response of the system subjected to harmonic and transient floor motion excitations. The differential equations of motion are integrated using Newmark-β method (Newmark, Rosenblueth, 1971) with a variable time step.

Figure (5.12) shows the dimensions of a typical cabinet housing telecommunication electronic equipment. The cabinet has a mass of 454 kg and is fastened to the floor by four half-inch diameter bolts. The mass is assumed to be evenly distributed throughout the cabinet. Based on dynamic testing, the cabinet has a fundamental frequency equal to 5 Hz. This value of frequency is used to estimate an equivalent GA for the shear beam model. From the free vibration analysis of a shear beam on a fixed base, it is found that
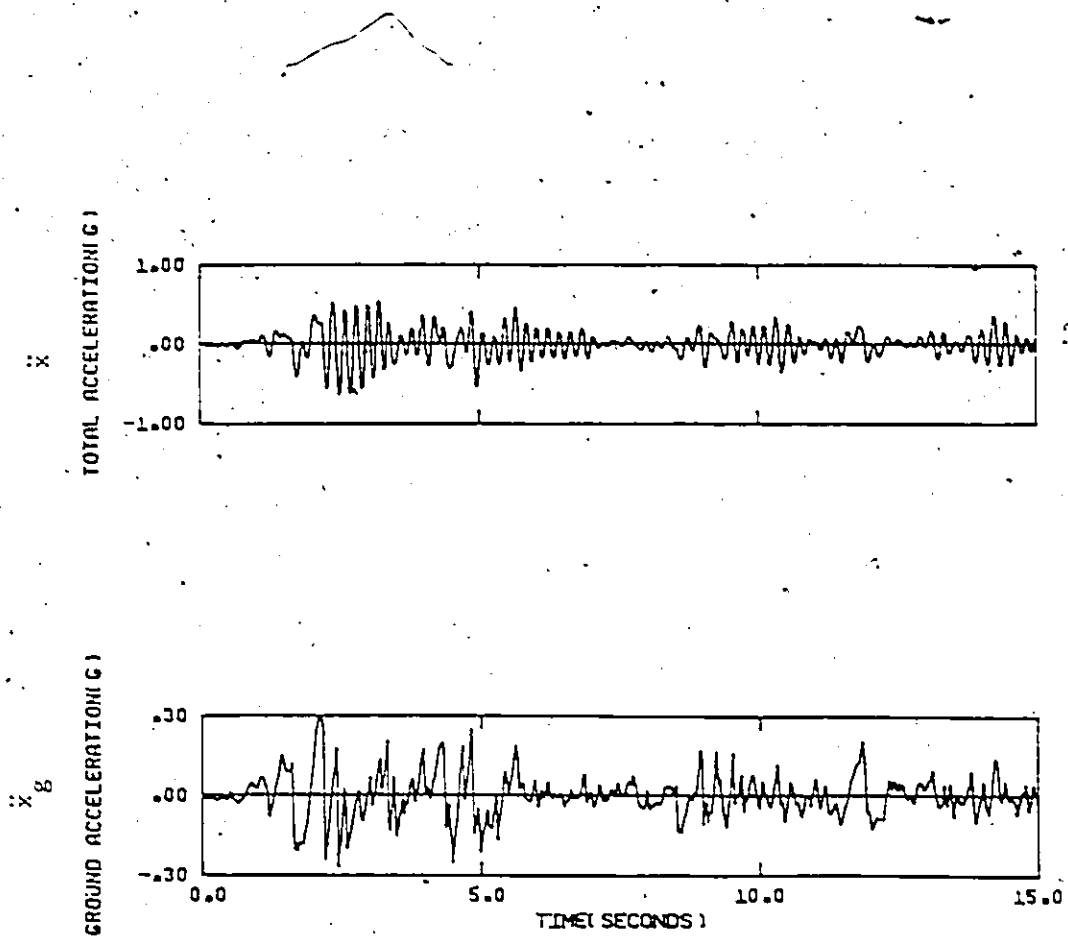
Fig. (5.10) Response of a SDOF·system on a fixed base
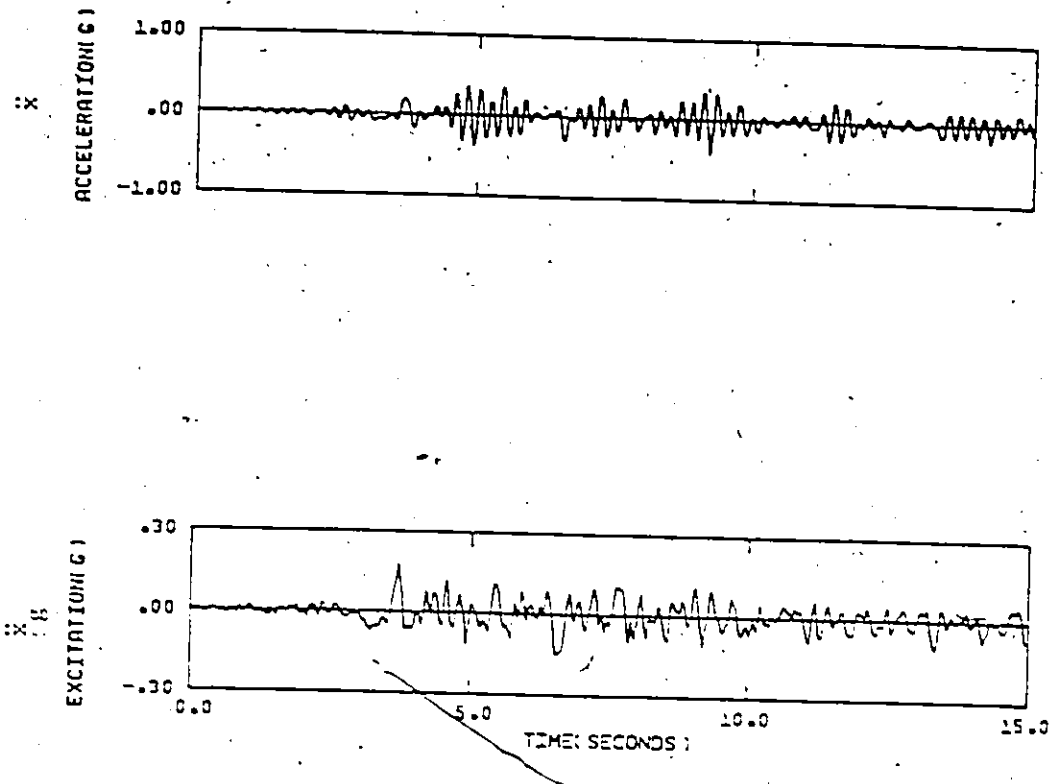(f_O=5 Hz, ξ=.05) to El Centro N-S component

Fig. (5.11) Response of a SDOF system on a fixed base
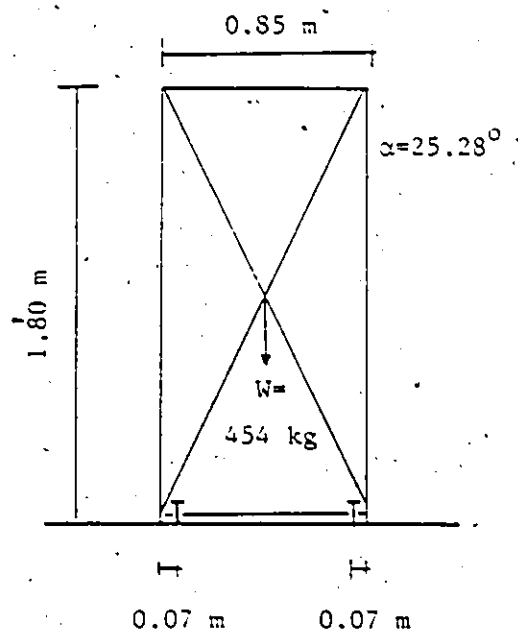(f₀=5 Hz, ξ=.05) to Taft S69E component

Fig. (5.12) Dimensions of Equipment

$$GA = \frac{16}{\pi^2} mh^2 \omega^2$$

(5.29)

The bolts are assumed to be made of carbon steel which has the following properties:

yield stress   = 248   MP

toughness   = 82,700   KN.m/m^3

resilience   = 152   KN.m/m^3

It is shown that the resilience is much smaller than the toughness. The bolts are assumed to be fastened such that their deformable length is 100 mm. Therefore, the maximum elastic deformation of the bolts just before yielding, D_y, is equal to 0.11 mm. The sum of the static stiffness of two bolts under uniaxial tension forces is equal to 520 MN/m. This high stiffness, the small resilience and the negligible elastic deformation justify the assumption that the bolts deform in a rigid-plastic manner. If it is assumed that the system is acted upon by a static load of value MA* at the center of mass, the value of the acceleration A* which will just cause one row of the bolts (two bolts) to yield in tension can be calculated by taking the moment of forces about the center of rotation. In this study, the value of the acceleration is found to be

$$A^* = 11.7 \, g = 114.77 \qquad m/sec^2$$

This value will provide a convenient normalization factor for other base motions used in this study.

Figure (5.13) shows the behaviour of the system under the effect of a harmonic base excitation, which has an acceleration amplitude of
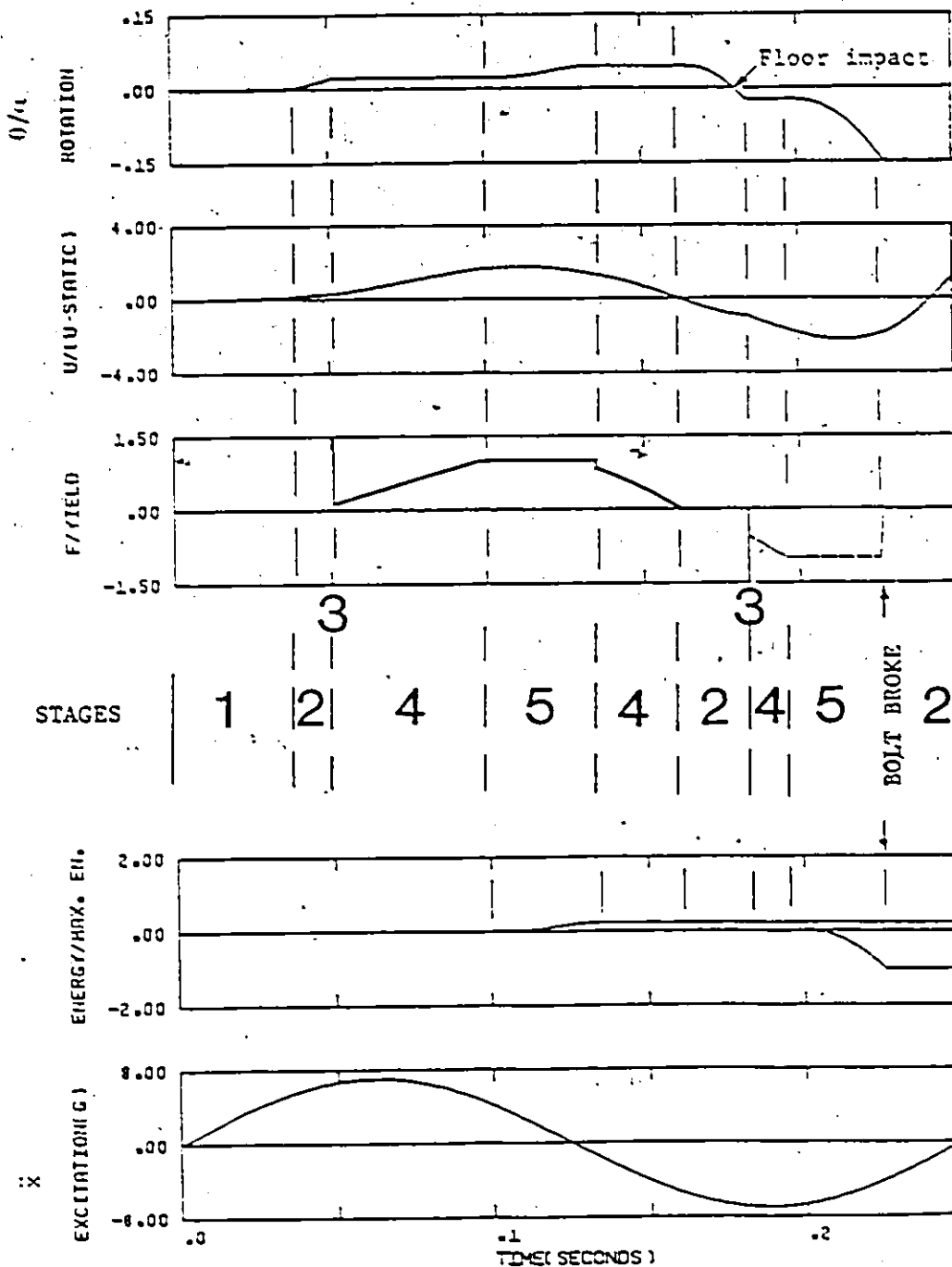
Fig. (5.13) Response of the system, supported by yielding bolts,
to harmonic excitation (a=0.6 A*, F=4 Hz. g_r=0.01)

0.6A* and a frequency of 4 Hz. An initial gap g_o equal to 7.8 mm is assumed. If we define the gap ratio g_r as

$$g_r = \frac{g_o}{I}$$

the initial gap corresponds to a gap ratio of 0.01 . Figure (5.13) shows the different stages of response. At the start (stage 1), the system responds as a SDOF system with the base plate at rest until uplift starts. Then the system starts to uplift (stage 2), but there is no force in the bolts. At $\theta = \theta_o$, impact between the base plate and the bolt takes place and an impulse is produced (stage 3). After that the angle θ remains constant while the bolt tension increases (stage 4). When the tension force reaches the yield strength, stage 5 begins and the bolt is stretched. Accordingly, the angle of rotation increases during this stage. When the force starts to decrease, the system returns to stage 4. As a result, the stretching stops and the angle of rotation remains constant. Stage 4 ends when the bolt tension becomes zero. At that instant, the plate separates from the bolt and the response enters stage 2. Then the angle θ continues to decrease until the base plate impacts with the rigid floor. After the impact, the angle of rotation changes sign from positive to negative and the response is described again by stages 2, 3, 4 and 5 . This time, however, the stressed bolt is the one on the left hand side of the equipment and the system is pivoted at the right edge of the base plate. During stage 5, the left bolt breaks. This time, stage 5 is followed by stage 2 and the angle of rotation increases without any restraint. The

overall response for 2.5 seconds of excitation is shown in Fig. (5.14).
In this case, the base plate rotates with a large angle. It impacts
with the floor several times until overturning occurs at 2.5 seconds
after the beginning of the excitation.

In the time histories shown for the subsequent cases, the
response parameters are normalized to different physical quantities.
The angle of rotation θ is normalized to the angle α. The magnification
factor is obtained by normalizing the deformation at the top of the
system, U, to the static displacement caused at the same point if the
system is subjected to a static load, uniformly distributed over the
height, with loading intensity per unit length equal to m times the
maximum base acceleration "a". The bolt forces are normalized to the
yield strength of the bolts. The negative and positive forces in the
plot correspond to tension forces in the left and right bolts,
respectively. The base shear of the SDOF system is normalized to the
weight W of the equipment. The energy absorbed by a bolt is normalized
to the bolt material toughness times its volume. The negative and
positive values of energy correspond to the energy absorbed by the left
and the right bolts, respectively. The excitation is presented as an
acceleration time history expressed in g's, the gravitational
acceleration.

To verify the computer program, the case of a system with very
small gaps is considered under both harmonic and transient floor motion
excitations. The response of these cases should approach the response
of the linear SDOF system on a fixed base. To ensure complete
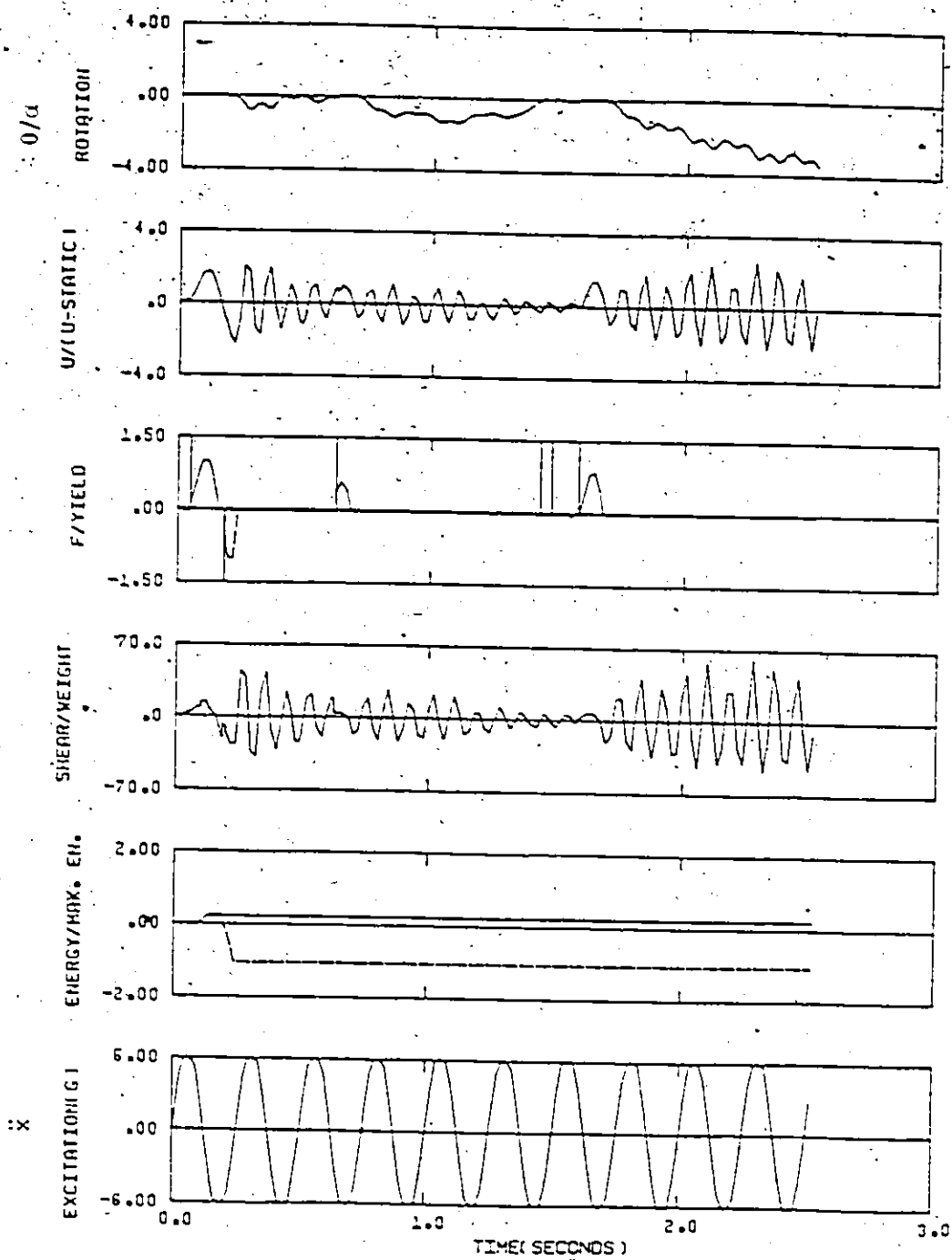equivalence between the two cases, no energy loss is permitted in the

Fig. (5.14) Response of the system, supported by yielding bolts,
to harmonic excitation (a=0.6 A*, F=4 Hz, g_r=0.01)

anchorage or during the impact with the floor. In other words, the bolts are considered rigid and non-yielding, and the restitution coefficient δ between the base plate and the floor is set equal to unity. Figure (5.15) shows the response of the system when the last two conditions are fulfilled. The small gaps provided correspond to ($g_r=0.0001$). The bolt's yield strength is increased ten times in the computation to simulate the rigid bolts. The response shown in Fig. (5.15) can be compared with the response of a linear SDOF system on a fixed base with a natural frequency $f_o=5$ Hz and damping $\xi=0.01$, for the same excitation, as shown in Fig. (5.16). The excitation is a sinusoidal base motion with a frequency of 5 Hz and an acceleration amplitude of 2g. The comparison of Figs. (5.15) and (5.16) indicates the equivalence between the two cases considered and provides a check on the accuracy of the program.

A similar comparison is made for a transient floor motion excitation. Figure (5.17) shows the response of the system when the gaps are very small ($g_r=0.0001$). The bolts are rigid and have a yield strength equal to $10F_y$, and the restitution coefficient is set equal to unity. The system is subjected to the floor motion caused by the ground acceleration of the El Centro (1940) N-S component shown in Fig. (5.10). The floor motion is normalized such that the peak floor acceleration has a value equal to $0.4A^{*}$. Figure (5.18) shows the response of a linear SDOF system on a fixed base ($f_o=5$ Hz, $\xi=0.01$) subjected to the same floor motion. The comparison between the two systems indicates agreement, as expected.
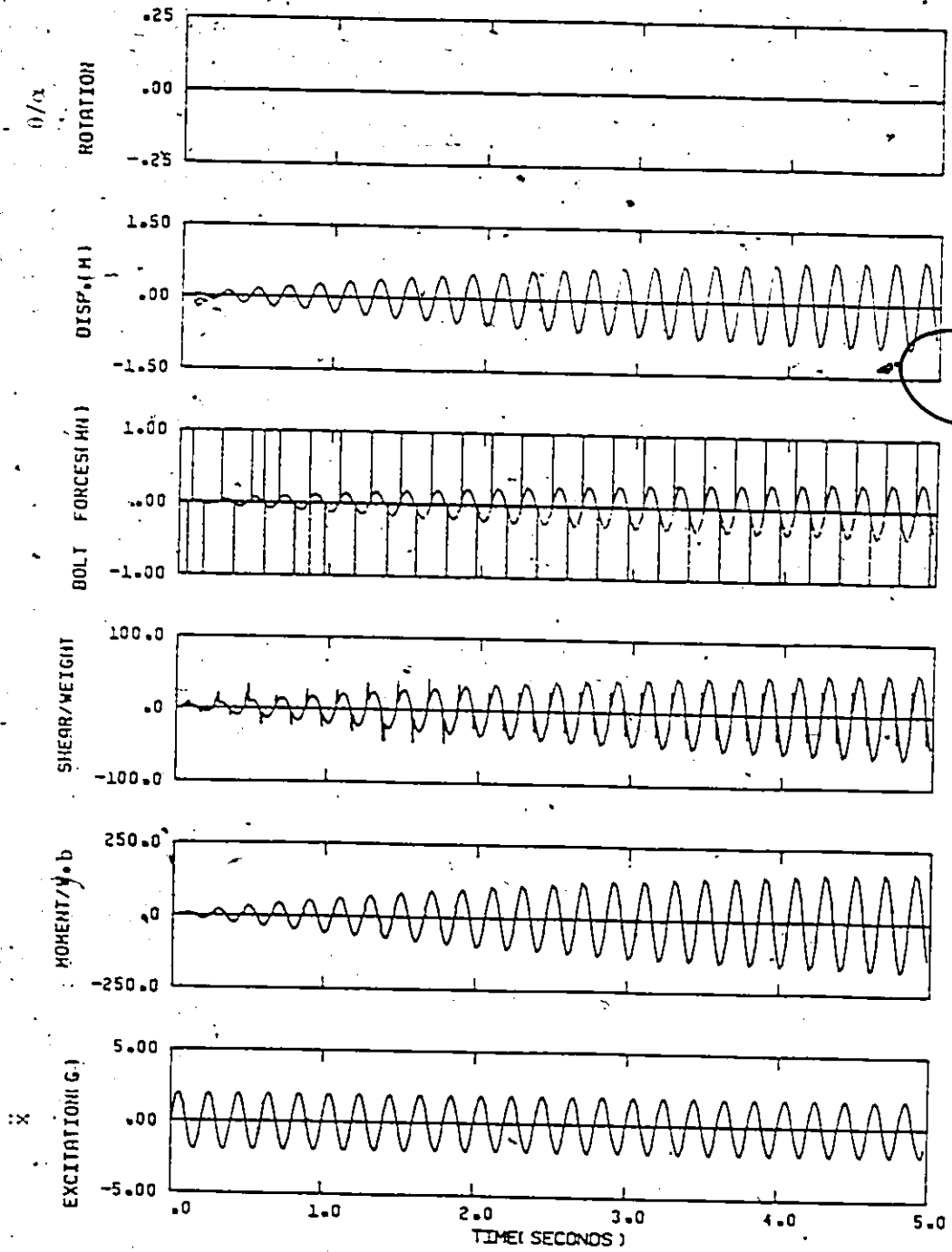
Fig. (5.15) Response of the system with very small gaps at resonance
(a=2g, F=5 Hz, bolts yield force=10 F_y, g_r=0.0001, δ=1.)
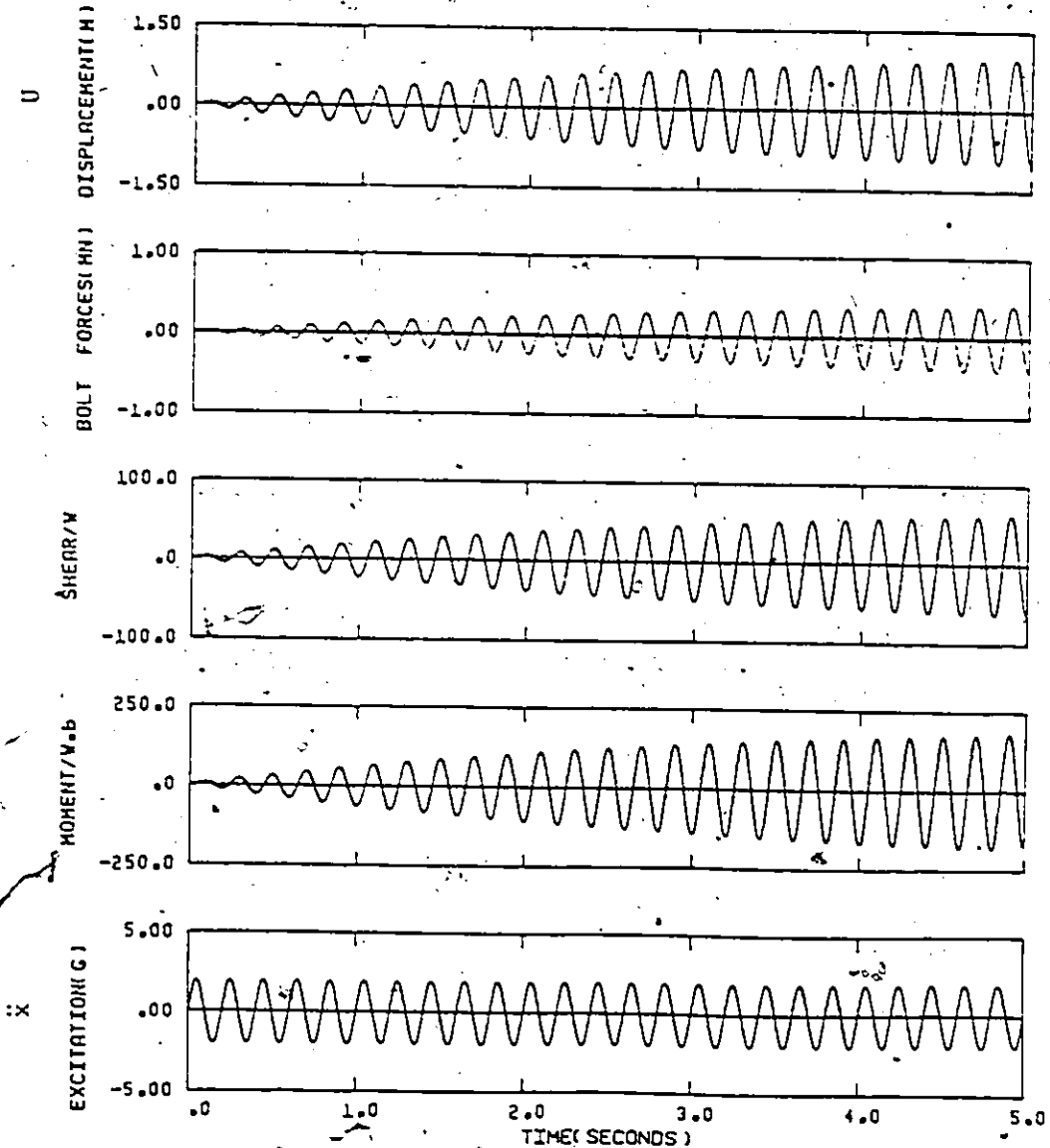
Fig. (5.16) Response of a linear SDOF system on a fixed base at resonance (a=2g, F=5 Hz)
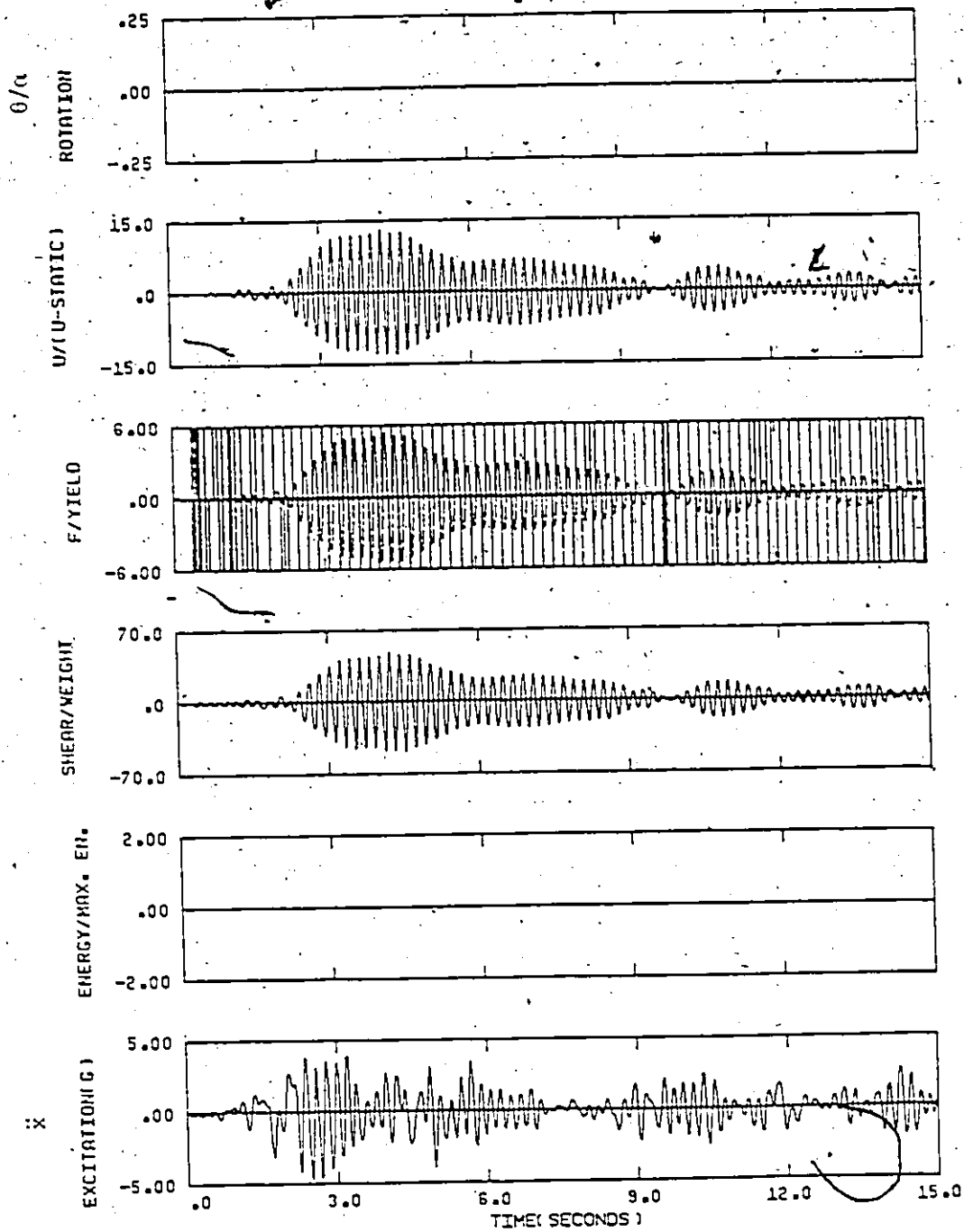
Fig. (5.17)   Response of the system with non-yielding bolt to El Centro
floor motion (f_O=5 Hz, ξ=0.01, g_r=0.0001, δ=1., a=0.4A*)
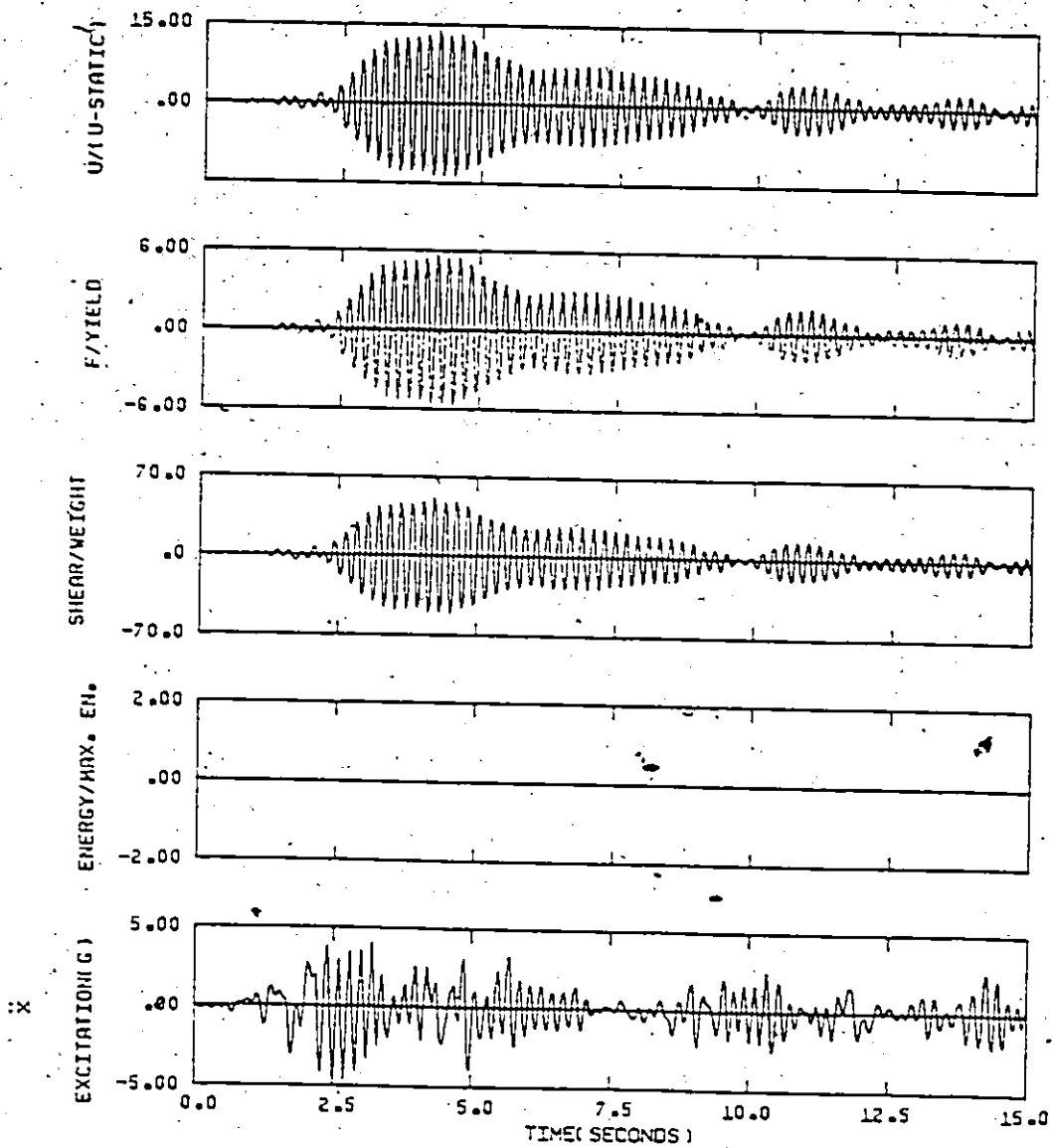
Fig. (5.18)   Response of a SDOF system on a fixed base (f_0=5 Hz, ξ=.01)
to El Centro floor motion (a=0.4 A^*)

5.7 Rigid-Plastic Bolts Versus Elasto-Plastic Bolts

In the previous description, the bolts, in the mathematical model, were assumed to be rigid-plastic. The validity of this assumption is investigated by comparing the corresponding results with those obtained if the bolts are assumed to be elasto-plastic. In the latter case, the rigid support assumed in stage 4 should be replaced by an elasto-plastic spring, as shown in Fig. (5.19). The spring has the force-displacement relationship shown in Fig. (5.20). The stiffness of the spring in the axial direction has a value of 520 MN/m. The response of this model, subjected to a harmonic excitation with an acceleration amplitude equal to $0.2A^*$ and a frequency of 4 Hz, is shown in Fig. (5.21). When the overall response shown in Fig. (5.21) is compared with the corresponding response of the rigid-plastic bolt model, shown in. Fig. (5.22), the levels of the response for the base rotation and the equipment deformation are found to be approximately the same. There exist, however, very high frequency oscillations in the bolt forces, during stage 4, in the case of the elasto-plastic bolts. This high frequency response oscillates around that of the rigid-plastic bolt model. This behaviour is due to the elastic nature of the springs which introduce an additional degree of freedom to the complete system in stage 4. This added degree of freedom has a very high natural frequency of 116 Hz. Due to the nature of the impact between the base plate and the bolts, this degree of freedom is also excited, causing "ringing" around the mean of the bolt response. The calculated details of this "ringing" force pattern and the corresponding changes in the angle of
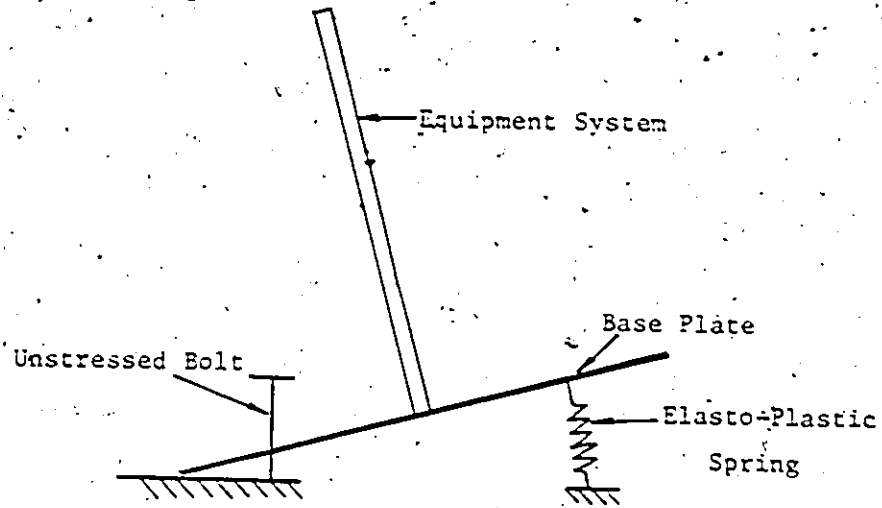
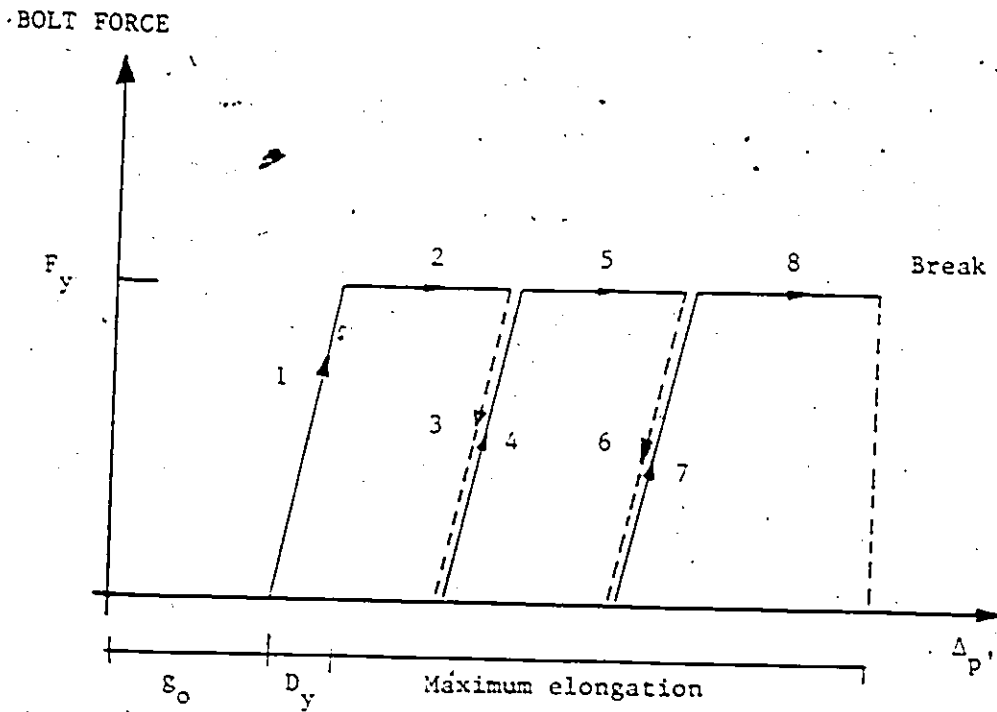Fig. (5.19) Model for the system with elasto-plastic bolts in stage 4

Fig. (5.20) Stress loops in elasto-plastic bolts
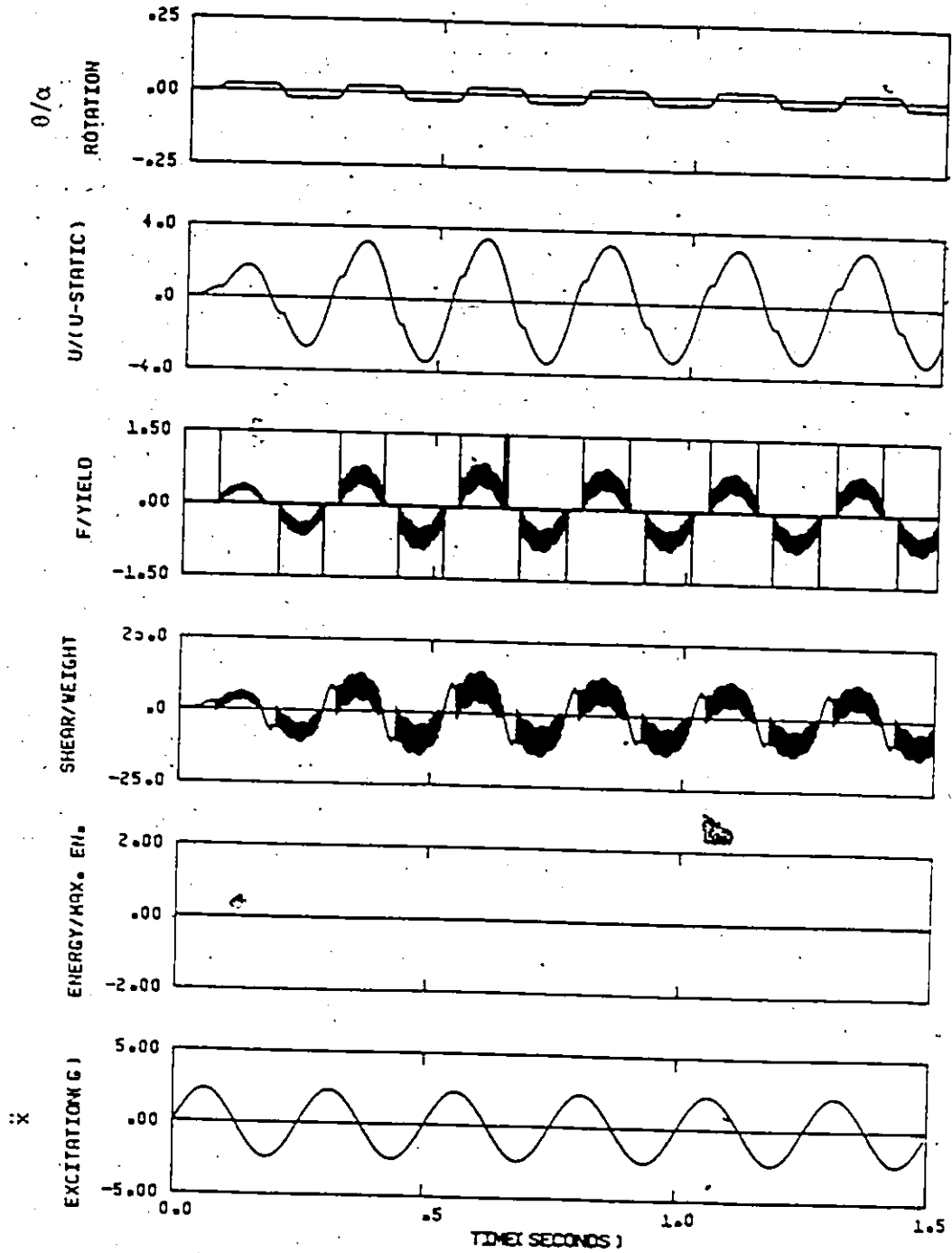
Fig. (5.21)   Response of the system with elasto-plastic bolts to
harmonic excitation (a=0.4 A*, F=4 Hz, g_r=0.01)
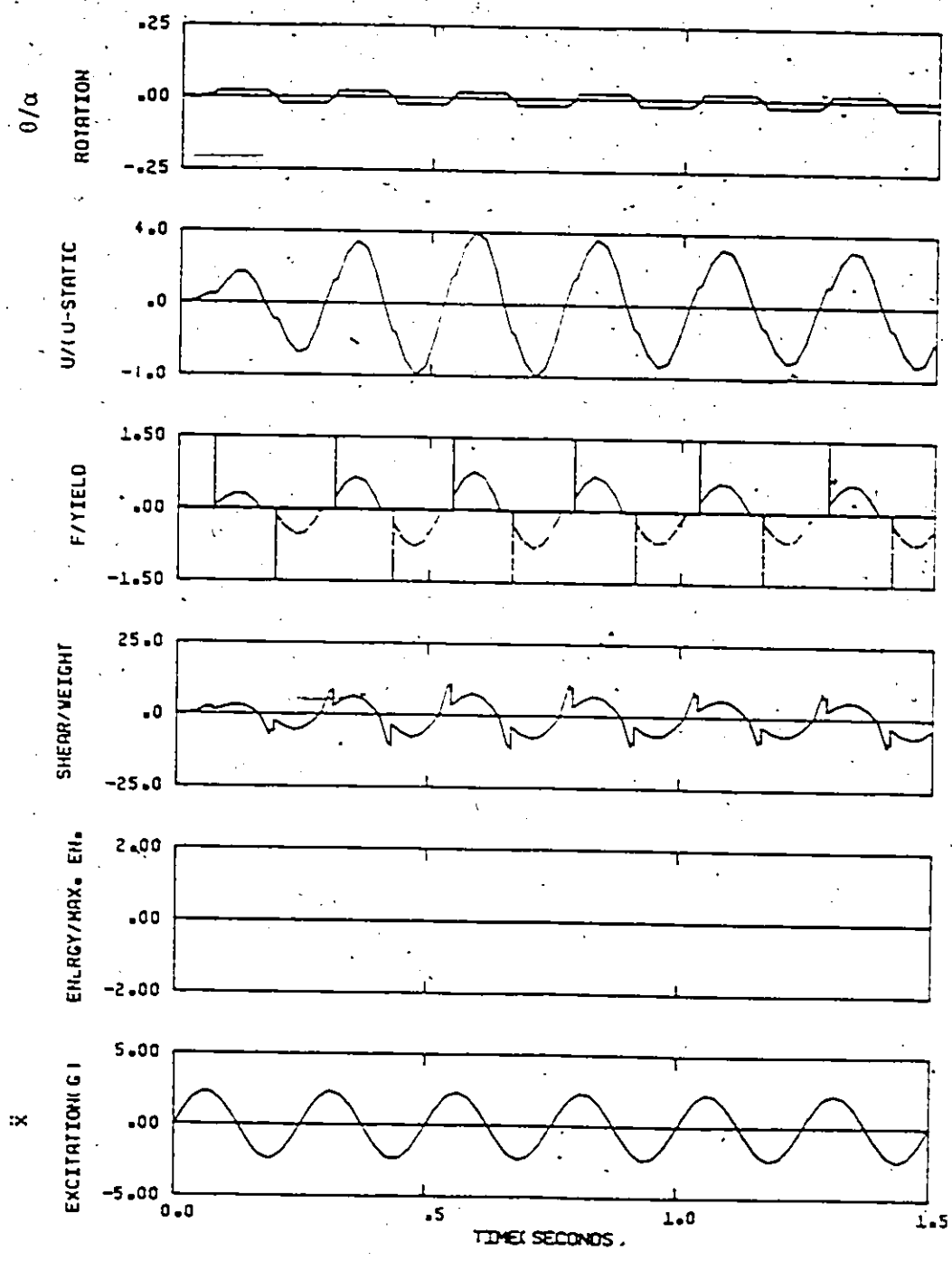
Fig. (5.22)   Response of the system with rigid-plastic bolts to
harmonic excitation (a=0.4 A*, F=4 Hz, g_r=0.01)

rotation depend on the integration time step used. Because the period of this stiff system is about 0.008 seconds, a much finer integration time step (say, less than 0.0001 seconds) is needed to obtain the fine details of the force variation in the bolts. However, since the overall response of the system is affected little by the high frequency fluctuations of the bolt forces, it is believed that the overall dynamic response of the equipment can be studied and realistic results obtained using the simpler rigid-plastic bolt model.

Next, a detailed study is done to investigate the behaviour of the equipment-anchor system under base excitation. A variable time step is used for the integration of the equations of motion. The largest time step applied is 0.001 seconds. Through each stage, an initial time step of 0.001 seconds is started with. At the transition intervals between the different stages, the time step is divided many times, if necessary, until the instant of transition between the two stages is defined accurately. The technique of variable time step is used to achieve accurate results at optimum computation effort. The accuracy of definition of the transition instants between the different stages is determined by satisfying different thresholds of accuracy. In general, they are taken to be 10^{-3} times the corresponding normalizing quantities. For example, a force estimation in the bolt within a tolerance of $0.001F_y$ is taken to be acceptable. An uplift displacement of point p' of the base plate within $0.001D_y$ from the bolt head is considered accurate enough for the contact condition.

5.8 Numerical Results

The main interest in this investigation is to study the seismic behaviour of equipment partially fixed on rigid floors. As shown in the previous section, even when a simple mathematical model is used, the problem is very complex and involves a number of parameters. Among these parameters are the size of the gap, the bolt's strength and the level of excitation. For a low level of excitation, the acceleration will not be sufficient to cause the base plate to uplift on its edges and the response will be identical to that of a system on a fixed base. For a higher level of excitation, tilting of the base plate and rocking of the system occur. Depending on the level and characteristics of the input base motion, the rocking amplitude may be small so that unrestrained rocking results. On the other hand, the rocking response may be sufficiently high that restrained rocking occurs. If the forces induced in the bolts remain below the yield strength, then the gap size within which rocking of the base plate is possible will remain the same as the initial gap size. If the excitation is sufficiently strong, however, the induced bolt forces will reach the bolt's yield strength and yielding will take place. The yielding of the bolts produces two significant changes to the system. First, it acts as an additional source of energy dissipation. Second, the gap between the bolt head and the base plate widens. Finally, the bolts may break because of excessive straining. Both rocking and yielding are highly nonlinear processes and they interact in a complex way to produce the various responses described.

To identify the effects of the various parameters on the dynamic

behaviour of the partially fixed equipment, the study will be divided
into two parts. In the first part, the gap size is assumed to remain
constant throughout the excitation. This situation can be achieved by
using bolts with strength far in excess of what is necessary for the
given level of base excitation. The purpose of this part is to study
the effect of restrained-base rocking on the dynamic response of the
equipment. In the second part of the study, the bolts are allowed to
yield, causing the gaps to increase in size until the bolts fail. In
each part of the study, the dynamic response is studied under two types
of base excitation, namely, harmonic base motion and two examples of
floor motion caused by earthquake ground motions.

In this chapter, the gap size is assumed to be constant and the
bolts to be non-yielding. The following parameters will be
investigated:

1. gap size,

2. level of input acceleration,

3. type of excitation (harmonic or earthquake floor motions), and

4. frequency of excitation (in the case of harmonic excitation).

The effect of each of these parameters on the response will be
discussed in detail. In the case of harmonic excitation, the results
are presented in the form of frequency-response curves. The horizontal
axis of those curves represents Ω_r, the ratio between the input
frequency Ω to the shear beam natural frequency on a fixed base ω. The
vertical axis represents the steady-state response U at the top of the
equipment, normalized to the static displacement of the corresponding

point caused by a static force, equal to $m\ddot{x}l_{max}$ per unit length, acting uniformly over the height 2h .

For the cases excited by earthquake floor motions, the results are presented in the form of time histories and tables which contain the maximum values of the response parameters.

5.8.1 Harmonic Excitation

5.8.1.1 Gap Effect

The effect of the gap size is investigated by choosing three different gap ratios, namely,

1. a large gap, $g_r = 0.03$

2. a small gap, $g_r = 0.01$

3. no gap (SDOF system on a fixed base), $g_r = 0$, or a very small gap, $g_r = 0.001$

Figure (5.23) shows the frequency-response curves of the system with non-yielding bolts for these three cases. The sinusoidal excitation applied has an acceleration amplitude equal to $0.4A^*$. At resonance ($\Omega_r = 1.0$), the case of no gap has a value for the magnification factor equal to 50. In general, the deformations of the systems with gaps decrease considerably as the gap size increases, as long as the frequency ratio is greater than or equal to unity. Below a frequency ratio equal approximately to (0.8), the systems with large gaps have a slightly higher response than the systems with small gaps.

It is also shown that the frequency ratio at which the maximum steady-state response occurs is less than unity for the systems with gaps. The shift of the natural frequency increases as the gap size is
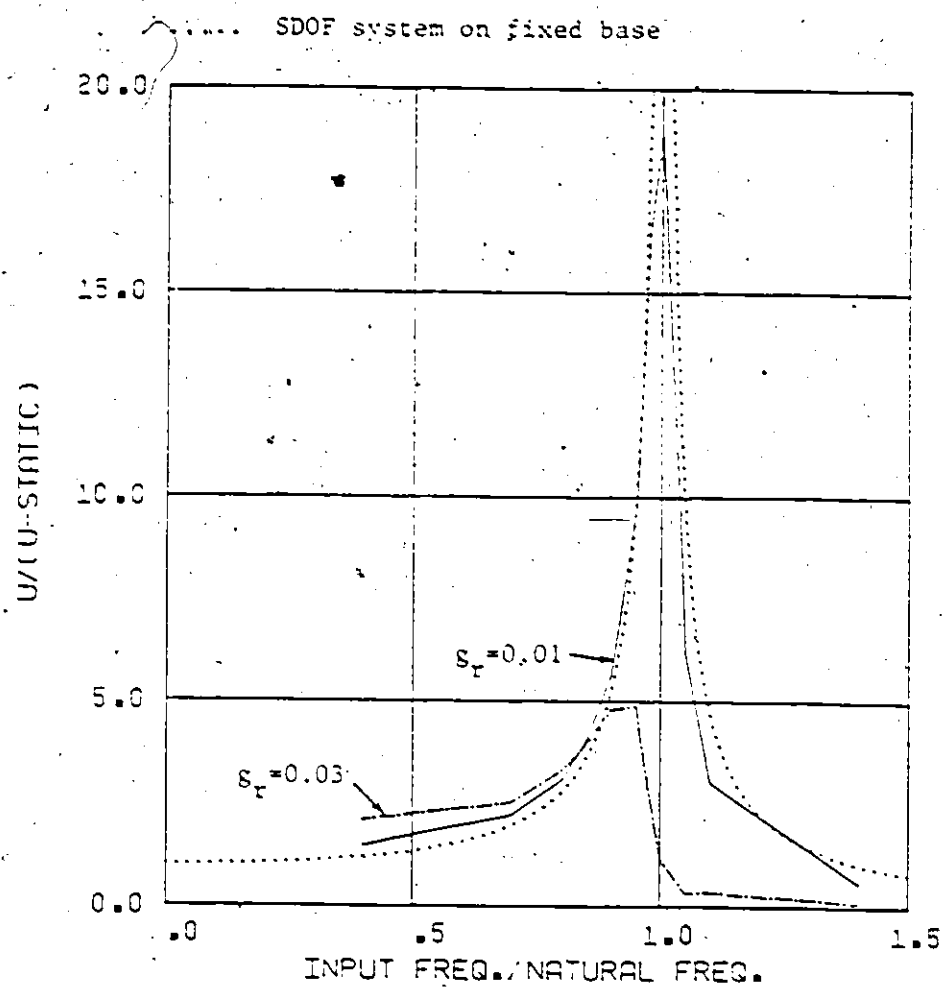
Fig. (5.23) Response of the system with non-yielding bolts for different gap ratios (a=0.4 A°)

increased.

In general, the deformation of a SDOF system mounted on a base that is allowed to rock is less than that of a system on a fixed base. This is because part of the energy supplied to the system is transferred to the rocking system as kinetic energy corresponding to the rigid body velocities. Also, during rocking, some energy is dissipated through the impact of the base with the floor.

5.8.1.2 Effect of the Input Acceleration Level

The input acceleration level is, in general, an important parameter in the non-linear problem. This effect is examined by keeping the gap ratio fixed at 0.01 and different levels of acceleration are applied to the system with non-yielding bolts. Figure (5.24) shows the frequency-response curves corresponding to four different levels of input amplitude. The deformation in the system increases as the input acceleration increases when the frequency ratio is greater than nearly (0.8). The increase in the response, however, is not proportional to the increase in the excitation level. For frequency ratios less than nearly 0.8, higher accelerations lead to slightly lower responses.

A comparison of Fig. (5.24) and Fig. (5.23) indicates similar behaviour. In other words, the variation of the response with the frequency for different gap ratios, at a constant acceleration level, has the same general behaviour as the response with the frequency for different acceleration levels at a constant gap size. The similarity indicates the equivalent effects of increasing the acceleration and decreasing the gap size on the system deformation.
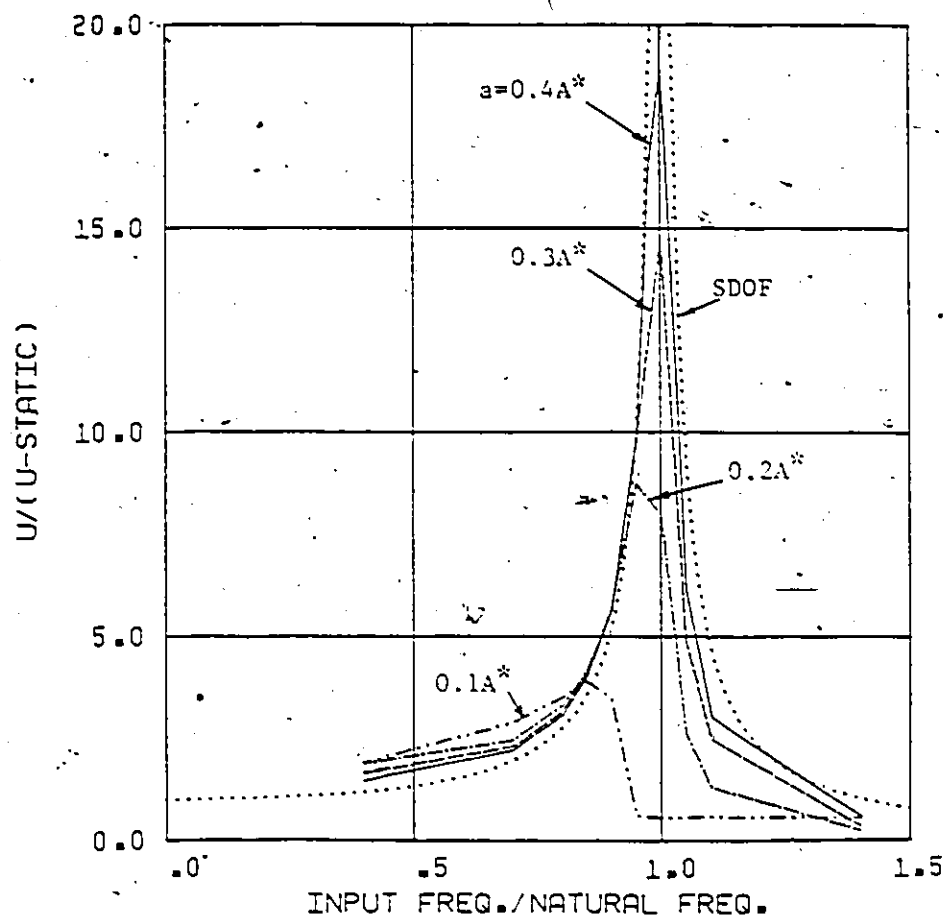
Fig. (5.24) Response of the system with non-yielding bolts for different levels of acceleration $(g_r=0.01)$

The shift of the natural frequency of the system with gaps can also be seen in Fig. (5.24). The shift increases as the input acceleration decreases.

5.8.2 Earthquake Floor Motion

The effect of the gap size on the response of the system, when it is subjected to floor motions resulting from earthquake excitations, is studied in this section. The input time history used is the floor motion induced by the N-S component of the El Centro (1940) earthquake record. Two levels of excitation are investigated with peak accelerations of $0.4A^*$ and $0.085A^*$, respectively. Three gap sizes are chosen, corresponding to gap ratios of $g_r=0.001$, 0.01 and 0.03. The responses of the cases studied are presented in time history plots. The response of the system for an acceleration level with a peak equal to $0.4A^*$ and a gap ratio of 0.001 has been shown already in Fig. (5.17). The responses of the system for the same excitation corresponding to the gap ratios $g_r=0.01$ and 0.03 are shown in Figs. (5.25) and (5.26), respectively. The response time histories illustrate that for the case of $g_r=0.01$, the base plate rocks with the full amplitude throughout the time history shown. For the case of $g_r=0.03$, the base plate rocks with the full amplitude mainly during the time of strong shaking.

The bolt forces, when the gap is very small, are considerably large within a significant part of the time history shown. For the "large gap" case, the bolts are stressed only at the time of strong shaking and the bolt forces are relatively small. The forces in the case of $g_r=0.01$ represent an intermediate condition between the other
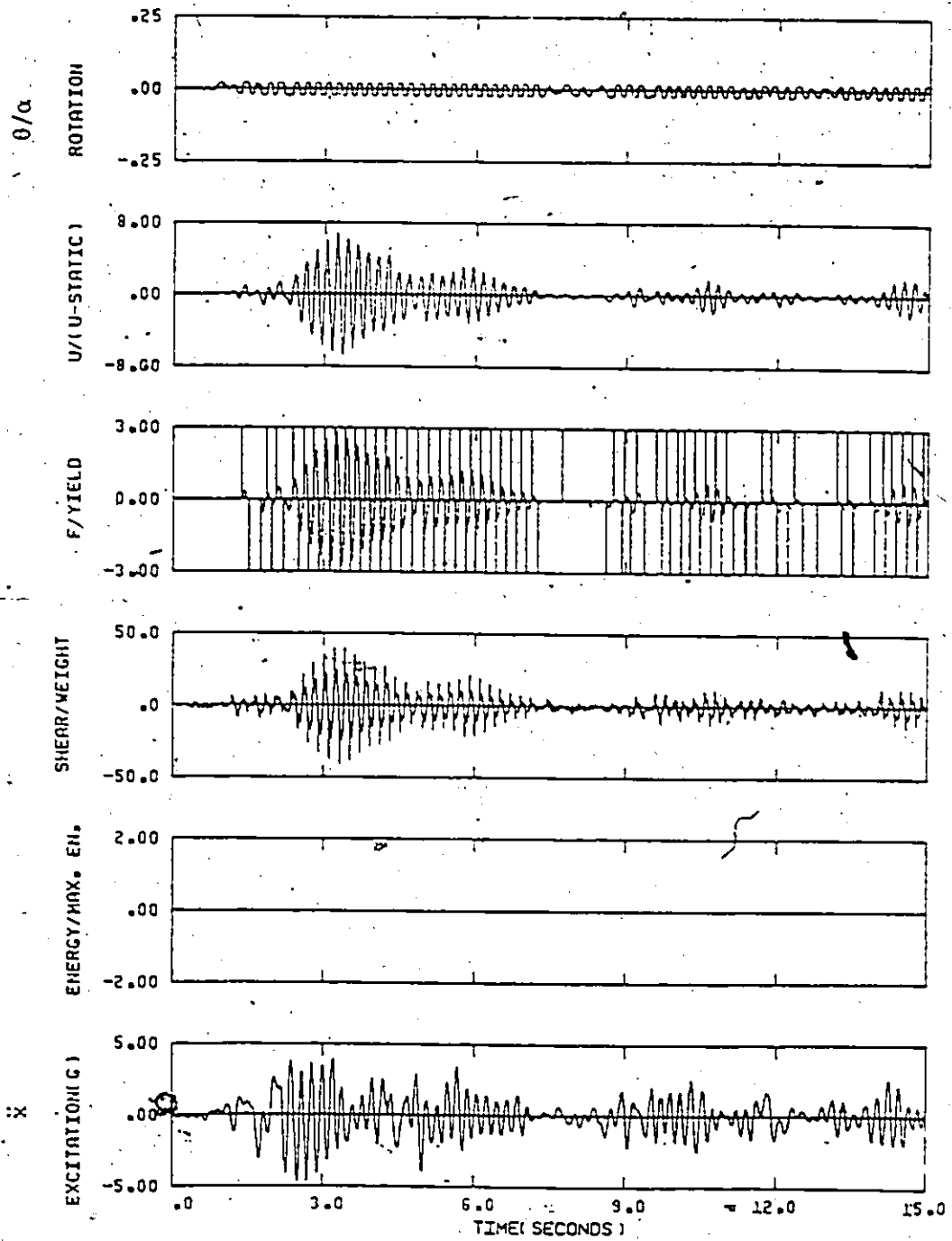
Fig. (5.25)   Response of the system with non-yielding bolts to El Centro
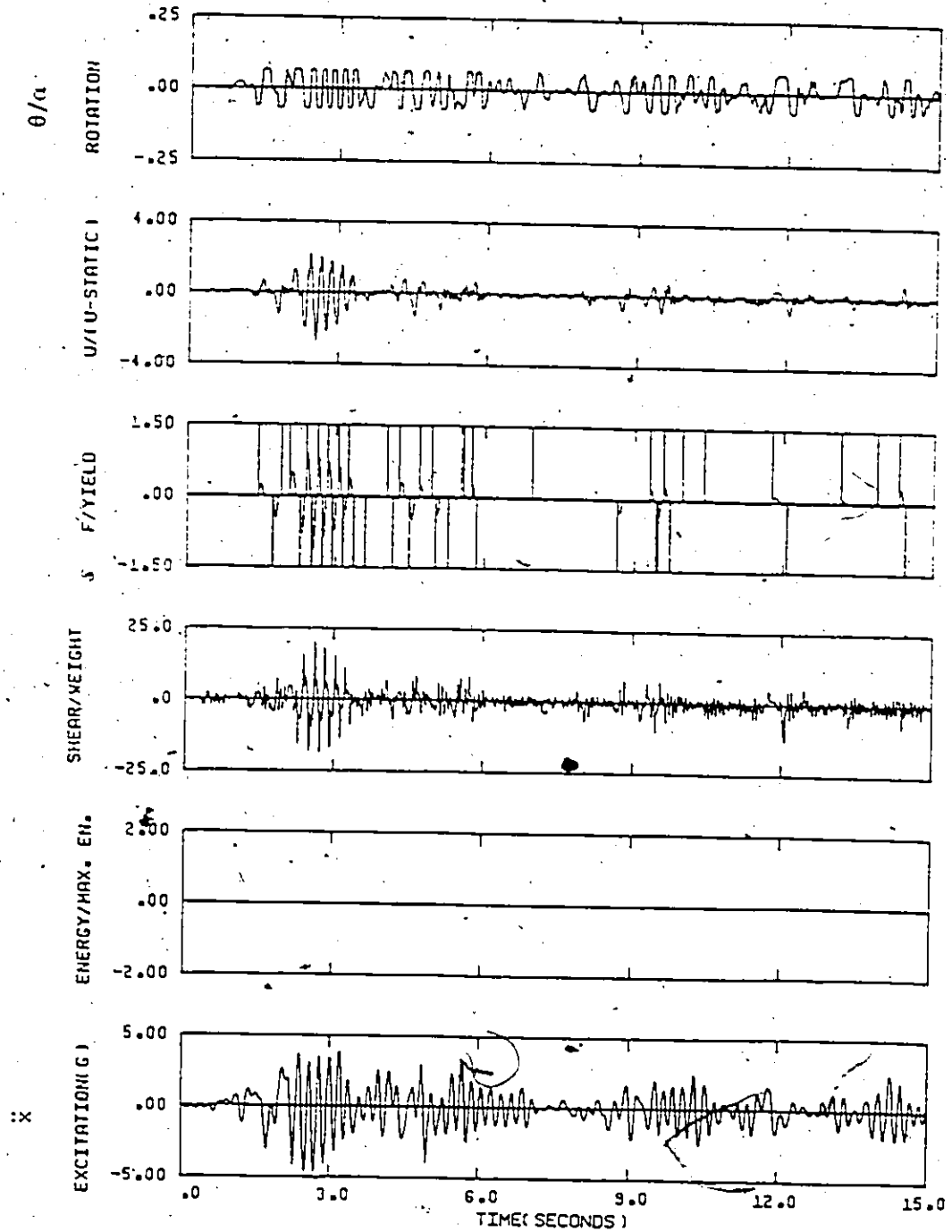floor motion (f_0=5 Hz, ξ=0.01, g_r=0.01, a=0.4A*)

Fig. (5.26)   Response of the system with non-yielding bolts to El Centro
floor motion (f_0=5 Hz, ξ=0.01, g_r=0.03, a=0.4A*)

cases of $g_r=0.001$ and $g_r=0.03$.

The equipment deformation, as measured by the response parameter U, is large when the gap is very small, for a relatively long duration. On the other hand, the deformation is decreased considerably when the gap is large. The response is significant only during the small interval of strong shaking, decaying to a small amplitude for the rest of the time history. The equipment response for the case of $g_r=0.01$ represents an intermediate case.

The base shear, varies with time in a way similar to the equipment response U. Also, the base shear is high for $g_r=0.001$, less for $g_r=0.01$ and small for $g_r=0.03$.

Comparison among these three cases shows that the equipment response is substantially reduced as the gap size increases. This trend is consistent with that observed for the steady-state response when the base motion is harmonic.

The peak values of the responses corresponding to an acceleration level with a peak of $0.085A^*$ are summarized in table (5.1). It can be seen that there is a considerable difference in the response amplitudes between the cases of very small gap and the other cases. However, the difference in the responses of the three cases of different gap size is very little. This behaviour can be explained as follows. For such a small level of excitation, the rocking amplitude is small and the response of the system is close to the state of unrestrained rocking, even for the case where the gap size corresponds to $g_r=0.01$. As a result, further increases in the gap size will not affect the response to any great extent.

Table (5.1)

Response to El Centro Floor Motion

Non-yielding bolts

$(a = 0.085A'')$

	0.001	0.01	0.02	0.03
Initial g_r	0.001	0.01	0.02	0.03
Final g_r	0.001	0.01	0.02	0.03
Max. F_i/F_y i=1 or 2	1.25	0.117	0.0876	0.1
Max. U/U-Static	14.02	1.737	1.403	1.58
Max. shear/W	10.8	3.6	3.72	3.79
Energy absorbed/ max. energy	0.0	0.0	0.0	0.0

The investigation of the response for the systems with non-yielding bolts led to the following conclusions.

1- For systems excited by harmonic excitations, the existence of the gaps decreases the response when the frequency ratio is greater than unity, the larger the gaps, the greater the reduction of the response.

2- The gaps also shift the natural frequency of the system to values below unity. Larger gaps lead to bigger shifts.

3- For the case of transient floor motions, the existence of the gaps also decreases the response of the mounted equipment relative to the case of complete fixation. Larger gaps lead to larger reductions in the response. The maximum reduction in the equipment response is obtained if the size of the gap is large enough to allow for a free-rocking situation.

CHAPTER 6

RESPONSE OF PARTIALLY FIXED EQUIPMENT

WITH

YIELDING BOLTS

6.1 Introduction

The bolts modelled as rigid-plastic members are characterized by two parameters; the yielding force F_y and the material toughness (the maximum energy that can be absorbed). If the excitation is strong enough to cause the bolts to yield, elongation of the bolts will result. If the elongation reaches the maximum limit, the bolts will break. During the elongation, the gap size increases and the system is allowed to rock with a larger angle of rotation. After yielding, there is no guarantee that the gaps on both sides will be equal. In fact, the elongation of the bolts is unequal in most cases, resulting in rocking with unequal gap sizes, even under harmonic excitations. If one bolt breaks, the second bolt may or may not break. If one or both bolts break, the system may or may not overturn, depending on the details of the transient response. Therefore, the response of the equipment system becomes much more complex if the inelastic behaviour of the bolts is taken into account.

In the following analysis, two simplifications are made.

a) The bolts are allowed to stretch indefinitely without breaking. This will provide information on the effect of an ever-enlarging gap on the system's response.

165

b) Although real bolts will fail if the elongation exceeds the
   maximum strain limit, it is assumed, in this analysis, that
   the complete system will fail if at least one bolt fails.

In the results presented, the failure points are marked by "X" and the points which represent yielding without breaking are marked by "o".

Similar to the cases studied in Chapter 5, this study will examine the effects of the partial fixation on the response of the equipment system. Both the harmonic excitation and the earthquake floor motion will be used as inputs. Also, a comparison will be made between the response of the systems with non-yielding bolts and that of the systems with yielding bolts.

6.2 Harmonic Excitation

6.2.1 Gap Effect on Yielding Systems

It should be pointed out that yielding of the bolts does not take place in the whole frequency range considered. The points where yielding of the bolts occurs and those where yielding does not occur should be distinguished, during the interpretation of the steady-state response results. Figure (6.1) shows the response curves for cases of different initial gaps (g_r=0.001 , 0.01 and 0.03) subjected to harmonic excitations with an acceleration amplitude equal to 0.4A*. For comparison, the response curves of the SDOF system on a fixed base are also shown. Figure (6.1) illustrates that, in the frequency range near to Ω_r=1, the responses of the systems with small initial gaps are less than those of the systems with large initial gaps. This is because the bolts of the former systems stretch more than those of the latter. As a
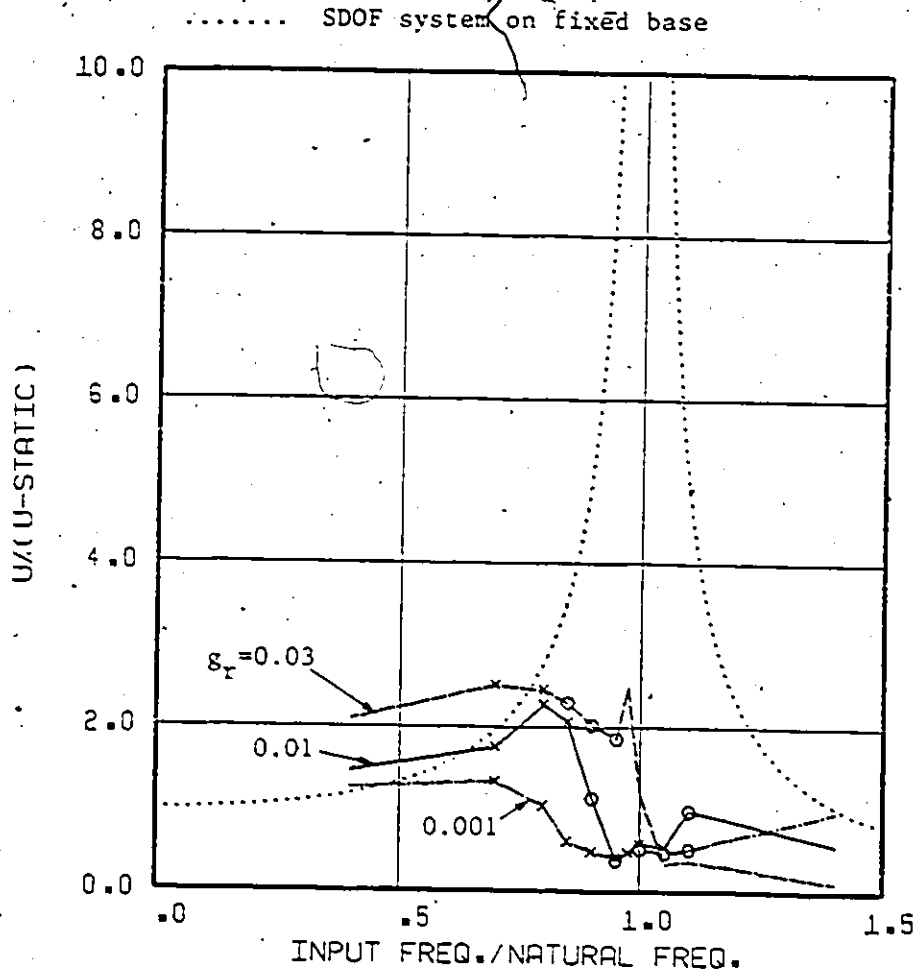
Fig. (6.1) Response of the system with yielding bolts for different gap ratios (a=0.4 A*)

result, by the time the steady state has been reached, the systems with small initial gaps have large final gaps. These large gaps allow the systems to rock with large angular amplitudes and consequently lower structural response U. In other words, yielding of bolts causes the gap size to vary with time and, therefore, the initial gap size is not sufficient to predict the system response during the dynamic excitations.

At high frequencies, the systems with larger initial gaps have lower response U than the systems with smaller initial gaps. The reverse is observed, however, at low frequency ratios, i.e., larger initial gaps lead to higher response U. In fact, at both the low and high frequency ratios (relative to the frequency ratio "unity"), the bolts do not yield and the response is similar to the cases with non-yielding bolts discussed in Chapter 5.

6.2.2   Effect of the Input Acceleration Level

For a range of acceleration amplitudes varying from $0.1A^*$ to $0.4A^*$, Figs. (6.2) and (6.3) illustrate the response curves for the systems with yielding bolts of different initial gap ratios. It should be realized that the final gap sizes at the steady state are different, in general, from the initial gap sizes. Two differences can be seen when the steady-state response curves of the systems with yielding bolts are compared to those of the systems with non-yielding bolts. First, the stretching of the bolts increases the gap size progressively and decreases the final steady-state response. Second, a lower level of excitation may lead to a higher response, as shown in Fig. (6.4). This
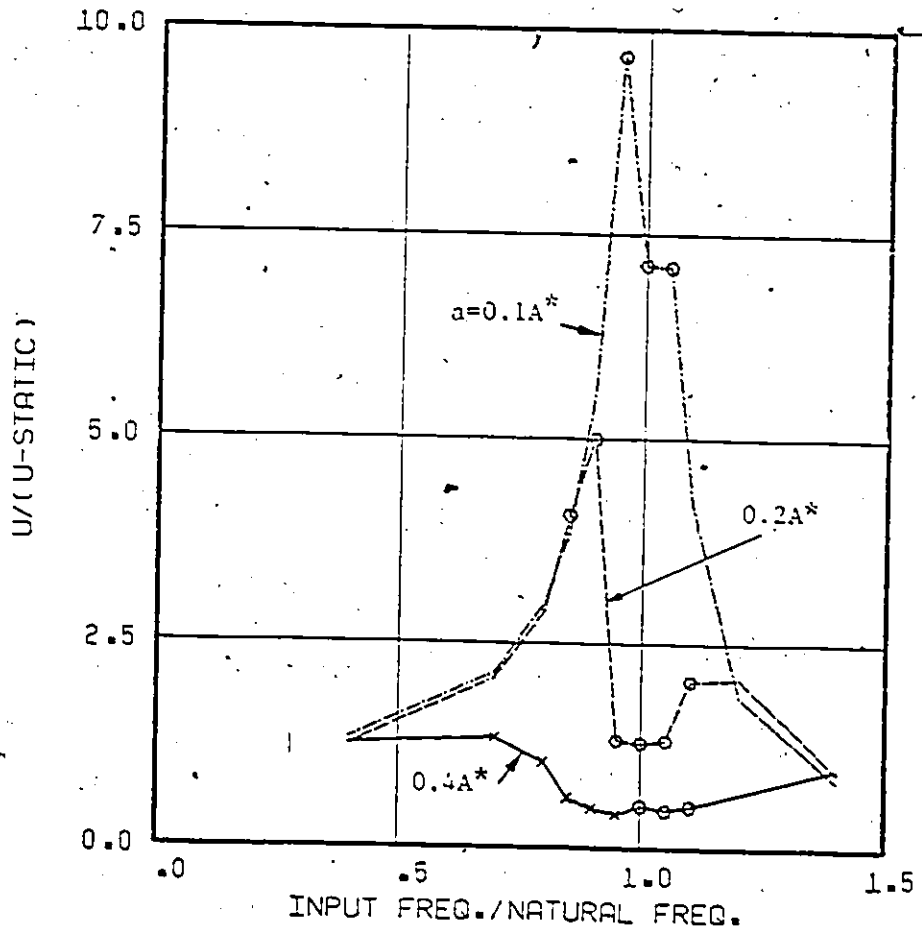
Fig. (6.2)   Response of the system with yielding bolts for
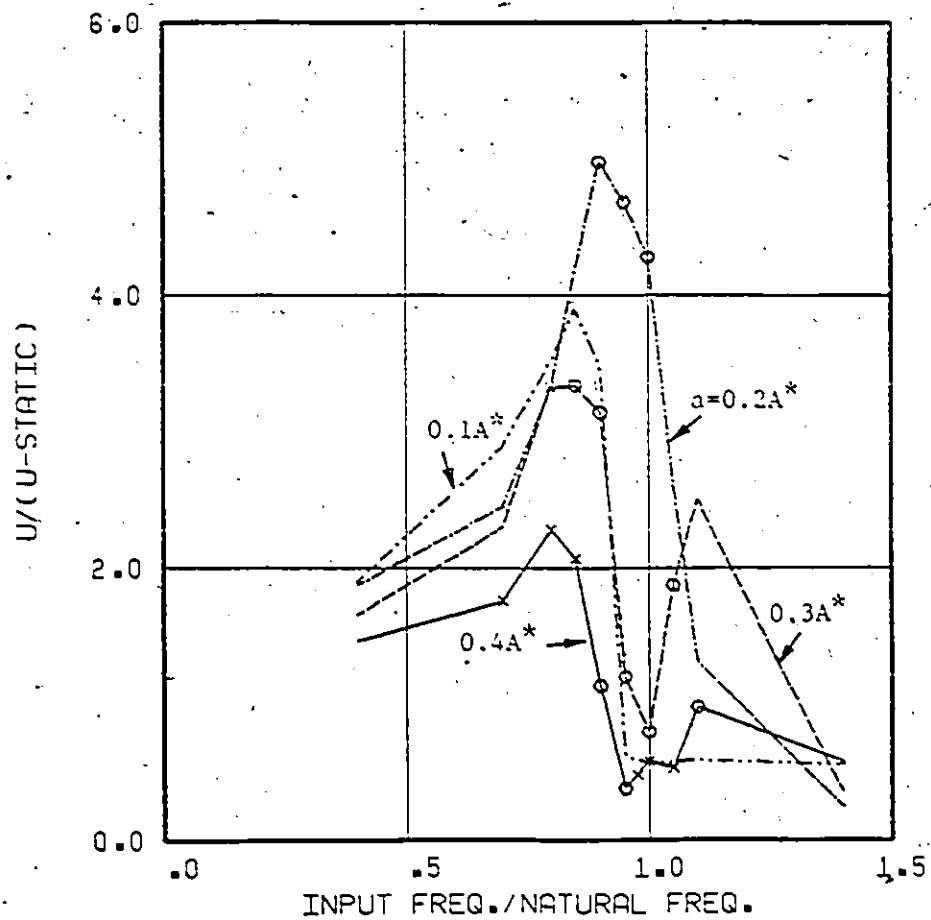   different levels of acceleration ($g_r=0.001$)

Fig. (6.3)   Response of the system with yielding bolts for
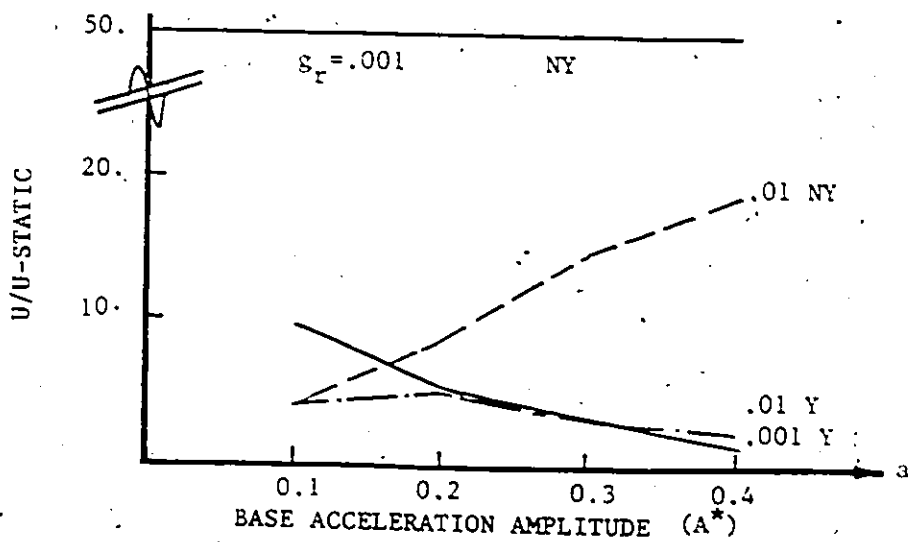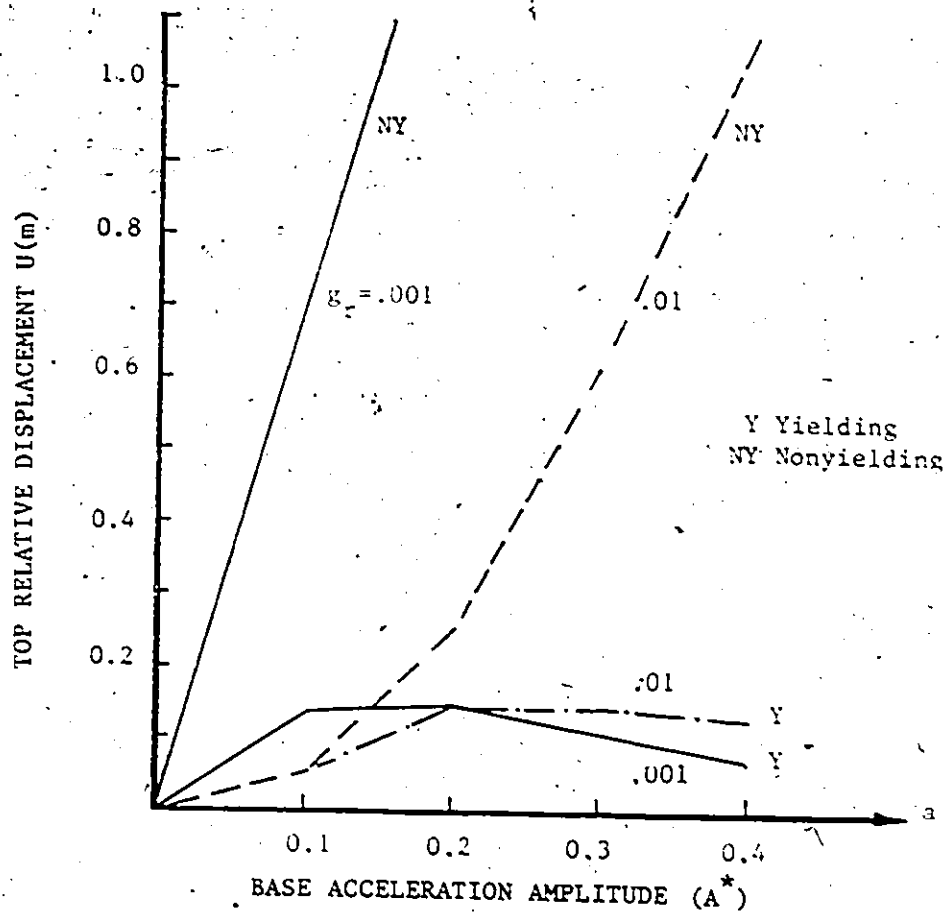different levels of acceleration ($g_r = 0.01$)

Fig. (6.4)   Response of the system with gaps versus base
acceleration amplitude (harmonic excitation)

is particularly evident when Ω_r is near to unity. This behaviour can be explained by the fact that although the initial gap sizes for all levels of excitation are identical, a higher level of excitation causes more extensive yielding of the bolts in the transient phase of the response. This results in a large gap through which the system can rock eventually during the steady-state response. Because large gaps tend to decrease the structural response, the steady-state response amplitude for a higher level of excitation is observed to be less than that for a lower level of excitation.

Exceptions to that behaviour occur when the forces induced in the bolts are less than their yield strength. Then, the responses of both the yielding and non-yielding systems are identical. This behaviour occurs in two cases, first when the input acceleration is not high enough, and second when the frequency ratio is far from unity. Figure (6.4) summarizes the variation of the frequency-response peaks as a function of the input acceleration amplitude for the systems with yielding and non-yielding bolts.

6.2.3 Comparison Between Systems With Yielding Bolts and Systems With Non-yielding Bolts

In the following, the steady-state responses of cases with different gap ratios are compared over a range of input acceleration amplitudes varying from $0.1A^*$ to $0.4A^*$. The results are shown in Figs. (6.5) to (6.7).

In general, the frequency-response curves of the systems with yielding bolts can be discussed by subdividing the curves into three

NY Nonyielding

U/(U-STATIC)

INPUT FREQ./NATURAL FREQ.
Fig. (6.5.b) a=.4A*

Y Yielding

U/(U-STATIC)
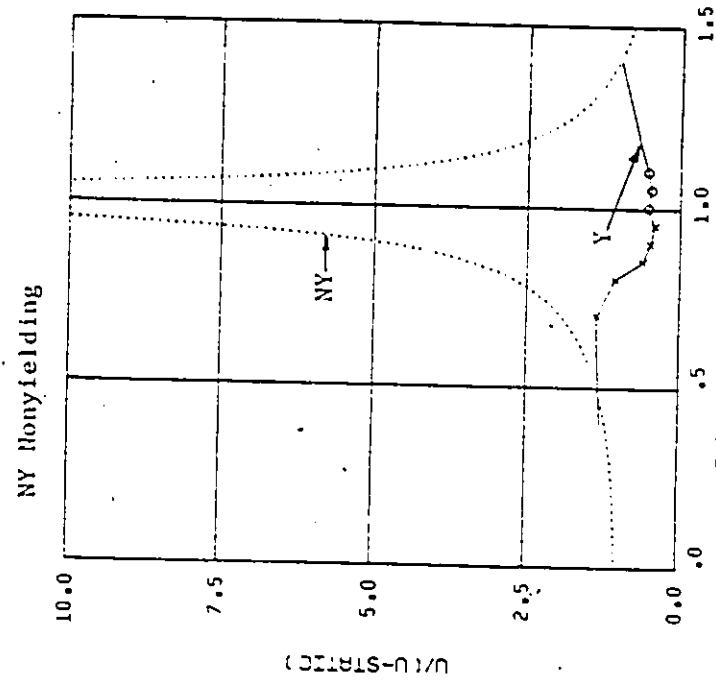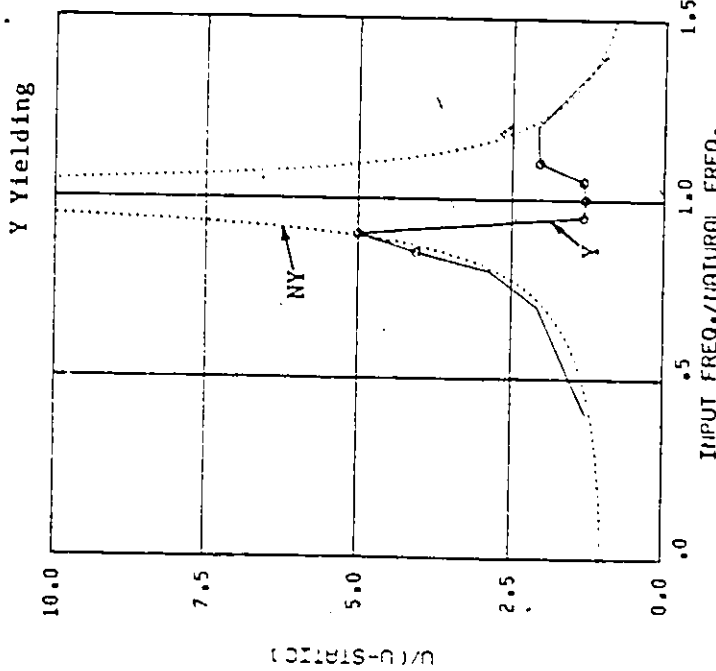
INPUT FREQ./NATURAL FREQ.
Fig. (6.5.a) a=.2A*

Fig. (6.5)   Responses of yielding versus non-yielding systems (g_r=.001)
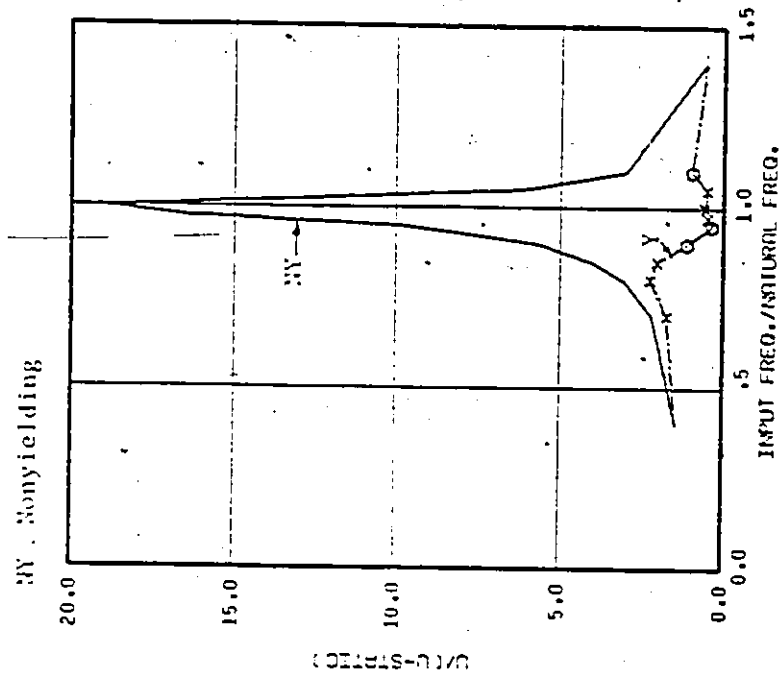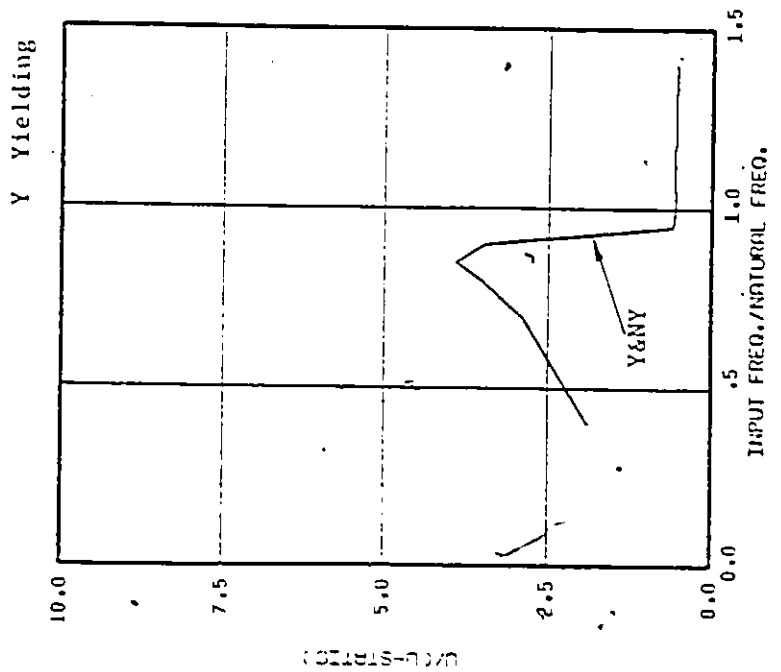
NY : Nonyielding

Fig. (6.6.b) a=.4A*

Y Yielding

Fig. (6.6.a) a=.1A*

Fig. (6.6) Responses of yielding versus non-yielding systems ($g_r=.01$)
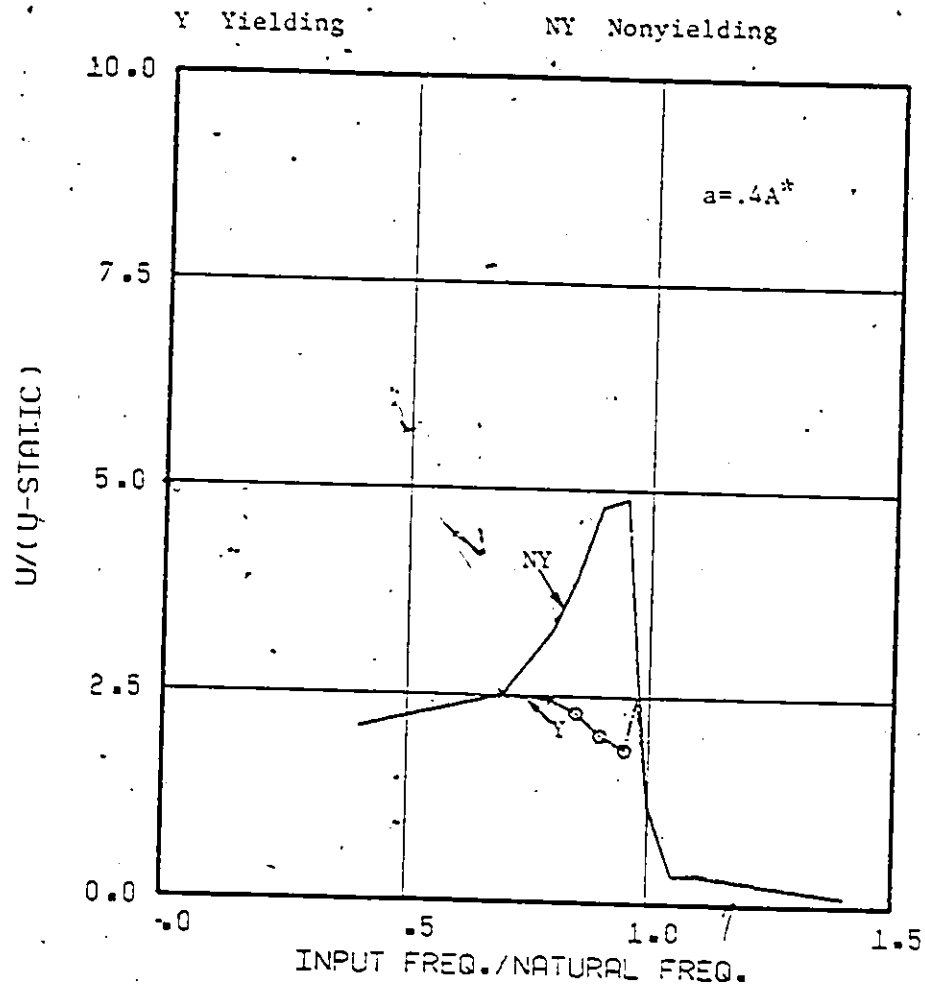
_Fig. (6.7)   Responses of yielding versus non-yielding
systems (g_r=.03)

ranges of the frequency ratio Ω_r, namely, low frequency ratios (less than 1.0), high frequency ratios (greater than 1.0), and intermediate frequency ratios (in the neighbourhood of 1.0). For frequency ratios far from unity, the response is not high, and the tensile force in the bolts is generally less than the yield strength. The response is, therefore, identical to that of the systems with non-yielding bolts. For frequency ratios in the neighbourhood of $\Omega_r=1.0$, the response of the systems with yielding bolts is different from that of the systems with non-yielding bolts. This difference becomes greater as the input acceleration increases and the initial gap decreases. Within that range of frequency, the bolts yield, and as a result, the gaps are enlarged. In many cases, the stretching exceeds the maximum limit and the failure of bolts is registered. The three zones of response can be recognized in Figs. (6.5.a) and (6.7). Figures (6.5.b) and (6.6.b) show that yielding of bolts can occur over a wide frequency range. This yielding zone disappears in the cases shown in Fig. (6.6.a).

An increase in the gap size has the same effect on the response as a decrease in the input acceleration. Accordingly, the definition of small or large gaps should take into consideration the input acceleration level. For example, a gap ratio equal to 0.01 can be considered relatively small for $a=0.2A^*$ because it will cause the bolts to yield. However, the same gap ratio can be considered relatively large for $a=0.1A^*$ because the bolt forces in this case are below the bolts' yield strength. Table (6.1) summarizes the bolts' behaviour in the various cases of steady-state response studied and shown in Figs.

Table (6.1)

Behaviour of Yielding Bolts

Under Harmonic Excitation

Gap ratio (g_r)	Input acceleration (A^*)	Bolts behaviour
0.001	0.1	Yield
0.001	0.2	Yield
0.001	0.4	Break
0.01	0.1	No yield
0.01	0.2	Yield
0.01	0.3	Break
0.01	0.4	Break
0.03	0.4	Break

(6.5) to (6.7).

6.3 Response to Earthquake Floor Motion

In the following sections, the response of the systems with gaps is studied under the effect of transient floor motions resulting from the N-S component of the El Centro (1940) earthquake.

If the bolts are allowed to stretch, they will absorb energy during the extension. The amount of stretching depends on the initial gap size, the input level and the time history of the input. There is a major difference between the response caused by transient excitation, such as floor motions induced by earthquakes, and that caused by harmonic excitation. In the latter case, the steady-state response that will be investigated takes place after the transient response and the stretching of bolts have been completed. In the case of transient excitation, it is only the peak values, which may take place at the same instant the bolts yield, that are of concern. During the calculation of the response of the equipment system, the bolts are allowed to stretch beyond the maximum limit, as they are assumed to be made of a material with unlimited toughness. Accordingly, the bolts will not break when the amount of energy absorbed exceeds the value corresponding to the toughness of the material in a real system. Once the actual toughness of the bolts is exceeded, however, it should be realized that failure would have occurred in a real system.

6.3.1 Gap Effect on Systems with Yielding Bolts

The responses of yielding systems with different gap ratios $(g_r = 0.001, 0.01$ and $0.03)$ under the effect of the El Centro induced

floor motion are presented in Figs. (6.8) to (6.10), respectively. The floor motion is normalized to have a peak acceleration equal to $0.4A^*$. From the response time histories of the three cases, the following observations are found.

In the case of the very small gap ($g_r=0.001$), the left and right bolts are stretched by different amounts, and the stretching takes place early, during the time of strong shaking. This is followed by rocking of the system with unequal amplitudes for the angle of rotation to the left and right. The energy absorbed by the left bolt exceeds the maximum limit defined by the toughness of the material, which indicates that a real bolt will fail and that the system may overturn. In the case of the small gap ($g_r=0.01$), only one bolt yields, but the extension is larger than that of the case when $g_r=0.001$. Therefore, a real bolt will fail in this case also. In the case of the large gap ($g_r=0.03$), only one bolt yields and the amount of energy absorbed is much less than the critical value for bolt failure. Thus the final gaps on the left and right sides of the base plate are nearly equal in this case. For all the cases considered, the yielding of the bolts (transition from stage 4 to stage 5) takes place early during the time of strong shaking.

A comparison of these three cases indicates that the lateral deformations U, for the cases of gap ratios equal to 0.001 and 0.01, are nearly equal, whereas there is a smaller response for the case of the large gap ($g_r=0.03$). The same behaviour applies also to the base shear. The final gaps for the three cases, however, are completely different. Table (6.2) summarizes the behaviour of the three cases considered and
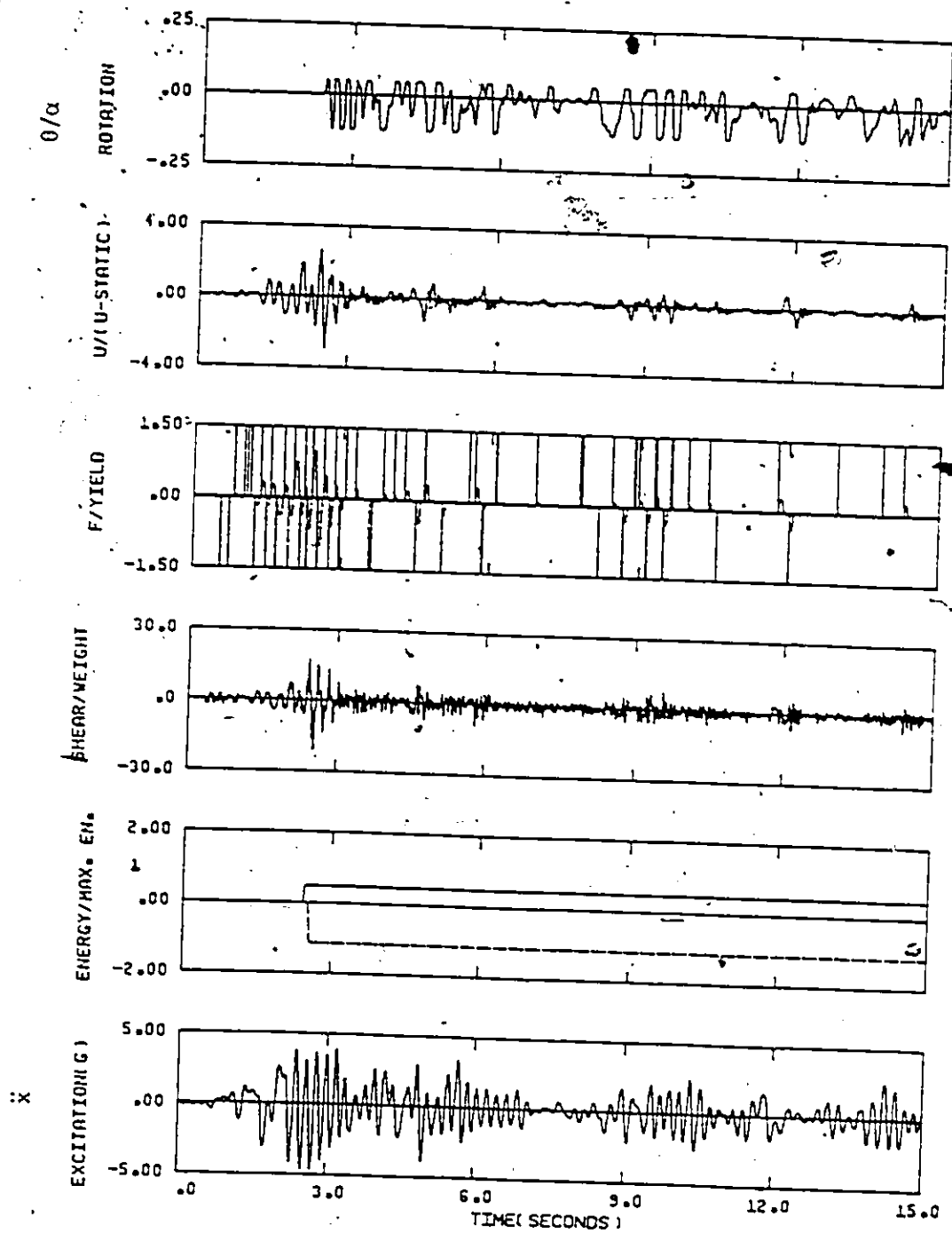
Fig. (6.8)   Response of the system with yielding bolts to El Centro floor motion (f_0=5 Hz, ξ=0.01, g_r=0.001, a=0.4A*)
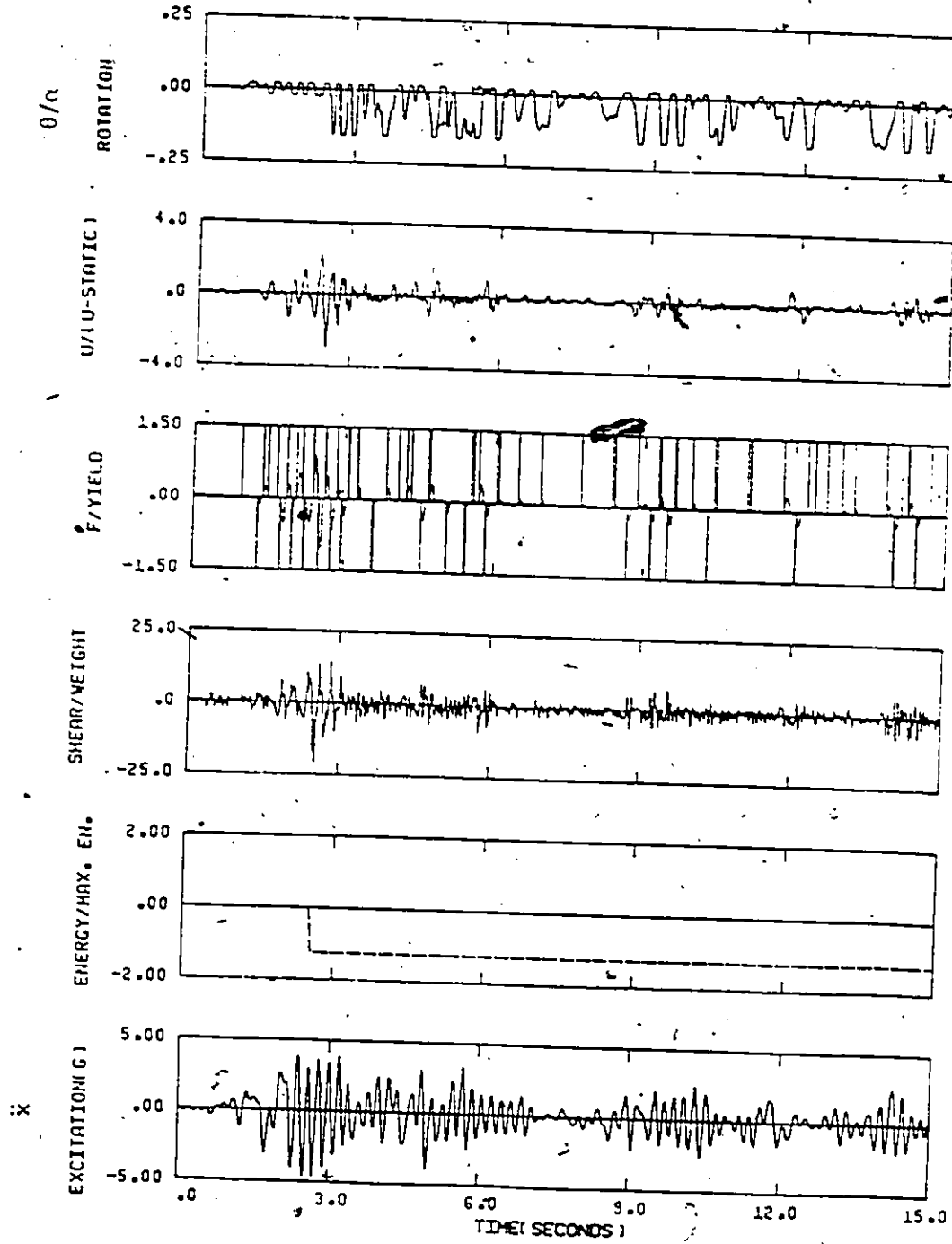
Fig. (6.9)   Response of the system with yielding bolts to El Centro floor motion (f_o=5 Hz, ξ=0.01, g_r=0.01, a=0.4A*)
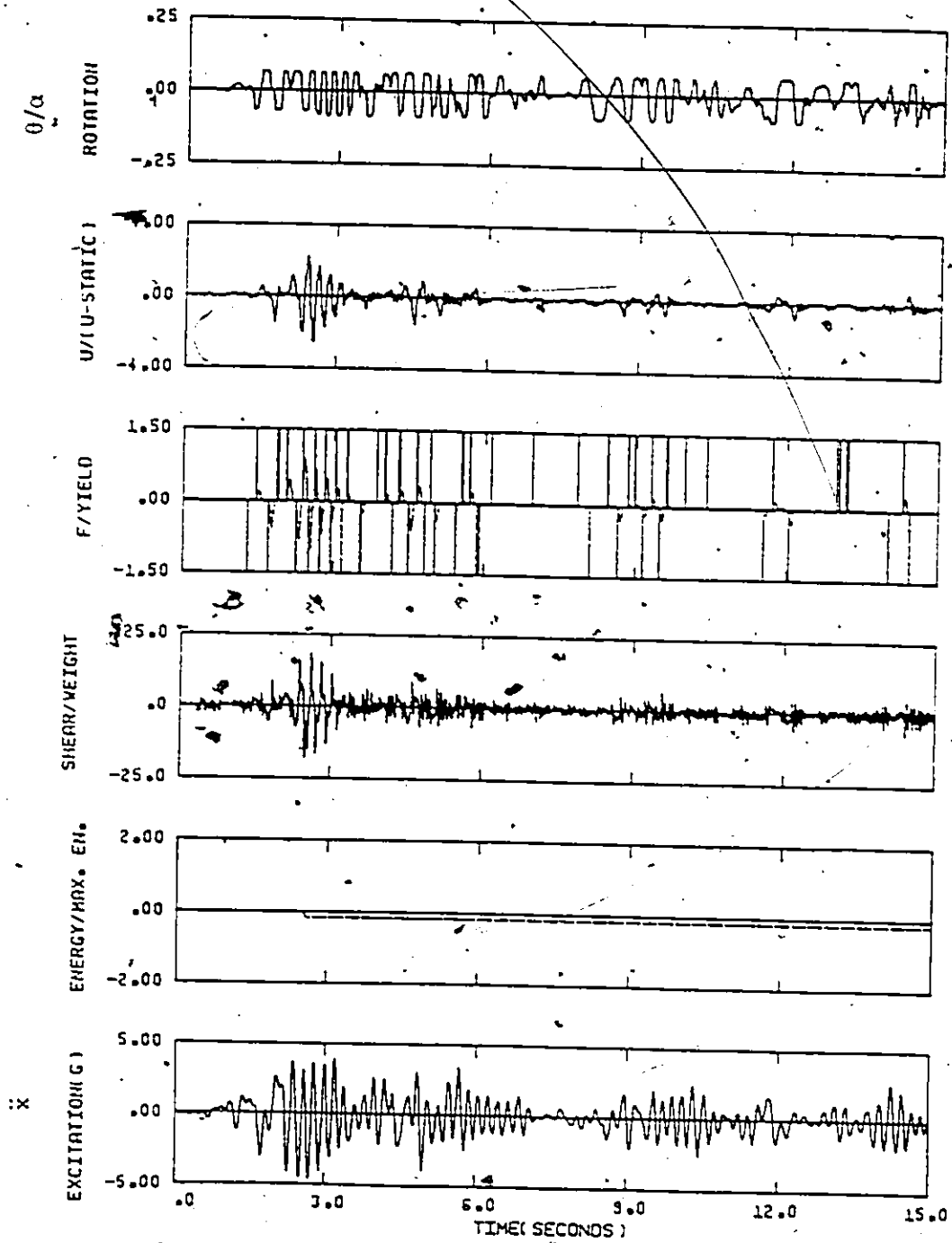
Fig. (6.10) Response of the system with yielding bolts to El Centro floor motion (f_0=5 Hz, ξ=0.01, g_r=0.03, a=0.4A*)

Table (6.2)

Response to El Centro Floor Motion

Yielding versus Non-yielding Bolts

$$(a=0.4A^*)$$

	Non-yielding Bolts			Yielding Bolts		
Initial g_r	0.001	0.01	0.03	0.001	0.01	0.03
Final g_r(left)	0.001	0.01	0.03	0.054	0.068	0.0377
Final g_r(right)	0.001	0.01	0.03	0.023	0.01	0.03
Max. F_i/F_y i=1 or 2	5.9	2.83	1.1	1.0	1.0	1.0
Max. U/U-Static	14.02	6.9	2.73	2.96	2.97	2.53
Max. shear/W	51.0	41.0	20.3	21.0	21.1	19.1
Energy absorbed/ max. energy(left)	0.0	0.0	0.0	1.13	1.24	0.16
Energy absorbed/ max. energy(right)	0.0	0.0	0.0	0.47	0.0	0.0
Failure	No	No	No	Yes	Yes	No

presents the peak values of the response time histories.

The results in Table (6.2) show two physical quantities worthy of discussion. The first quantity is the sum of the energy absorbed by the left and right bolts, which can also be measured by the sum of the extensions in both bolts. The second quantity is the sum of the final sizes of the gaps at the left and right sides of the base plate, which is nearly proportional to the sum of the absolute values of the amplitudes of the positive and negative angles of rotation. Later, this sum of absolute angles will be referred to as the "total rocking angle".

It is found that the sum of bolt extensions or the sum of the energy absorbed by the two bolts increases as the initial gap decreases. The sum is small for the case with the large gap, $(g_r=0.03)$, greater for the case with the small gap, $(g_r=0.01)$, and maximum for the case with the very small gap, $(g_r=0.001)$. This quantity can be considered a measure of the severity of excitation for the systems with gaps.

The sum of the final gap sizes is nearly equal for all cases, although the initial gap sizes are unequal. This indicates that, for a certain level of excitation applied to the system, the bolts will extend by different amounts, but the final total rocking angles will be nearly equal. If a critical gap size is defined for a specific input, such that the bolt(s) will yield fully until it is just about to break, the critical gap ratio, for the case of $a=0.4A^*$, is somewhere between 0.01 and 0.03.

6.3.2 Effect of the Input Acceleration Level

In the following, the initial gap ratio is fixed to 0.01 , and

the acceleration level of the floor motions is varied between 0.2A* and
0.4A*. Figures (6.11) and (6.12) present the response time histories
when the system is subjected to the El Centro induced floor motion,
normalized to have acceleration peaks equal to 0.2A* and 0.3A*,
respectively. The response of the case with a=0.4A* is shown in Fig.
(6.9). A comparison of the response time histories of the three cases
leads to the following observations. Higher input accelerations lead to
more stretching of the bolts and, consequently, larger values for the
total rocking angle. In the case of low-level excitation, a=0.2A*, the
bolts do not yield. In the case of a=0.3A*, one bolt yields but the
extension does not exceed the maximum extension limit of a real bolt.
For the case of high excitation level, a=0.4A*, one bolt yields and the
extension exceeds the maximum limit of a real bolt, indicating that
failure occurs. In the last two cases, the yielding of the bolts
(transition from stage 4 to stage 5) takes place only once during the
time of strong shaking. Table (6.3) shows the peak values of the
different cases considered. The base shear increases less rapidly as
the input acceleration is increased. As for the lateral deformation of
the system U, Fig. (6.13) illustrates the variation of the response
peaks as a function of the peak floor acceleration "a", in absolute and
normalized units. It is shown that the deformation of the system
increases less rapidly as the floor acceleration is increased. When the
response is normalized to the corresponding static displacement,
however, the magnification factor decreases as the input increases.
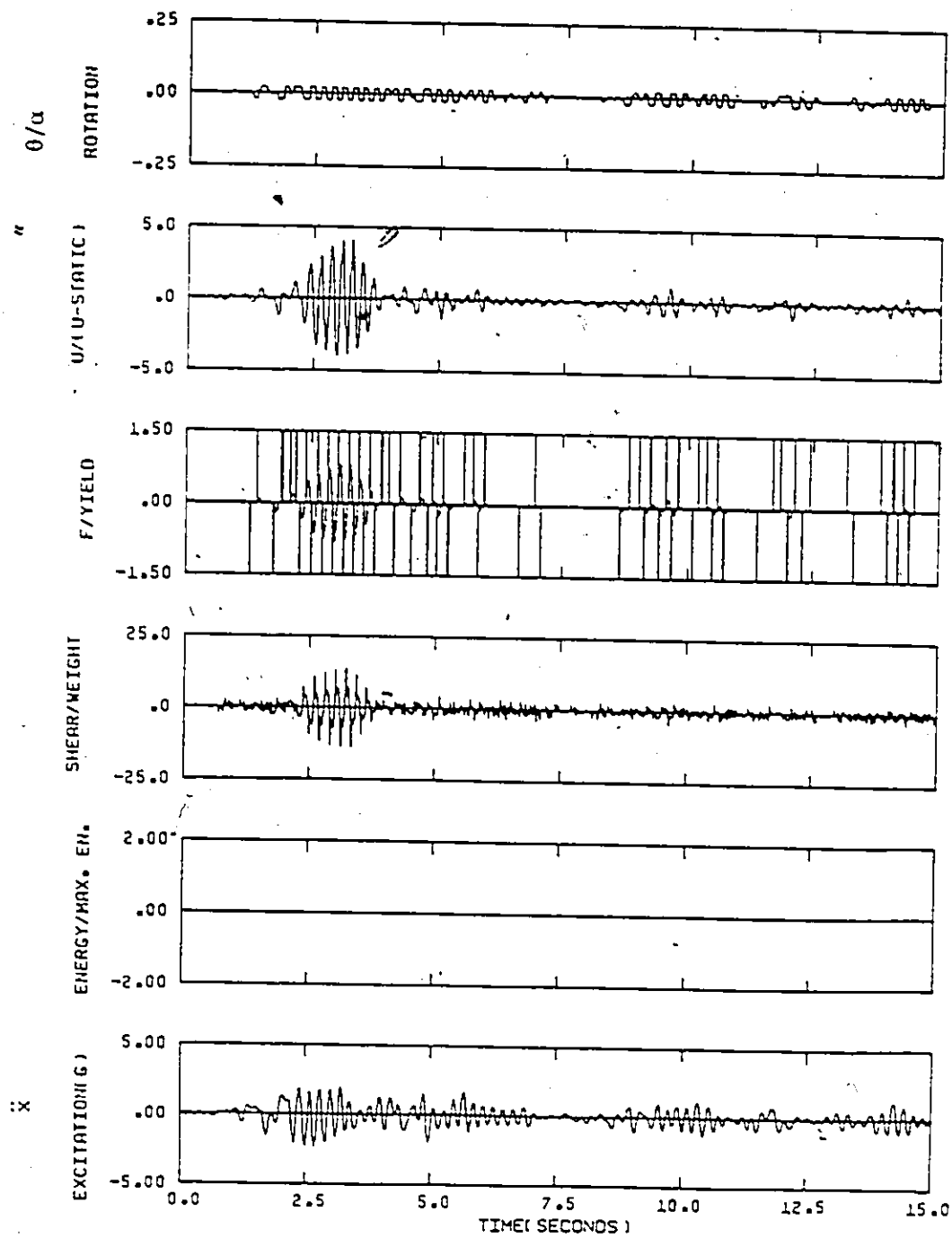
Fig. (6.11)   Response of the system with yielding bolts to El Centro floor motion (f_o=5 Hz, ξ=0.01, g_r=0.01, a=0.2A*)
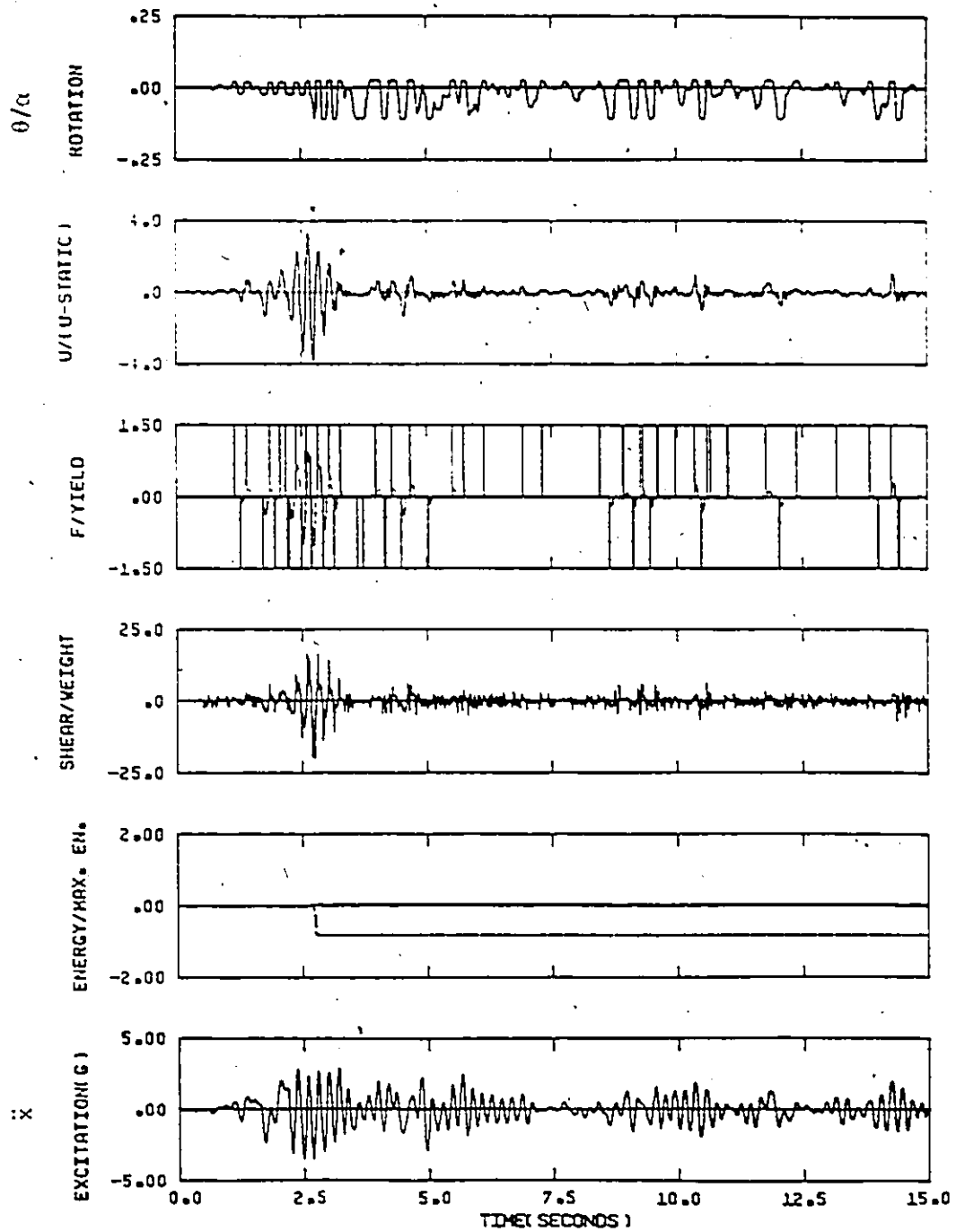
Fig. (6.12) Response of the system with yielding bolts to El Centro floor motion (f_o=5 Hz, ξ=0.01, g_r=0.01, a=0.3A*)

Table (6.3)

Response to El Centro Floor Motion

Yielding Bolts

Effect of Input Acceleration Level

$$(g_r = 0.01)$$

Peak floor acceleration a	$0.2A^*$	$0.3A^*$	$0.4A^*$
Initial g_r	0.01	0.01	0.01
Final g_r(left)	0.01	0.047	0.068
Final g_r(right)	0.01	0.011	0.01
Max. F_i/F_y $i=1$ or 2	0.88	1.0	1.0
Max. U/U-Static	4.138	3.838	2.97
Max. shear/W	13.8	19.9	21.1
Energy absorbed/ max. energy(left)	0.0	0.8	1.24
Energy absorbed/ max. energy(right)	0.0	0.03	0.0
Failure	No	No	Yes
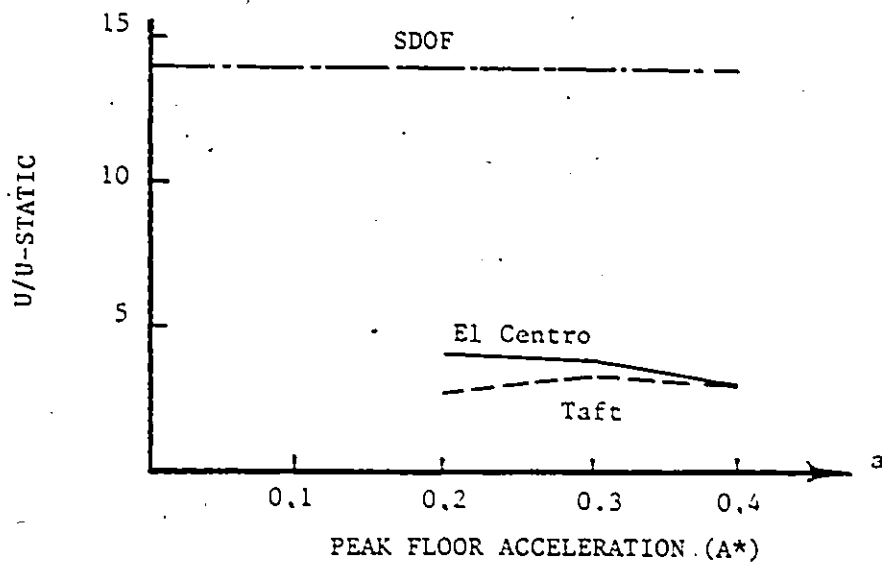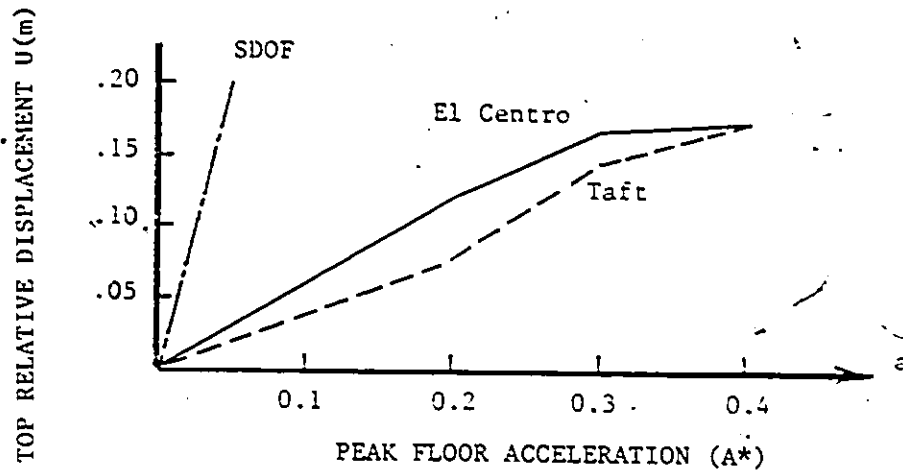
Fig. (6.13)   Response of the system with gaps and yielding bolts versus
              base acceleration amplitude (floor motion excitation)

6.3.3 Comparison Between Systems with Yielding Bolts and Systems with Non-yielding Bolts

In this section, the comparison is carried out for different gap ratios. Figures (5.17), (5.25) and (5.26) have already shown the responses of systems with rigid bolts for the cases of gap ratios equal to 0.00001, 0.01 and 0.03, respectively, when the rocking systems are subjected to the El Centro induced floor motion. Figures (6.8) to (6.10) present the responses of the corresponding cases when the bolts are allowed to yield. All the cases have a peak floor acceleration equal to 0.4A*. The peak values of the corresponding response time histories are presented in Table (6.2). When each case with yielding bolts is compared to the corresponding case of the same initial gap ratio with non-yielding bolts, the following observations are found. There are considerable reductions in the lateral deformation U and in the base shear in the cases with yielding bolts compared to those with non-yielding bolts. The reductions are large for the case with the very small gap ratio, smaller for the case with $g_r=0.01$ and minor for the case of the large gap ratio.

6.4 Effect of Earthquake Type (Numerical Results of Taft Induced Floor Motion)

Since earthquake motions differ in shape and frequency content, their effects on systems may also differ even if their peaks are equal. In the previous sections, the N-S component of the El Centro (1940) earthquake record was used to study the effects of earthquakes on the partially fixed systems. The purpose of this section is to examine how

general the conclusions are, based on the El Centro earthquake excitation alone. In this part, the floor motion caused by the Taft (1952) S69E component, shown in Fig. (5.11), is used as input to the equipment. The floor motion obtained is normalized to have a peak acceleration equal to $a=0.2A^*$, $0.3A^*$ or $0.4A^*$, respectively. Each floor motion is then applied to a system with yielding bolts of a gap ratio equal to 0.01. Figures (6.14) to (6.16) present the corresponding time histories of these cases, respectively. These Figures show that, when the floor motion has a peak acceleration $a=0.2A^*$, neither bolt yields and the base plate rocks with amplitudes corresponding to the initial gap ratio. When the peak acceleration is equal to $0.3A^*$, both bolts yield equally. Yielding of the bolts (transition from stage 4 to stage 5) takes place only once at the time of strong shaking. Accordingly, the rocking amplitudes of the base plate increase more than the initial amplitudes before yielding. In the case of the largest input with $a=0.4A^*$, one of the bolts yields at the time of strong shaking. The yielding extends beyond the maximum limit for failure of real bolts, and is followed by asymmetric rocking.

The base shear increases when the input acceleration is raised from $a=0.2A^*$ to $0.3A^*$. It is not affected, however, by further increase in acceleration. The same behaviour is also noticed for the lateral deformation U with small differences in the magnification factor among the three cases, as shown in Fig. (6.13).

Table (6.4) compares the response peaks for the three cases considered. A comparison of Table (6.3) and Table (6.4) indicates that the responses of both groups follow the same trend with respect to the
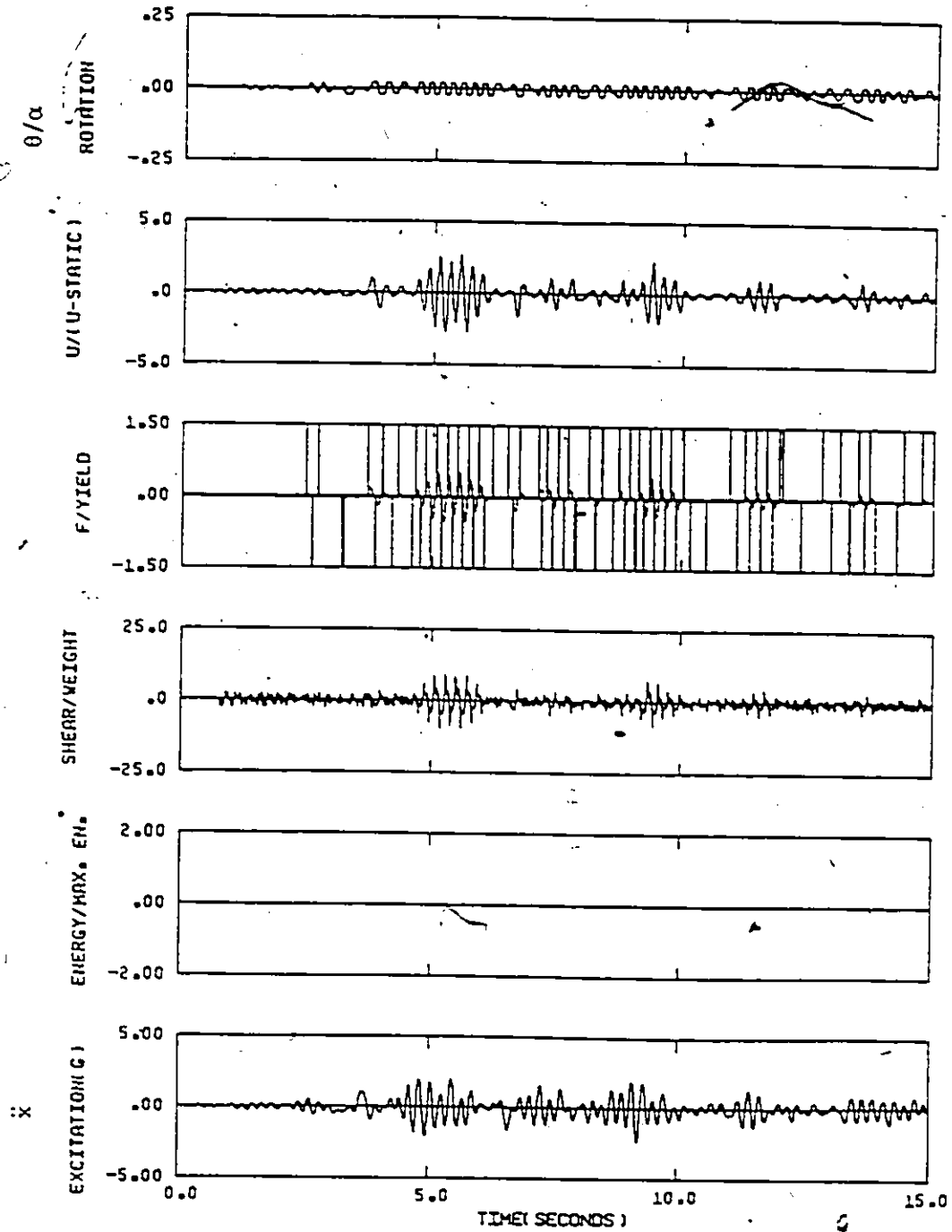
Fig. (6.14)   Response of the system with yielding bolts to Taft
floor motion (f_0=5 Hz, ξ=0.01, g_r=0.01, a=0.2A*)
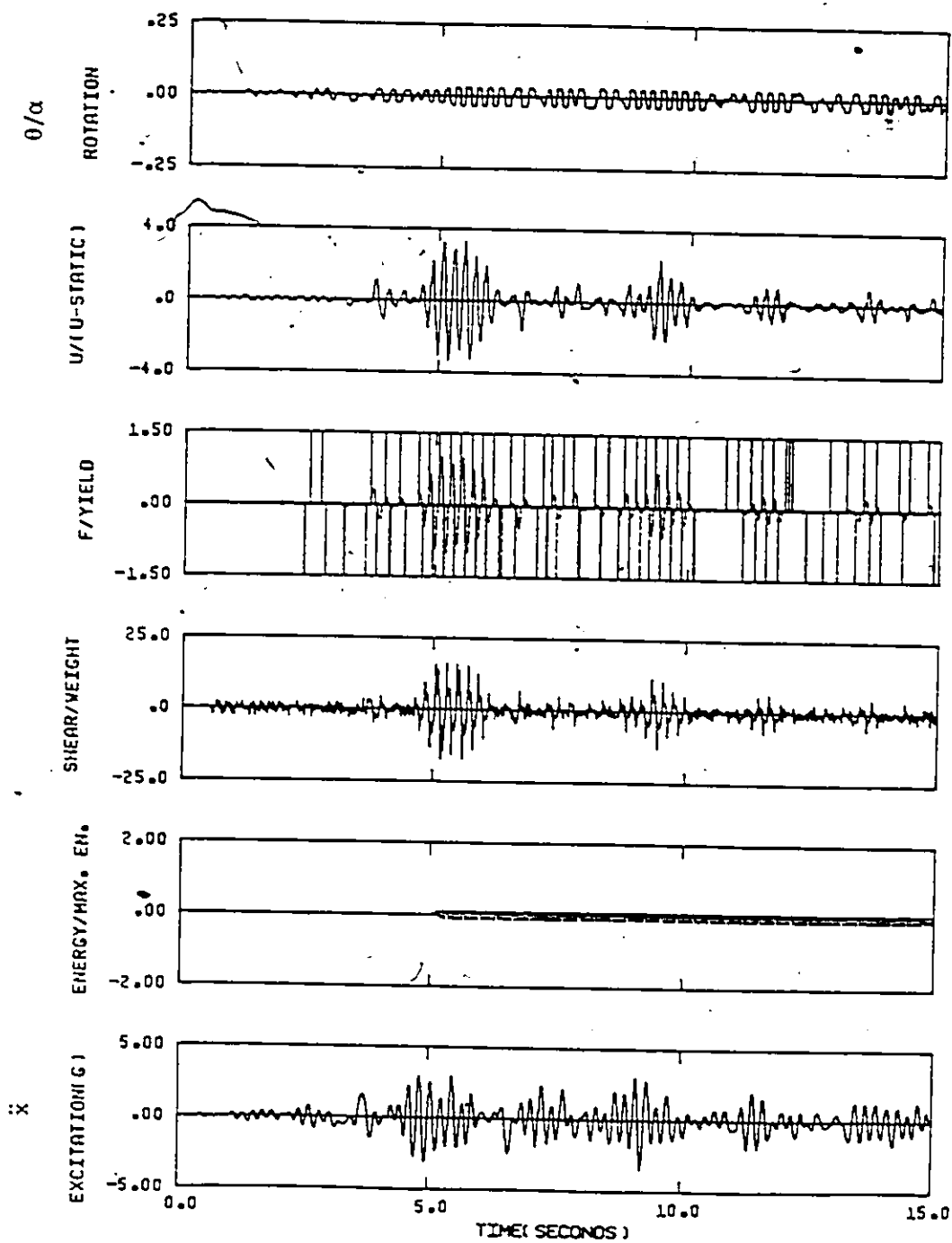
Fig. (6.15) Response of the system with yielding bolts to Taft floor motion (f_0=5 Hz, ξ=0.01, g_r=0.01, a=0.3A$^\bullet$)
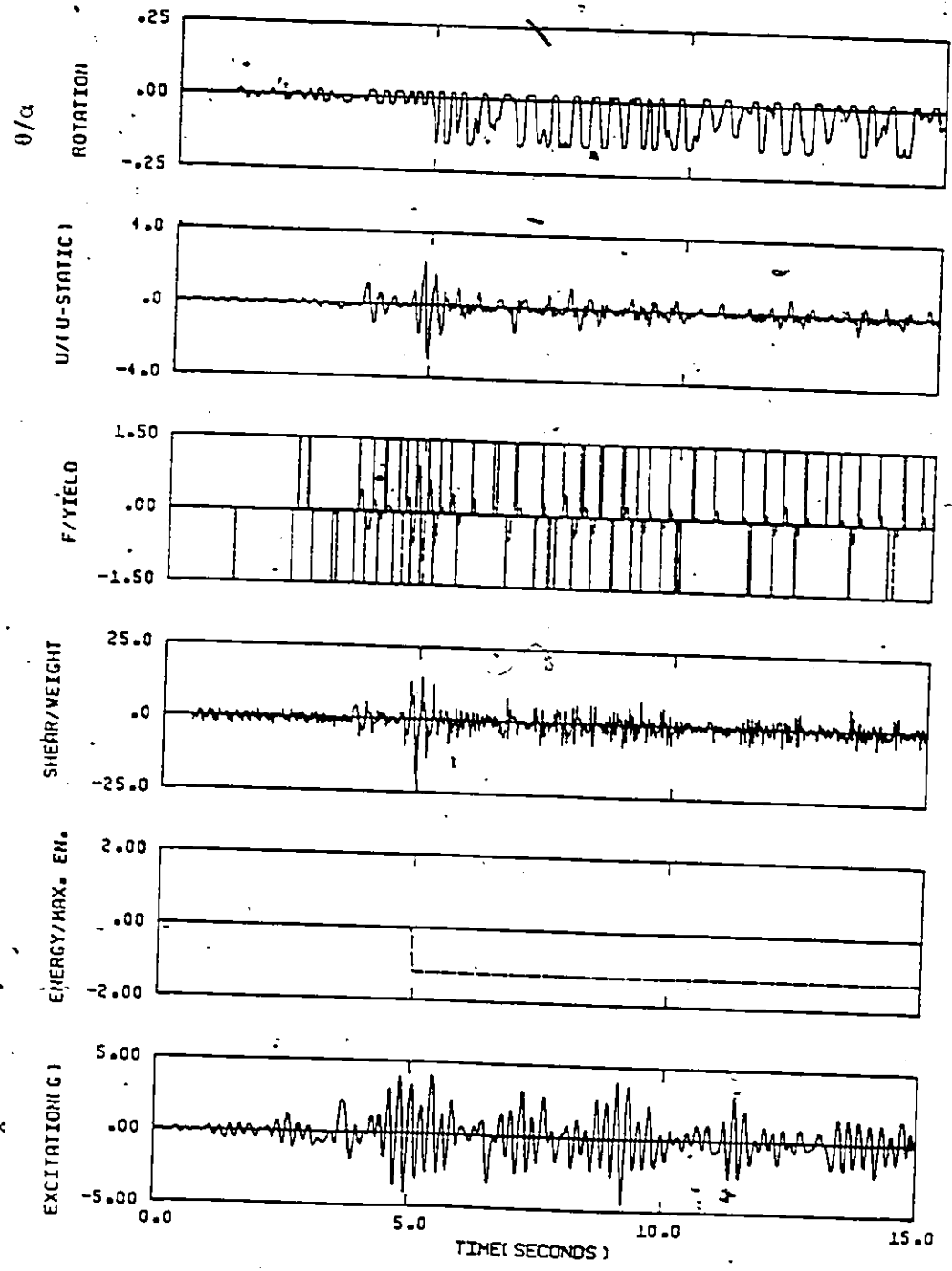
Fig. (6.16) Response of the system with yielding bolts to Taft
floor motion (f_O=5 Hz, ξ=0.01, g_r=0.01, a=0.4A*)

Table (6.4)

Response to Taft Floor Motion

Yielding Bolts

Effect of Input Acceleration Level

$(g_r=0.01)$

	$0.2A^*$	$0.3A^*$	$0.4A^*$
Peak floor acceleration a			
Initial g_r	0.01	0.01	0.01
Final g_r(left)	0.01	0.015	0.067
Final g_r(right)	0.01	0.014	0.01
Max. F_i/F_y i=1 or 2	0.99	1.0	1.0
Max. U/U-Static	2.71	3.35	3.01
Max. shear/W	9.61	21.1	21.9
Energy absorbed/ max. energy(left)	0.0	0.1	1.23
Energy absorbed/ max. energy(right)	0.0	0.08	0.0
Failure	No	No	Yes

effect of the gap size and the level of excitation. All the other features of response explained in Section (6.3.2) for the El Centro induced floor motion apply for the Taft induced floor motion. The behaviour of the yielding system subjected to the Taft floor motion is also compared in Fig. (6.13) with that of the system subjected to the El Centro floor motion. It can be seen that when the floor motions are normalized to have equal peak floor accelerations, the responses of the rocking systems are of the same order of magnitude. The differences in the lateral deformation U or the magnification factor are maximum at a low level of excitation, decrease gradually as the input level increases and disappear at a=0.4A*.

In general, the comparison between the responses of the systems subjected to the El Centro and the Taft induced floor motions indicates that the response level for the partially fixed systems does not appear to be highly dependent on the earthquake motion source if all other parameters are kept the same (floor natural frequency and damping).

6.5   Shift of Natural Frequency

As was shown in the case of harmonic excitation, both yielding and non-yielding systems have natural frequencies shifted from the natural frequency of the linear system on a fixed base. Larger gaps cause larger shifts. To investigate the equipment response to earthquake excitations, it was assumed that both the equipment (on a fixed base) and the supporting structure have the same natural frequency (5Hz). In fact, the effect of the frequency shift, an effect which may be significant to the response, was ignored. To investigate the effect

of the frequency shift, the response of the equipment is studied in a case where the supporting structure has a natural frequency of 4 Hz and a gap ratio of 0.01 is assumed. Figure (6.17) shows the floor motion resulting from the response of a SDOF system with a natural frequency of 4 Hz and a damping ratio equal to 0.05, subjected to the Taft (1952) S69E component. Figure (6.18) shows the response of the equipment system subjected to this resulting floor motion, normalized to have a peak acceleration "a" equal to $0.4A^*$.

Figure (6.18) shows that one bolt yields (i.e., goes from stage 4 to stage 5) twice and the energy absorbed exceeds the maximum limit for failure of real bolts. After yielding, asymmetric rocking response occurs. When the resulting response is compared with the response shown in Fig. (6.16), which corresponds to the case when the effect of the frequency shift is ignored, it is found that the lateral deformation U and the base shear are not affected by the frequency shift. However, the bolt stretching and the energy absorption increase by about 12%, which indicates that the excitation becomes more severe if the structure has a natural frequency equal to 4 Hz. Table (6.5) summarizes the comparison between the two cases considered in Figs. (6.16) and (6.18).

6.6 Design Considerations

The parametric study using the El Centro induced floor motion showed that the magnification factor corresponding to the system on a fixed base is nearly equal to 14 . This value drops to a range between 2.5 and 6 for the partially fixed systems, the value depending on the input level, the initial gap ratio and the rigidity of the bolts. This
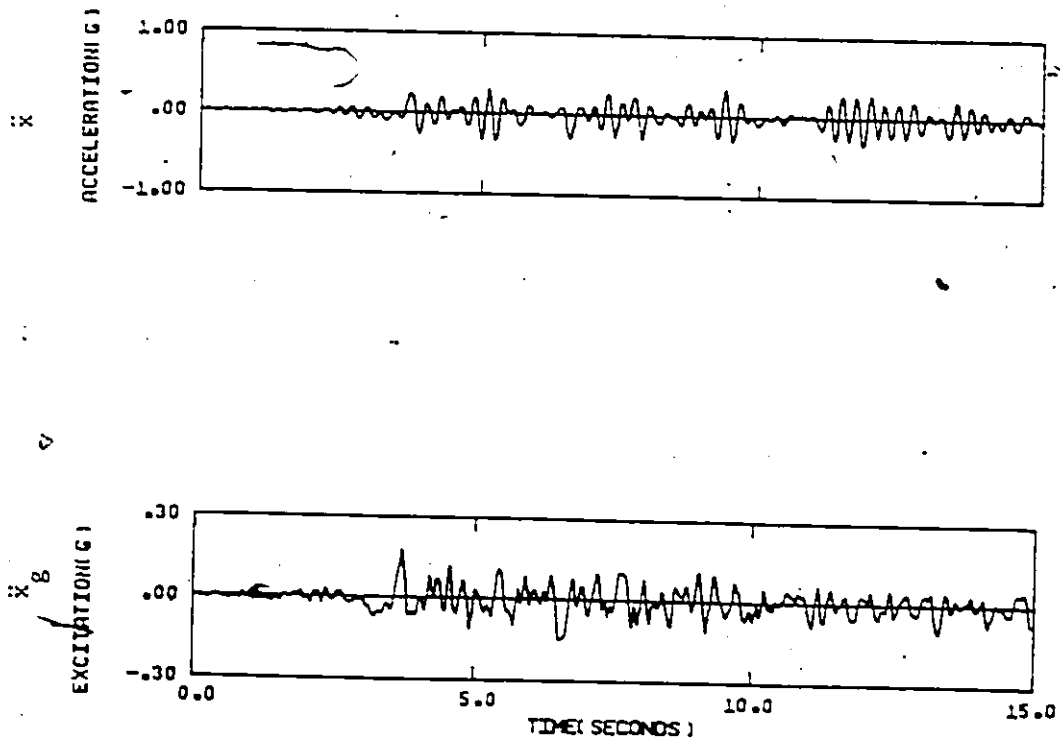
Fig. (6.17)   Response of a SDOF system on a fixed base (f_o=4 Hz, ξ=.05) to Taft S69E component
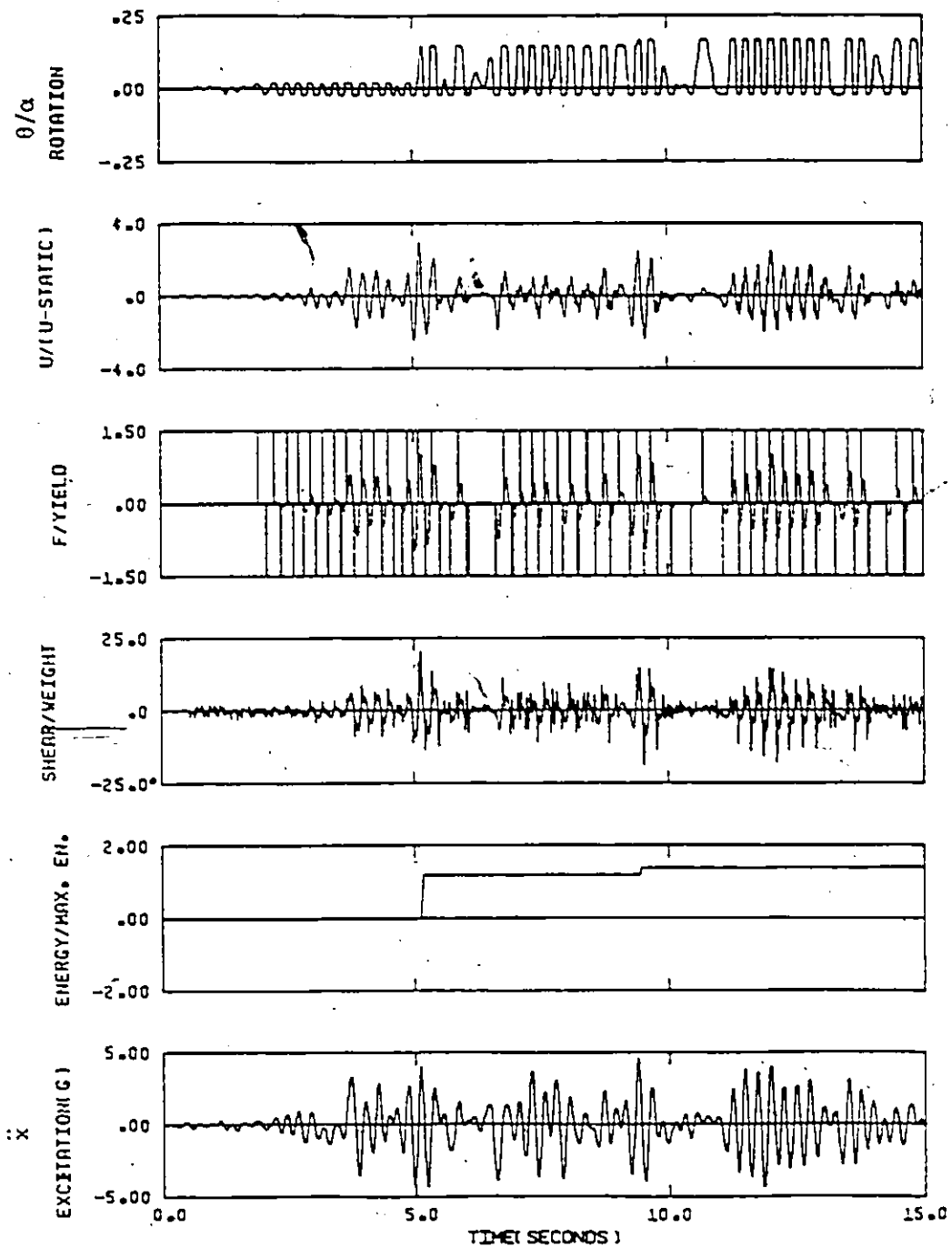
Fig. (6.18)   Response of the system with yielding bolts to Taft floor motion (f_0=5 Hz, ξ=0.01, g_r=0.01, a=0.4A, structure frequency=4 Hz)

Table (6.5)

Response to Taft Floor Motion

Yielding bolts

$(a=0.4A^*,\ g_r=0.01,\ $ Equipment frequency$=5\,Hz)$

Structure frequency (Hz)	4.0	5.0
Initial g_r	0.01	0.01
Final g_r(left)	0.01	0.067
Final g_r(right)	0.074	0.01
Max. F_i/F_y $i=1$ or 2	1.0	1.0
Max. U/U-Static	2.94	3.01
Max. shear/W	20.6	21.9
Energy absorbed/ max. energy(left)	0.0	1.23
Energy absorbed/ max. energy(right)	1.37	0.0
Failure	Yes	Yes

considerable-reduction in response shows the benefit to be gained by allowing the equipment to uplift.

The acceleration level that can be used for the design of the bolts is dependent on the gap size and the criterion required for the bolt behaviour. If the bolts are not allowed to yield, the system should not be exposed to an acceleration greater than $0.066A^*$ when no gap is provided. A design factor can be defined as the ratio between the design floor acceleration used in the static approach and the corresponding peak acceleration used in the dynamic approach which will have an equivalent effect on the equipment. In the previous case, therefore, the design factor is equal to 14. If the gap ratio is equal to 0.01, however, the system will resist up to a maximum acceleration of $0.2A^*$, which corresponds to a design factor equal to 5. For a system with a gap ratio equal to 0.03, the design factor is reduced to (3.3). In other words, for a given bolt size, a gap, deliberately provided in the system, will render it capable of withstanding a higher level of floor excitation.

If the bolts are allowed to yield but not to break, the maximum floor acceleration, the anchorage system can withstand, is about $0.3A^*$ and $0.4A^*$ for systems with gap ratios equal to 0.001 and 0.03, respectively. Accordingly, the corresponding design factors are equal to 3.3 and 2.5, respectively.

On the other hand, the final gap ratios tell us approximately how large a gap is required for a certain input to keep the bolt forces below the yield level. For floor motions with peak accelerations equal

to $0.2A^*$, $0.3A^*$ and $0.4A^*$, it is recommended that gaps with ratios equal to 0.01, 0.015 and 0.04, respectively, be provided.

The design of the equipment frame is governed by the maximum base shear that would occur during the excitation. The design base shear depends on the size of the gap provided and on the criterion required for the bolts' behaviour. In the case where no gap is provided, the maximum base shear that would occur to the system is equal to $10.8V_o$, where V_o is the static base shear and is equal to Ma. If the system is anchored such that a gap is allowed, the design base shear drops to $6V_o$ and $4V_o$, with gap ratios equal to 0.01 and 0.03, respectively, while the tensile forces in the bolts are always less than the yield strength. However, if the anchor system is allowed to yield but not to break, the design base shear is approximately equal to $5.6V_o$.

In general, it is recommended that equipment be allowed to rock on its base by providing gaps in the fastening system. Partial fixation has two advantages over complete fixation. First, it reduces the deformation of the mounted system and, consequently, the design base shear. Second, it decreases the required yield strength for the bolts.

It is also recommended that bolts with relatively large material toughness be used. This will allow the gaps, if they are relatively small, to increase to the required size during the excitation, before the bolts fail. The bolts can be fastened in such a way that a sufficient deformable length for the bolts will be provided. This will increase their ability to absorb energy without changing their yield strength. It is more practical, however, to increase the gap size to the required value. Larger gaps are recommended for higher floor

acceleration levels.

CHAPTER 7

SUMMARY AND CONCLUSIONS

This study investigates the rocking response of equipment resting freely on a rigid floor and also the effect of restrained rocking on the response of partially fixed equipment under the effect of seismic excitations. The equipment which rests freely is modelled as a rigid rectangular block. Whereas the partially fixed equipment is modelled as a shear beam attached to a rigid rocking base plate which in turn is fastened to the floor by two bolts. The bolts are modelled as rigid-plastic members. The overturning of the rigid rectangular block is studied under the effect of three types of base motion, namely, pulsive, critical and harmonic excitations, whereas the response of the partially fixed equipment is studied under the effect of harmonic and earthquake excitations.

The minimum conditions for overturning of the rigid rectangular block are derived, using an energy approach, for three different cases of excitation composed of a single pulse of base acceleration, namely, a triangular pulse with decreasing acceleration, a triangular pulse with increasing acceleration, and a half-sine pulse. The results obtained lead to the following conclusions.

1- The minimum peak acceleration required for overturning has large values for small pulse durations and monotonically decreases as the pulse duration increases.

204

2- The most severe pulse which will require the least peak acceleration for a specified duration is the rectangular type.

3- Independent of the shape of the pulse, a very short duration pulse can be approximated as an impulse with a normalized area equal to unity.

In this study, critical excitations composed of rectangular and triangular pulses are investigated. Conditions leading to the amplification of the response of the rigid block during the excitation are derived. The investigation lead to the following conclusions.

1- The extent of response amplification depends on the restitution coefficient, the initial angle of rotation, and the peak acceleration of the pulses.

2- The critical acceleration required to amplify the motion by a specified ratio decreases monotonically as the initial angle and the restitution coefficient increase.

3- Critical excitations which are equivalent in the context of overturning lead to completely different responses of the conventional linear SDOF systems. Accordingly, linear elastic spectra do not appear to be an adequate representation for measuring the severity of base motions insofar as the overturning of the rigid blocks is concerned.

Under the effect of harmonic excitation, the rigid block may vibrate periodically, overturn, or remain stationary. Considering the frequency-acceleration domain for the excitation, steady-state periodic motion is possible within a wedge in the domain. As the restitution coefficient decreases, the upper and lower limits for this wedge shift

upwards. For a specified acceleration amplitude, the maximum steady-state response amplitude occurs at a low frequency and the response amplitude decreases monotonically as the excitation frequency increases. If the periodic motion is unstable, overturning of the rigid block can occur. For situations with stable steady-state periodic motion, overturning can still occur if the transient phase of the response exhibits excessive rotations. From the results obtained, it is found that, as the restitution coefficient decreases, the system becomes more stable against overturning and can withstand higher accelerations. In this study, simpler approximate relations governing the existence of the steady-state periodic motion are derived and applied. The approximate relations are found to be accurate for practice.

In this study, the effect of uplift on the response of partially fixed systems is investigated. The parameters of interest are: a) the gap size, b) the bolts' rigidity, and c) the excitation parameters. The results obtained lead to the following conclusions.

1- For systems restrained by non-yielding bolts, the existence of gaps decrease the deformation of the mounted equipment relative to the base as compared to the case of complete fixation. The maximum reduction in the deformation of the equipment is obtained when the size of the gaps is large enough to allow free rocking.

2- For harmonic excitations with low frequency ratios, the introduction of gaps does not affect the deformation of equipment restrained by non-yielding bolts.

3- Existence of gaps also decreases the natural frequency of the

system. This effect is enhanced at low excitation levels for the systems restrained by non-yielding bolts and is decreased for the systems with yielding bolts.

4- In the systems with yielding bolts, the presence of the gaps affects the deformation of the equipment more than in the systems with non-yielding bolts.

5- The total rocking angle after all stretching takes place is not sensitive to the initial gap size, and depends on the level of excitation.

6- For a specified excitation level, the bolts in the systems with smaller initial gaps experience more stretching. Accordingly, more ductility demand is placed on the bolts in such systems.

7- Because of the shift in the natural frequency of the partially fixed equipment, the case of equipment mounted on a structure the natural frequency of which is less than that of the mounted equipment (on a fixed base), can be more critical than that where both natural frequencies are identical.

In general, from the results obtained by the analysis of restrained rocking of equipment, the following recommendations are made:

1- It is recommended that equipment be allowed to rock on its base by providing gaps in the fastening system. Partially fixed equipment systems have two advantages over completely fixed systems. First, the deformation of the mounted system and the design base shear are reduced. Second, the design bolt's yield strength is decreased, especially, when the bolts are required to remain elastic.

2- It is useful to design the bolts to yield but not to break. This will reduce the equipment deformation considerably. This design will be difficult to achieve in practice, however, unless the toughness of the bolt's material is sufficiently large.

3- It is recommended that a ductile kind of material be used for the bolts. This will accommodate the stretching in the bolts when the forces induced in them reach their yield strength.

4- The bolts can be fastened in such a way that a sufficient deformable length for the bolts will be provided. This will increase their ability to absorb energy without changing their yield strength. It is more practical, however, to increase the gap size to the required value. Larger gaps are recommended for higher floor acceleration levels. In general, a gap ratio equal to 0.03 is found to be sufficiently large for the case considered.

5- In this study, it is assumed that the equipment is not deformable in the vertical direction. In fact, the columns of the equipment frame are usually stiff in the vertical direction and the natural frequency of equipment due to the axial deformation is relatively high. If the beams, inside the equipment, are relatively flexible, however, their lateral vibration should be considered.

6- It is also assumed, in this study, that the impact forces occur instantaneously. Therefore, their effect is considered as a sudden change in the momenta. For future research, however, the effect about impact should be studied in more detail, taking into

consideration the effect of wave propagation in the equipment
frame column.

APPENDIX A

AREA OF ACCELERATION-TIME DIAGRAM

FOR

IMPULSIVE EXCITATIONS

The area of pulsive acceleration-time diagram A_t is expressed as

$$A_t = \int_0^{2h} \ddot{x} \, dt \tag{A.1}$$

To overturn the rigid block, by an initial angular velocity, the initial kinetic energy of the block must equal the potential energy of the block at the position of overturning. Therefore, using small angle approximation, we have:

$$\frac{1}{2} . I_0 \, \dot{\theta}^2 = WR \, \frac{\alpha^2}{2} \tag{A.2}$$

The momentum principle implies that:

$$\int_0^{2h} M \ddot{x} \, h \cdot dt = I_0 \, \dot{\theta} \tag{A.3}$$

or

$$M h \int_0^{2h} \ddot{x} \, dt = Mh \, A_t = I_0 \, \dot{\theta} \tag{A.4}$$

Substituting the expression of the angular velocity given by equation (A.2) into equation (A.4) and solving for A_t, we get:

$$A_t = \frac{g\alpha}{p} \tag{A.5}$$

Thus the area of the normalized acceleration time diagram becomes equal to:

$$\frac{p\,A_t}{g\alpha} = 1$$

REFERENCES

1. Aslam, M., Godden, W.G. and Scalise, D.T. (1980), "Earthquake Rocking Response of Rigid Bodies," Journal of the Structural Division, American Society of Civil Engineers, Vol. 106, No. ST2, pp. 377-392.

2. Beck, J.L. and Skinner, R.I. (1974), "The seismic Response of a Reinforced Concrete Bridge Pier Designed to Step," Earthquake Engineering and Structural Dynamics, Vol. 2, No. 4, pp. 343-358.

3. Berezin, I.S. and Zhidkov, N.P. (1965), Computing Methods, Addison-Wesley.

4. Clough, R.W. and Huckelbridge, A.A. (1977), "Earthquake Simulation Tests of a Three-Story Steel Frame with Columns Allowed to Uplift," Report No. UCB/EERC 77-22, Earthquake Engineering Research Center, University of California, Berkeley, California.

5. Evison, R.J., Prietstley, M.J.N. and Carr, A.J. (1977), "Rocking Foundations," Research Report No. 77-8, Department of Civil Engineering, University of Canterbury, New Zealand.

6. Housner, G.W. (1963), "The Behaviour of Inverted Pendulum Structures During Earthquakes," Bulletin of the Seismological Society of America, Vol. 53, No. 2, pp. 403-417.

7. Huckelbridge, A.A. (1977), "Earthquake Simulation Tests of a Nine-Story Steel Frame with Columns Allowed to Uplift," Report No. UCB/EERC 77-23, Earthquake Engineering Research Center, University of California, Berkeley, California.

8. Ishiyama, Y. (1980), "Review and Discussion on Overturning of Bodies by Earthquake Motions," BRI Research Paper No. 85, Building Research Institute, Ministry of Construction, June 1980.

9. Ishiyama, Y. (1982), "Motions of Rigid Bodies and Criteria For Overturning by Earthquake Excitations," Earthquake Engineering and Structural Dynamics, Vol. 10, No.5, pp. 635-650.

10. McManus, K.J., Priestly, M.J.N. and Carr, A.J. (1980), "The Seismic Response of Bridge Structures Free to Rock on Their Foundations," Research Report No. 80-4, Department of Civil Engineering, University of Canterbury, New Zealand.

11. Meek, J.W. (1975), "Effects of Foundation Tipping on Dynamic

Response," *Journal of the Structural Division*, American Society of Civil Engineers, Vol. 101, No. ST7, pp. 1297-1311.

12. Meek, J.W. (1978), "Dynamic Response of Tipping Core Building" *Earthquake Engineering and Structural Dynamics*, Vol. 6, No. 5, pp. 437-454.

13. Muto, K., Umemura, H. and Sonobe, Y. (1960), "Study of Overturning Vibrations of Slender Structures," Proceedings of the Second World Conference on Earthquake Engineering, Tokyo, 1960.

14. Newmark, N.M. and Rosenblueth, E. (1971), *Fundamentals of Earthquake Engineering*, Prentice Hall.

15. Ogawa, N. (1980), "A Study on Overturning Vibration of Rigid Structures," Proceedings of the Seventh World Conference on Earthquake Engineering, Istanbul, 1980.

16. Ogawa, N. (1980), "A Study on Overturning Vibration of Rigid Structures," Trans. of AIJ, No. 287, Jan. 1980, pp. 51-63 (in Japanese)

17. Priestly, M.J.N., Evison, R.J. and Carr, A.J. (1978), "Seismic Response of Structures Free to Rock on Their Foundations," *Bulletin of the New Zealand National Society of Earthquake Engineering*, Vol. 11, No. 3, pp. 141-150.

18. Psycharis, I.N. (1981), " Dynamic Behaviour of Rocking Structures Allowed to Uplift," Report No. EERL 81-2, Earthquake Engineering Research Laboratory, California Institute of Technology, Pasadena, California.

19. Sexton, H.J. (1976), Discussion of reference 10, *Journal of the Structural Division*, American Society of Civil Engineers, Vol. 102, No. ST6, pp. 1262-1263.

20. Spanos, P.D. and Koh, A.S. (1984), "Rocking of Rigid Blocks Due to Harmonic Shaking," *Journal of Engineering Mechanics Division*, American Society of Civil Engineers, Vol. 110, No. ST11, pp. 1627-1642.

21. Wolf, J.P. (1976), "Soil-Structure Interaction with Separation of Base Mat from Soil (Lifting-off)," *Nuclear Engineering and Design*, Vol. 38, No. 2, pp. 357-384.

22. Wolf, J.P. (1977), "Seismic Response Due to Travelling Shear Wave Including Soil-Structure Interaction with Base Mat Uplift," *Earthquake Engineering and Structural Dynamics*, Vol. 5, No. 4, pp. 337-363.

23. Yim, C.S., Chopra, A.K. and Penzien, J. (1980), "Rocking Response

of Rigid Blocks to Earthquakes," Report No. UCB/EERC 80-2, Earthquake Engineering Research Center, University of California, Berkeley, California.

24. Yim, C.S. and Chopra, A.K. (1983), "Effects of Transient Foundation Uplift on Earthquake Response of Structures," Report No. UCB/EERC 83-9, Earthquake Engineering Research Center, University of California, Berkeley, California.